UCLA
UCLA Electronic Theses and Dissertations

Title

Improved Therapeutic Efficacy of Cancer Gene Therapy using Retroviral Replicating Vectors Designed for Multiple Transgene Transduction

Permalink

https://escholarship.org/uc/item/10j817dq

Author

Hermann, Kip James

Publication Date

2015

Peer reviewed|Thesis/dissertation

eScholarship.org Powered by the California Digital Library
University of California

UNIVERSITY OF CALIFORNIA

Los Angeles

Improved Therapeutic Efficacy of Cancer Gene Therapy using RRVs Designed for Multiple Transgene Transduction

A dissertation submitted in partial satisfaction of the requirements for the degree Doctor of Philosophy in Molecular and Medical Pharmacology

by

Kip James Hermann

2015

ABSTRACT OF THE DISSERTATION

Improved Therapeutic Efficacy of Cancer Gene Therapy using Retroviral Replicating Vectors Designed for Multiple Transgene Transduction

by

Kip James Hermann

Doctor of Philosophy in Molecular and Medical Pharmacology

University of California, Los Angeles, 2015

Professor Noriyuki Kasahara, Co-Chair

Professor James A. Byrne, Co-Chair

Retroviral Replicating Vectors (RRVs) carrying the human codon optimized yeast cytosine deaminase (yCD2) suicide gene are currently in Phase I/II clinical trials for treatment of high-grade glioma. These vectors are highly tumor specific due to their intrinsic inability to infect non-dividing cells, and their restriction by the innate immune system, which is often suppressed in the tumor microenvironment.[1]. Currently, this system relies on delivery of a single transgene, yCD2, to the tumor mass[2]. However, the current 'gold standard' in medical care is to treat cancer with a multi-drug regimen to combat the heterogeneous nature of tumors. As RRV therapy progresses, it must also address the issue of heterogeneity and seek to deliver more therapeutics to the cancer. These studies explore the possibility of using RRVs armed with multiple transgenes to improve the therapeutic efficacy of RRV-mediated cancer gene therapy. Super Core Promoter and P2A Sequences Facilitate Combined Delivery of a Suicide Gene and Cytokine by a Single Retroviral Replicating Vector

We examined the use of independent intrinsic promoter to drive RRV transgene expression in multiple cell lines. As transgene space in limited in RRVs, a smaller promoter was studied. Super Core Promoter (SCP1)[3] was found to have varying degrees of protein expression across different cell lines. As certain immune factors are confined to a therapeutic window, low expression of transgene by SCP1 was used in U87 cells to express cytokine mouse granulocyte macrophage colony-stimulating factor (mGM-CSF) along with yCD2. Protein levels of yCD2 dropped, but the transgene still remained functional, while levels of mGM-CSF remained within the therapeutic range.

Delivery of Two Retroviral Replicating Vectors Pseudotyped With Different Non-Interfering Envelopes Increases Transgene Expression and Therapeutic Efficacy

The MLV 4070A envelope, suffers from "superinfection resistance", a phenomenon in which a virus is unable to infect cells that have already been infected by a virus expressing the same envelope protein. By switching out the envelope of RRV for different viral envelopes, the efficiency of cotransduction was studied across multiple cell lines. Results showed that cotransduction efficiencies varied between cell lines, potentially as a function of receptor availability or intrinsic viral immunity. Based on results from these studies, prime candidates for cotransduction of U87 cells were established. Simultaneous cotransduction using two RRVs, expressing the noninterfering 4070A (AC3) and gibbon ape leukemia virus (GALV) envelopes, resulted in increased transgene expression from AC3-RRV, whereas transgene expression from GALV-RRV decreased slightly when compared to transduction with a single RRV.

Enveloped-Linked Oligonucleotide P2A Increases Transgene Expression From Retroviral Replicating Vectors

In order to increase transgene expression of larger transgenes without compromising transgene stability, P2A[4,5] was attached to the end of 4070A and GALV envelope proteins. P2A proved to increase protein expression in most cell lines compared to SCP1, however, the vector copy number per cell decreased. GALV pseudotyped RRV with P2A was then used to cotransduce

cells in combination with AC3-yCD2. Expression of the yCD2 transgene increased, while expression of the GALV-RRV transgene decreased slightly. Functional assays revealed that cotransduction with two RRVs resulted in increased cell death, except at the highest concentrations of ganciclovir. Thus use of pseudotyped RRVs to deliver multiple transgenes has the potential to increase the therapeutic efficacy of RRV-mediated gene therapy.

The dissertation of Kip James Hermann is approved.

Lily Wu

Jerome A. Zack

Steven J. Bensinger

James A. Byrne, Committee Co-Chair

Noriyuki Kasahara, Committee Co-Chair

University of California, Los Angeles

2015

TABLE OF CONTENTS

ABSTRACT OF THE DISSERTATION ii
COMMITTEE v
TABLE OF CONTENTS vi
LIST OF FIGURES AND TABLES vii
VITA viii

INTRODUCTION 1

CHAPTER ONE Super core promoter and P2A sequences facilitate combined delivery of a suicide gene and cytokine by a single retroviral replicating vector
Introduction 4
Materials and Methods 6
Results 10
Discussion 12

CHAPTER TWO Delivery of two retroviral replicating vectors pseudotyped with different non-interfering envelopes increases transgene expression and therapeutic efficacy
Introduction 23
Materials and Methods 24
Results 27
Discussion 32

CHAPTER THREE Enveloped-linked oligonucleotide P2A increases transgene expression from retroviral replicating vectors
Introduction 45
Materials and Methods 46
Results 49
Discussion 52

CONCLUSIONS AND FUTURE DIRECTIONS 66
REFERENCES 81

LIST OF FIGURES AND TABLES

CHAPTER ONE

Figure 1-1 17
Figure 1-2 18
Figure 1-3 19
Figure 1-4 20
Figure 1-5 21
Figure 1-6 22

CHAPTER TWO

Table 2-1 38
Table 2-2 39
Figure 2-1 40
Figure 2-2 41
Figure 2-3 42
Figure 2-4 43
Figure 2-5 44

CHAPTER THREE

Figure 3-1 57
Figure 3-2 58
Figure 3-3 59
Figure 3-4 61
Figure 3-5 62
Figure 3-6 64
Figure 3-7 65

SUPPLEMENTARY

Supplementary Figure 1-1 70
Supplementary Figure 2-1 71
Supplementary Figure 2-2 78
Supplementary Figure 2-3 79
Supplementary Figure 3-1 80

VITA

Education

2009 B.S., Psychological Biology
University of California at Los Angeles
Los Angeles, California

PUBLICATIONS

1. Matsumoto H, Haga K, Ohno I, Hiraoka K, Kimura T, Hermann K, Kasahara N, Anton P, McGowan I. (2014) Mucosal gene therapy using a pseudotyped lentivirus vector encoding murine interleukin-10 (mIL-10) suppresses the development and relapse of experimental murine colitis. BMC Gastroenterol. 14:68

2. Haga K, Tomioka A, Liao CP, Kimura T, Matsumoto H, Ohno I, Hermann K, Logg CR, Jiao J, Tanaka M, Hirao Y, Wu H, Kruse CA, Roy-Burman P, Kasahara N. (2009) PTEN knockout prostate cancer as a model for experimental immunotherapy. J Urol 181:354-62

3. Mareninova OA, Hermann K, French SW, O'Konski MS, Pandol SJ, Webster P, Erickson AH, Katunuma N, Gorelick FS, Gukovsky I, Gukovskaya AS. (2009) Mechanisms of regulating cytochrome C release in pancreatic mitochondria. Gut 58:431-42

4. Odinokova IV, Sung KF, Mareninova OA, Hermann K, Evtodienko Y, Andreyev A, Gukovsky I, Gukovskaya AS. (2009) Impaired autophagic flux mediates acinar cell vacuole formation and trypsinogen activation in rodent models of acute pancreatitis. J Clin Invest 119:3340-55

5. Odinokova IV, Sung KF, Mareninova OA, Hermann K, Gukovsky I, Gukovskaya AS. (2008) Mitochondrial mechanisms of death response in pancreatitis. J Gastroenterol Hepatol 23 Suppl 1:S25-30

MANUSCRIPTS IN PREPARATION

1. Timberlake N, Hermann K, Yoo J, Inagaki A, Lin A, Logg C, Taylor P, Jolly D, Kasahara N. Reduced systemic spread, without loss of tumor toxicity, of a retroviral replicating vector with miR142-3p targets in the ψ and 3'LTR.

2. Hermann K, Truong B, Logg CR, Kasahara N. Delivery of two retroviral replicating vectors pseudotyped with different non-interfering envelopes increases transgene expression and therapeutic efficacy.

3. Hermann K, Inagaki A, Truong B, Collins SA, Logg CR, Kasahara N. Super core promoter and P2A sequences facilitate combined delivery of a suicide gene and cytokine by a single retroviral replicating vector.

4. Hermann K, Inagaki A, Truong B, Collins SA, Logg CR, Kasahara N. Enveloped-linked oligonucleotide P2A ncreases transgene expression from retroviral replicating vectors.

5. Truong B, Hermann K, Vega-Crespo A, Chang K, Sjarif J, Lee PC, Lipshutz GS, Wu L, Byrne J. OCT4-dependant safeguarding for site-specific gene therapy of human pluripotent stem cells.

6. Vega-Crespo A, Hermann K, Awe J, Chang K, Truong B, Lee PC, Schoenberg B, Lipshutz GS, Wu L, Byrne J. Investigating the functionality of the OCT4 short response element in human induced pluripotent stem cells.

ABSTRACTS

1. Kubo, S., Takagi-Kimura, M., Logg, C. R., Hermann, K., Kasahara, N. Dual-vector prodrug activator gene therapy using retroviral replicating vectors derived from amphotropic murine leukemia virus and gibbon ape leukemia virus. (Abstract presented at the 18th Annual Meeting of the American Society of Gene & Cell Therapy, New Orleans, LA; May 13-16, 2015.)

2. Timberlake, N., Lin, A., Hermann, K., Logg, C., Liu, Y., Kamijima, S., Diago, O., Wong, K., Anderson, C., Gammon, D., Yang, E., Gruber, H., Jolly, D. J., Kasahara, N. MicroRNA 142-3p Attenuates Spread of a Replicating Retroviral Vector in Hematopoietic-Lineage Derived Cells. (Abstract presented at the 17th Annual Meeting of the American Society of Gene & Cell Therapy, Washington DC, May 21-24, 2014.)

3. Tomioka, A., Haga, K., Liao, C.-P., Kimura, T., Logg, C., Matsumoto, H., Ohno, I., Hermann, K., Tanaka, M., Uemura, H., Hirao, Y., Roy-Burman, P., Kasahara, N. Immunotherapy using tumor-specific cytotoxic T lymphocytes (CTLs) for PTEN knock-out spontaneous prostate cancer model. (Abstract presented at the 99th Annual Meeting of the American Association for Cancer Research, San Diego, CA, April 12-16, 2008.) AACR Meeting Abstracts, Apr 2008; 2008: 4480.

Introduction

Glioblastoma multiforme (GBM), the most common form of malignant glioma in adults, infiltrates surrounding normal brain tissue, making complete surgical resection impossible. Despite improvements in neurosurgery, chemotherapy, and radiation therapy, the overall prognosis for GBM is still only 12-15 months. At best, current treatments only delay recurrence. Hence, there is considerable need for effective new approaches for this devastating disease; notably, gene therapy is one of the approaches that have been extensively tested for treatment of gliomas.

Gene therapy often demands highly efficient transfer of transgenes from the vector into the entire tumor mass to achieve a therapeutic effect. However, there have been difficulties in the past achieving such efficiency *in vivo*. In a phase III clinical trial for GBM using a conventional, non-replicating retroviral vector, less than <0.002% of the tumor was successfully transduced. Non-replicating adenoviral vectors have also failed to penetrate the tumor mass, instead, leaving a small number of transduced cells along the needle tract[6]. To increase the efficiency of transgene spread, many groups have designed viruses capable of tumor-selective replication. With viral replication, each transduced tumor cell itself becomes a virus-producing cell, sustaining further transduction events even after initial administration. Among replicating viruses being developed as oncolytic agents, murine leukemia virus (MLV)-based retroviral replicating vectors (RRV; also known as replication-competent retrovirus (RCR) vectors) have the unique ability to replicate without immediate lysis of host cells and maintain viral persistence through stable integration. Due to MLV's intrinsic inability to infect quiescent normal cells with intact innate immunity, RRV transduction is highly selective for rapidly dividing cancer cells[1]

RRV can efficiently transduce and stably propagate in a variety of cell lines in culture and tumors in vivo, thereby achieving a large in situ amplification effect after initial injection of a small inoculum. The Kasahara lab,[7] and others, have found that intratumoral injection of RRV with as little as 10e4 total infectious units resulted in viral spread and transgene delivery throughout entire subcutaneous and intracranial tumor masses in vivo, resulting in significant

therapeutic benefit in both human xenograft and syngeneic rodent[2] intracranial tumor models. The ability of RRV to stably integrate and persist in a reservoir of residual infected glioma cells is highly advantageous, enabling re-infection of recurrent tumors even as they resumed growth. A single intratumoral injection of 10e6 RRV carrying the cytosine deaminase (CD) suicide gene, followed by multiple cycles of systemic treatment with the non-toxic pro-drug 5-fluorocytosine (5-FC), achieved 100% survival for >135-day follow-up period, compared to 0% survival of controls in <40 days ($p<0.0001$)[2]. Notably, no virus was detected in any normal tissues, even after intravenous injection, in immunocompetent mice[2].

Based on these preclinical results, clinical trials are now underway (https://clinicaltrials.gov/; NCT01156584, NCT01470794, NCT01985256) using an RRV expressing the CD suicide gene. More than 70 glioma patients have been injected with RRV, and all have tolerated the treatment well, as no vector-related toxicity was observed. Promising symptomatic and radiologic signs of therapeutic benefit have been seen, but subsequent tumor progression has been observed in many patients, suggesting that the 'reservoir' of integrated virus is eliminated at lower dose levels. Thus, strategies to improve the potency of RRV gene therapy are warranted.

RRVs continue to produce virus within the tumor mass that can be transferred to neighboring, dividing tumor cells. However, some cells within the tumor mass avoid transduction by the RRVs, allowing them to escape the therapeutic effect of the vector. Evasion of transduction can lead to recurrence of tumor growth. Previous studies with RRVs have sought to deliver a single transgene into the tumor mass. However, this approach is limiting and far different from the clinical gold standard of chemotherapeutics, which recognizes the heterogeneity of the tumor mass and uses multiple drugs to either synergistically attack the tumor or attack varying pathways to ensure any cells that have bypassed a given pathway will not survive. Should RRV-mediated therapy be able to mimic chemotherapy by taking advantage of multiple pathways, it could rival the effects of chemotherapy on the targeted tumor, while avoiding the unwanted systemic side effects generally associated with chemotherapy.

However, there are two major restraints of RRVs when attempting to deliver multiple transgenes: (1) the size of the transgene is limited by the virus, so usually, only one transgene can fit into one virus and (2) the envelope of the virus binds its own receptor, blocking further transduction of an already infected cell. Despite these issues, the transgene cassette can be configured to carry multiple transgenes in a single RRV by minimizing the space taken up by promoters and linkers. RRVs can also be pseudotyped with different envelopes that do not block each other.

Chapter 1: Super Core Promoter and P2A Sequences Facilitate Combined Delivery of a Suicide Gene and Cytokine by a Single Retroviral Replicating Vector

Introduction

The efficacy of cancer gene therapy is limited both by the efficiency of gene transfer to tumor cells and the transgene expression level within each transduced cell. Early gene therapy clinical trials, utilizing non-replicating viral vectors, yielded poor results, in large part due to the inability of the vectors to effectively transduce the entire tumor mass. For instance, in one of the largest cancer gene therapy clinical trials to date, a non-replicating retroviral vector, encoding the Herpes Simplex Virus thymidine kinase (TK) suicide gene, achieved <0.002% transduction of patient gliomas, and no survival benefit was observed compared to standard therapy[8]. Lang *et al* demonstrated that transduced cells were limited to the area immediately surrounding the needle track[6]. In order to improve tumor transduction efficiency, we are developing tumor-selective retroviral replicating vectors (RRV; also known as replication-competent retrovirus (RCR) vectors) as novel gene therapy agents. One such virus, Toca 511, is currently under investigation in Phase I/II clinical trials for the treatment of advanced stage glioma (https://clinicaltrials.gov/; NCT01156584, NCT01470794, NCT01985256).

RRV Toca 511 encodes the yeast cytosine deaminase suicide gene (yCD2) downstream of an internal ribosomal entry site (IRES)[2]. yCD2 converts the nontoxic prodrug, 5-fluorocytosine (5-FC) into the chemotherapeutic drug 5-fluorouracil (5-FU), which works by (1) inhibiting thymidylate synthase (TMS), thereby decreasing the pool of available thymidine, and (2) at higher concentrations, integrating directly into the cellular RNA and DNA. Pre-clinical animal models of Toca 511, demonstrate high levels of tumor transduction and evidence of transgene expression throughout the tumor mass[2]. However, the homogeneity of xenograft tumors likely does not adequately reproduce the complex environment of human cancer. Chemotherapeutic regimens usually require multiple drugs to attack the heterogeneous cancer mass, as the

administration of a single drug can result in selection for cancer cells that are resistant to the drug in question. While the current clinical protocol for Toca 511 involves the delivery of a single transgene from a single virus, delivery of multiple transgenes may increase the clinical efficacy of RRV-mediated gene therapy. For example, combined delivery of a suicide gene and immune stimulating factor may increase tumor clearance as well as prime immune memory cells against tumor cells recurrence. Recently, Coffin *et al* demonstrated that delivery of granulocyte macrophage colony-stimulating factor (GM-CSF) delivered by an attenuated form of HSV can result in resistance to tumor challenge after the initial therapy[9]. These studies have progressed to clinical trials for the treatment of melanoma[10].

A major obstacle to developing RRVs that deliver multiple transgenes is the inherent limited transgene capacity of the virus. Error prone MLV reverse transcriptase naturally truncates, or "drops-out", genetic material that is unnecessary and detrimental to viral replication. The likelihood that exogenous genetic material will be dropped-out increases with the size of the insert. Previous studies have shown that inserting more than 1.4kb of exogenous material results in rapid drop-out[11]. In the current RRV design, the IRES sequence, which is 553 bps in length, occupies nearly a third of the RRV's limited capacity for exogenous genetic material. Recent studies in promoter function have led to the development of a Super-Core Promoter (SCP1), which combines four potent and robust promoter motifs into a single promoter SCP1[3] occupies only 74 bps, and therefore allows more space for the insertion and expression of multiple transgenes in a single RRV. With this increase in transgene space, other options now present themselves, as pairs of genes can now be inserted into the transgene space. By using a small oligonucleotide, P2A, which causes ribosomal skipping and cleavage during translation[4,5], two transgenes can be expressed from a single promoter thereby further conserving the transgene space in the RRV.

In this study, novel RRVs were developed encoding multiple transgenes through the use of SCP1 and P2A. RRVs containing the original IRES sequence were compared to RRVs with

transgenes driven by the SCP1 promoter and P2A oligonucleotide. RRV vector copy number, RNA expression of the transgene transcript, protein expression levels, and transgene function were all studied using different RRVs. Primary studies focused on the transgene expression level by studying fluorescence proteins. We then sought to determine the effect of P2A on the yCD2 transgene. Finally, we designed novel RRVs that functionally express both yCD2 and mGM-CSF, and show that mGM-CSF delivered by RRV is successfully secreted.

Materials and Methods

Cloning

pRRV-S1-emd was cloned by ligating the SCP1 sequence provided by BioBasic with 5' MluI and 3' HpaI sites, emd in with 5' HpaI and 3' NotI sites, and backbone RRV with 5' NotI and 3 MluI sites. pRRV-S1-p53 was cloned by creating a p53 product with 5' HpaI and 3' NotI site and replacing that with the emd transgene. pRRV-pRRV-S1-emd-P2A was cloned by annealing P2A oligonucleotides containing 5' BamHI site and 3' SmaI and NotI sites. SCP1-emd was isolated from a PCR reaction producing emd without a stop codon as well as 5' MluI and 3'BamHI site. Both were then ligated into the pRRV-SCP1-emd backbone cut at 5' MluI and 3' NotI and gel extracted at 10.9 kb. pRRV-S1-yCD2-P2A and pRRV-S1-Stb-P2A were constructed in a similar fashion as pRRV-S1-emd-P2A. Once these plasmids were cloned, pRRV-S1-emd-P2A-Stb, pRRV-S1-Stb-P2A-emd, pRRV-SCP1-yCD2-P2A-emd, pRRV-SCP1-emd-P2A-yCD2, and pRRV-S1-yCD2-P2A-mGM-CSF were all cloned in a very similar manner. For the 3' transgene, PCRs were done to produce a blunt 5' and a 3' containing NotI. The 5' transgene containing the P2A sequence was then excised with ClaI and SmaI. Corresponding inserts were then ligated into pRRV-S1-yCD2-P2A backbone cut with ClaI and NotI and gel extracted at 10.7 kb.

Cell Culture

293T human embryotic kidney cells (ATCC-CRL-3216), U87 (ATCC-HTB-14), and TU2449 cells were grown in DMEM (Corning Cellgro Ref# 10-0130-CV). PC3 human adenocarcinoma (ATCC-CRL-1435) were grown in RPMI (Corning Cellgro Ref# 10-040-CV). TU2449 mouse glioma cell lines[12] were provided by Dr. Matthias Renner and grown in DMEM. All media was supplemented with 10% FBS (Hyclone) and 1% Pen-Step.

Viral Production

Viruses were produced on 293T cells by calcium-phosphate mediated transfection, as previously described. Functional viral titers were calculated by transduction of U87s at various volumes, then treatment with AZT 24-hours later. Quantitation was done by either FACs in the case of either emd, or qPCR in the case of yCD2 or TKO.

Transduction

Cells were transduced with an MOI of 0.05. 4 ug/mL polybrene was supplemented into the media to promote transduction. Cell cultures were grown out for 14 days before analysis to assure complete transduction.

FACs analysis

Cells were analyzed by a BD Biosciences FACs Canto II. Negative controls were run and gated for the live population of cells, 10,000 of these samples were then run for emd+ or Stb+ fluorescence. Untransduced negative control cells were gated in the lower quadrant of the emd-Stb axises. Transduced cells were then run and analyzed for percent population and MFI by FlowJo (www.flowjo.com).

Genomic DNA/RNA Extraction

Genomic DNA extraction kit was provided by Qiagen DNeasy Blood and Tissue Kit (Qiagen Cat# 69506. Cells were either processed directly or frozen at -80C before processing. RNA was isolated by Aurum total RNA minikit (BioRad Cat# 7326820) from 10cm plates directly with the lysis buffer. Both gDNA and RNA isolations were done according to the kit manufacture's protocol.

qPCR

10 ng-1 µg of RNA was reverse-transcribed to cDNA utilizing Transcriptor First Strand cDNA Synthesis Kit (Roche Applied Sciences, 04379012001) following the manufacturer instructions. Primers and probes were designed from Roche's Universal Probe Library. Primers for the genes were synthetized at Valuegene Inc. Quantitative PCR relative expression experiments were performed on a LightCycler 480 Real-Time PCR System (Roche), and data was further analyzed with LightCycler 480 Software release 1.5.0. with 1-10 ng of sample in a total of 20 µL of reaction mix consisting of 10 µM UPL probe, 20 µM each of forward and reverse primers, and 20 µM 2X-LightCycler 480 Probes Master Mix. Triplicate experimental samples were paired using the all-to-mean pairing rule ΔCt value calculation with three housekeeping genes run in triplicate for advanced relative quantification.

Viability Assay

Viability assays were done with Promega CellTiter 96® AQ_{ueous} One Solution Cell Proliferation Assay (Cat#G3580). Cells were split into 2x10^3 cells per well on a 96-well plate and treated with prodrug one day after seeding. Media was removed from wells before addition of fresh media containing 20uL assay solution and 100uL media. Plates were then analyzed in a BioTek Synergy H1 Hybrid Reader at 490 nm. Plates were analyzed on days 3, 6, and 8 for TU2449 cells and days 3, 6, and 9 for U87 cells. Fro each day, time points were taken every half hour up to 4 hours.

Western Blot

Western Blots were done using whole cell lysate from cultured cells 21 days post-transduction. Wells were loaded with between 15-90ug/well, depending on abundance of protein. Antibodies used were cytosine deaminase antibody from Thermo Scientific (Cat# PA1-85365) and mGM-CSF from R&D Systems (Cat# AF-415-NA). Beta-Actin controls were from Santa Cruz (Cat#sc-47778). Secondary antibodies used were Rabbit Anti-Goat IgG H&L (HRP) (Cat#ab6741) to conjugate mGM-CSF and Rabbit anti-sheep IgG H&L (HRP) (Cat#ab97130) to conjugate CD,

both from abcam. Primary antibody dilutions were done at 1:500 and secondary antibodies at 1:2000. Membranes were blocked with 5% milk in TBS. Primary antibodies were incubated overnight at 4C in TBS supplemented with 0.1% Tween and 5% milk. Secondaries were incubated at room temperature for 1 hour in 5% milk T-TBS. Beta-Actin antibody was only incubated at RT for 1 hour as the antibody itself is already conjugated to HRP.

Intracellular Staining

Intracellular staining for CD was done by fixation of TU2449s in 4% paraformaldehyde, then permeation of the cellular membrane by 0.1% Triton. Cells were then stained with anti-Toca CD provided by Tocagen. Secondary staining was done with goat anti-mouse IgG (H+L)-Alexa 488 from Thermo (Cat#A-11001). Cells were then analyzed by FACs as described above. Controls were run either without primary antibody or without both primary and secondary antibody. Two washes with staining buffer BD Pharmigen (Cat#554656) were carried out between each step.

mGM-CSF ELISA

mGM-CSF ELISA was carried out with Biolegend mouse GM-CSF ELISA MAX Standard (Cat#432201). Supernatant was removed 2 hours before harvesting for analysis and replaced with fresh media. Supernatant was removed from 6-well plates, filtered, and frozen at -80C. When ready for analysis, SN was thawed and diluted into cell culture medium (DMEM) and diluted at x10, x100, and x1000. Protocol was then followed according to the Biolegend company's protocol. In short, 96-well plates were incubated overnight at 4C with primary antibody, then blocked one hour, standards and solutions were added for two hours, followed by 1 hour incubation with the Detection antibody, 30 minutes with Avidin-HRP, 15 minutes TMB Substrate Solution, and finally, Stop Solution (2N H_2SO_4). The plate was then read on BioTek Synergy H1 Hybrid Reader at 450 and 570 nm. Absorbance at 570 nm was subtracted from 450 nm. Dilutions that appeared on the standard curve were used as data points. Cell were counted after SN harvest in order to establish cytokine per cell levels. SN and cells were collected at days 4, 7, 11, 14, 18, and 25.

Results

Expression of SCP1-driven transgenes varies between cell lines.

In order to evaluate the ability of SCP1 to drive RRV transgenes in different cells lines, we transduced 293T, PC3, U87, and TU2449 cells at an MOI of 0.05 with both AC3-IRES-emd and AC3-S1-emd (Figure 1-2). Cells were cultured for 14 days to allow full transduction of the cell population to occur. After 14 days, vector copy numbers per cell and transgene RNA expression levels were assayed by qPCR, and transgene protein expression was measured by FACS. The emerald GFP (emd) transgene was expressed at higher levels when driven by the LTR, through IRES, in all cell lines studied, although the extent of the differences varied (Figure 1-2D). The lowest difference was in 293T cells, where SCP1 resulted in a roughly 15% decrease in mean fluorescence intensity (MFI), while in U87s the decrease in MFI was 95%. Despite the change in MFI, the vector copy number per cell remained relatively constant for both RRVs in U87 and PC3 cell lines, varying from 1-2 vectors per cell (Figure 1-2A). Interestingly, the vector copy number was significantly higher in 293T and TU2449 cells. In 293T cells the vector copy number increased up to 6 copies per cell for both RRVs. TU2449 cells transduced with AC3-emd had 8 vector copies per cell, which increased 50% to 12 copies per cell when transduced with AC3-S1-emd. Transgene RNA expression levels also varied between cell lines. When transduced with AC3-S1-emd, transgene RNA levels increased 30% and 55% in 293T and PC3 cells respectively, compared to transduction with AC3-emd (Figure 1-2B). Transgene RNA expression in U87 cells transduced with AC3-S1-emd actually decreased by about 25% compared to AC3-emd, while expression levels were equal in TU2449 cells. These results indicate that transgene expression is more dependent on the promoter driving expression than the number of vector copies per cell.

Use of SCP1 and P2A allows functional expression of two transgenes from a single RRV

After establishing that SCP1 can drive RRV transgene expression in U87 cells, we next asked whether this promoter, in combination with the oligonucleotide P2A, could be used to drive the expression of two transgenes from a single vector. We constructed AC3-S1 vectors containing both the emd and Strawberry (Stab) fluorescent proteins linked by P2A (Figure 1-3). Since P2A results in addition of 18 amino acids to the C-terminus of the upstream gene, and addition of a proline to the N-terminus of the downstream gene, vectors were designed with each fluorescent protein in both orientations, upstream and downstream, relative to the P2A sequence. This was done to investigate whether transgene expression levels were affected by linkage to P2A. There was no decrease in protein expression for transgenes in either orientation relative to P2A. In fact, as previously described, the proteins showed a very linear relationship (Figure 1-3). The P2A amino acid sequence causes ribosomal skipping, such that the proteins should be physically separated and expressed at equimolar levels[4,5].

We next engineered vectors expressing yCD2 and emd, in both orientations relative to P2A, in order to establish whether P2A had an effect on yCD2 function. Fully transduced U87 cells were exposed to varying concentrations of 5-FC and cell viability was measured by MTS (Figure 1-4B). IRES-driven yCD2 achieved higher levels of cell killing at lower concentrations of 5-FC (5uM to 50uM) as compared to SCP1-driven yCD2. At 100uM 5-FC, the cytotoxic effect of SCP1-driven yCD2 RRVs was similar to that of AC3-IRES-yCD2. Interestingly, there was a significant increase in cytotoxicity when yCD2 was positioned upstream from P2A compared to when it positioned downstream. This was true even at the highest tested concentration of 5-FC, 500uM. At this concentration, AC3-IRES-yCD2 had a much greater cytotoxic effect, potentially due to increased levels of converted 5-FC integrating directly into the RNA and DNA. Surprisingly, FACS analysis of the surviving cell population after 5-FC treatment revealed enrichment for emd positive cells, indicating that a portion of the RRV-transduced cell population can survive 5-FC treatment (Figure 1-4A).

Co-delivery of the cytokine, mGM-CSF, and the suicide gene, yCD2, from a single RRV

Once functionality of yCD2 had been established in both orientations of the SCP1-P2A vector, the cytokine mGM-CSF was cloned downstream of SCP1-yCD2-P2A since yCD2 in the 5' orientation showed favorable cytotoxicity. Also, mGM-CSF contains a signal peptide at the 5' end, so the additional proline attached by P2A could cause some changes in the peptide that could result in it being unable to secrete from the cell. Mouse TU2449 cells were transduced with AC3-IRES-yCD2, AC3-IRES-mGM-CSF, and AC3-SCP1-yCD2-P2A-mGM-CSF, and allowed 14 days to achieve full transduction. qPCR analysis showed a 20% increase in vector copy number in cells infected with AC3-IRES-yCD2 compared to AC3-SCP1-yCD2-P2A-mGM-CSF, whereas cells infected with AC3-IRES-mGM-CSF showed a 20% decrease in vector copy number compared to AC3-SCP1-yCD2-P2A-mGM-CSF (Figure1-5A). Transgene RNA levels showed the same increases and decreases of roughly 20% (Figure 1-5B). Western blot and intracellular staining revealed significantly lower levels of yCD2 expression when the transgene was driven off of SCP1 compared to IRES (Figure 1-5C and E). However, this decrease in protein expression had little effect on cytotoxicity at higher concentrations of prodrug. Cells expressing either IRES- or SCP1-driven yCD2 were less than 5% viable by day 9 at 5-FC concentrations exceeding 50uM (Figure 1-6A). Western blot analysis of intracellular mGM-CSF expression showed very high expression levels in TU2449 cells transduced with RRV-IRES-mGM-CSF, but could not detect mGM-CSF in cells transduced with RRV-SCP1-yCD2-P2A-mGM-CSF (Figure 1-5D). However, mGM-SCF was detectable in the supernatant of these cells by ELISA, although the expression was consistently 10-fold reduced compared to cells expressing IRES-driven mGM-CSF (1-6B). Importantly, mGM-CSF expression from SCP1 was more within the normal *in vivo* range (30-300 ng/10^6 cells/hr according to Serafini *et al*[13]).

Discussion

RRVs represent a promising new field for cancer therapy. However, the current protocol for RRV-mediated gene therapy involves the use of a single transgene and prodrug. This is in

contrast to current chemotherapy-based treatments, which entail the use of multiple drugs in order to combat the heterogeneity of the cancer mass. The high mutation rate of cancer cells can lead to the outgrowth of cells that are resistant to the effects of delivered transgenes. Combination therapy involving the delivery of multiple therapeutic payloads may therefore increase the efficacy of RRV-mediated cancer gene therapy. Here we developed novel RRVs capable of delivering two transgenes from a single vector, and as proof of concept, we utilized vectors expressing the suicide gene, yCD2, in combination with GM-CSF.

RRV transgene expression varied depending both on the cell line transduced and the promoter driving expression. Across cell lines, the number of vector copies per cell also varied, likely due to the availability of viral receptors. The MLV 4070A envelope binds to the inorganic phosphate transporter, Pit2. This envelope is subject to "superinfection resistance," a phenomenon in which a cell that is already infected with a certain virus cannot be re-infected by a virus bearing the same envelope. This is thought to result from sequestration of the viral receptor after viral entry. Therefore, in the case of 4070A, increased vector copy number could be caused by increased Pit2 expression on the cell surface. However, despite decreased expression of PiT2 in HEK293T cells compared to U87 cells[14], the vector copy number in 293Tcells infected with RRV expressing 4070A envelope, was higher than that in U87 cells. RNA expression levels do not necessarily correlate with surface protein expression, however, so the surface availability of PiT2, and/or the rate of receptor recycling, could still be greater in 293Ts than in U87s, accounting for the difference in vector copy number in these two cell lines. Other factors that could affect the vector copy number per cell include the availability of dNTPs for reverse transcription or the expression levels of intrinsic viral restriction factors.

While the number of viral integration events is a major determining factor in the expression level of RRV-delivered transgenes, expression is also dependent on the efficiency of transcription and translation of integrated viral genes. While transgene expression from the SCP1 promoter was very high in HeLa and 293T cells, our results show that protein expression of transgenes

driven by SCP1 varies depending on the cell line. This is likely a result of variable levels of transcription factors between cell lines. Because SCP1 is an artificial promoter, it was synthesized and tested in HeLa cells for functionality. Using a single cell line to optimize the promoter would lead to selection for that cell line's specific transcription factors to be favored by the artificial promoter. The side effects of such selection can be seen in the decreased SCP1-driven transgene expression levels in U87 cells. Achieving maximal transgene expression in cancer cells may not always be desirable, however. For instance, high levels of GM-CSF expression result in the conversion of monocytes to myeloid suppressor cells, *in vivo*[13]. As shown here, use of the SCP1 promoter decreased the expression of mGM-CSF to more optimal levels for therapeutic effect compared to IRES-driven GM-CSF. These sub-maximal levels of transgene expression could also be applied to other transgenes where maximum expression levels are not required or are detrimental.

Our data demonstrate that the oligonucleotide linker, P2A, can be used to produce equimolar amounts of two different transgenes from a single RRV. Although not necessary for the particular applications in this study, the ability to produce equimolar amounts of transgene could be useful in other situations. Regardless, the small size of P2A substantially increases the space available in the RRV for therapeutic transgenes. Ongoing research has found promising results from attaching the P2A sequence to the end of the envelope protein of RRVs. Linking transgenes to the envelope gene, via P2A, allows transgene expression to be driven by the LTR promoter. Unlike transgenes driven off of IRES, which are translated from both viral RNA splice forms, transgenes linked to the envelope gene would only be translated from one.

Despite our promising results with the P2A sequences, there are some potential drawbacks. Linking two genes via P2A results in modifications to the amino acid sequence of both genes—addition of 18 amino acids to the C-terminus of the upstream gene, and addition of a proline to the N-terminus of the downstream gene. These modifications could have dire effects on the protein function. In this study, yCD2 had slightly higher activity when oriented upstream of P2A.

The active site of yCD is much closer to the N-terminus than the C-terminus in the folded protein structure of yCD[15] (Supplementary 1-1). The proximity of the N-terminus to the active site may explain why the activity of yCD2 was slightly decreased when it was oriented downstream of P2A and thus had an additional proline at the N-terminus. These results demonstrate the importance of carefully characterizing proteins that are linked by P2A.

When compared to the IRES-driven yCD2, SCP1-driven yCD2, in either orientation relative to P2A, effected less cell death at lower concentrations of 5-FC (5 or 10 uM). However, at higher concentrations (50 and 100 uM) SCP1- driven yCD2 began to catch up to the killing curve of AC3-IRES-yCD2. Surprisingly, FACS analysis of the population of cells that survived 5-FC treatment, revealed enrichment for cells expressing the fluorescent marker, indicating that these cells had in fact been transduced, suggesting that even when fully transduced with yCD2, the presence of 5-FC is not enough to kill the entire population of cancer. This poses a problem, as recurrence is a main issue in cancer therapy, in which a small portion of the cancer mass survives and regrows into a tumor that is more resistant to the effects of the original treatment. Our results demonstrate and additional innovations or modifications may be required to achieve complete tumor cell killing by RRVs .

A promising candidate for the improvement of RRV-mediated cancer therapy is to combine it with immunotherapy. Thought to be the new frontier in cancer therapy, adding itself to the list of chemotherapy, radiotherapy, and surgery, immunotherapy involves training the body's own immune system to recognize cancer cells and mount an immune response. This strategy has already been applied to the field of oncolytic virotherapy; the Herpes Simplex Virus (HSV) was armed with GM-CSF to induce an immune response after lysis of melanoma cells[9,10]. This study, along with the fact that GM-CSF is one of the most commonly studied and applied cytokines in cancer therapies[16,17], made it an ideal transgene to combine with yCD2 in RRV. In this study, we demonstrated that delivery of mGM-CSF to TU2449 cells by RRV resulted in secretion of mGM-CSF. These levels of secreted mGM-CSF varied depending on the RRV

used, with AC3-IRES-mGM-CSF causing production of roughly 10 times the amount of mGM-CSF in the supernatant of infected cells as AC3-SCP1-yCD2-P2A-mGM-CSF. These results also demonstrated that the proline attached to the N-terminus of the signal peptide of mGM-CSF by P2A did not interfere with secretion of the protein, consistent with previously published results[5]. Additionally, our results confirm that genes linked by P2A are physically separated after translation as yCD2 was intracellularly localized. Most importantly, the levels of mGM-CSF were decreased by SCP1 expression as compared to IRES, but this decrease was actually advantageous, as it brought the levels of mGM-CSF into a range (30-300 ng/10^6 cells/hr[13]) that recruits APCs to the tumor mass rather than stimulating monocytes to mature into myeloid suppressor cells. Although the expression of mGM-CSF from AC3-IRES-mGM-CSF was significantly higher, it also did not exceed the 1500 ng/10^6 cells/hr mark that leads to overstimulation. Theoretically, after transduction of the tumor mass, GM-CSF expression will recruit monocytes to the tumor and those will mature into APCs. Once these APCs have established themselves in the tumor, 5-FC can be delivered and cause cells in the tumor to lyse, releasing tumor associated antigens. APCs, already having infiltrated the tumor, can now easily process and display these antigens to the immune system, which can seek out and destroy any remaining tumors presenting these antigens. The body's natural immune system is suppressed in the tumor environment, but with the introduction of an immune cytokine to the RRV, the immune system can now re-establish a foothold in the tumor mass and clear out any of the remaining cancer. The combination delivery of a suicide gene and immune modulating factor from a single RRV has potential to greatly increase the therapeutic efficacy of RRV-mediated gene therapy.

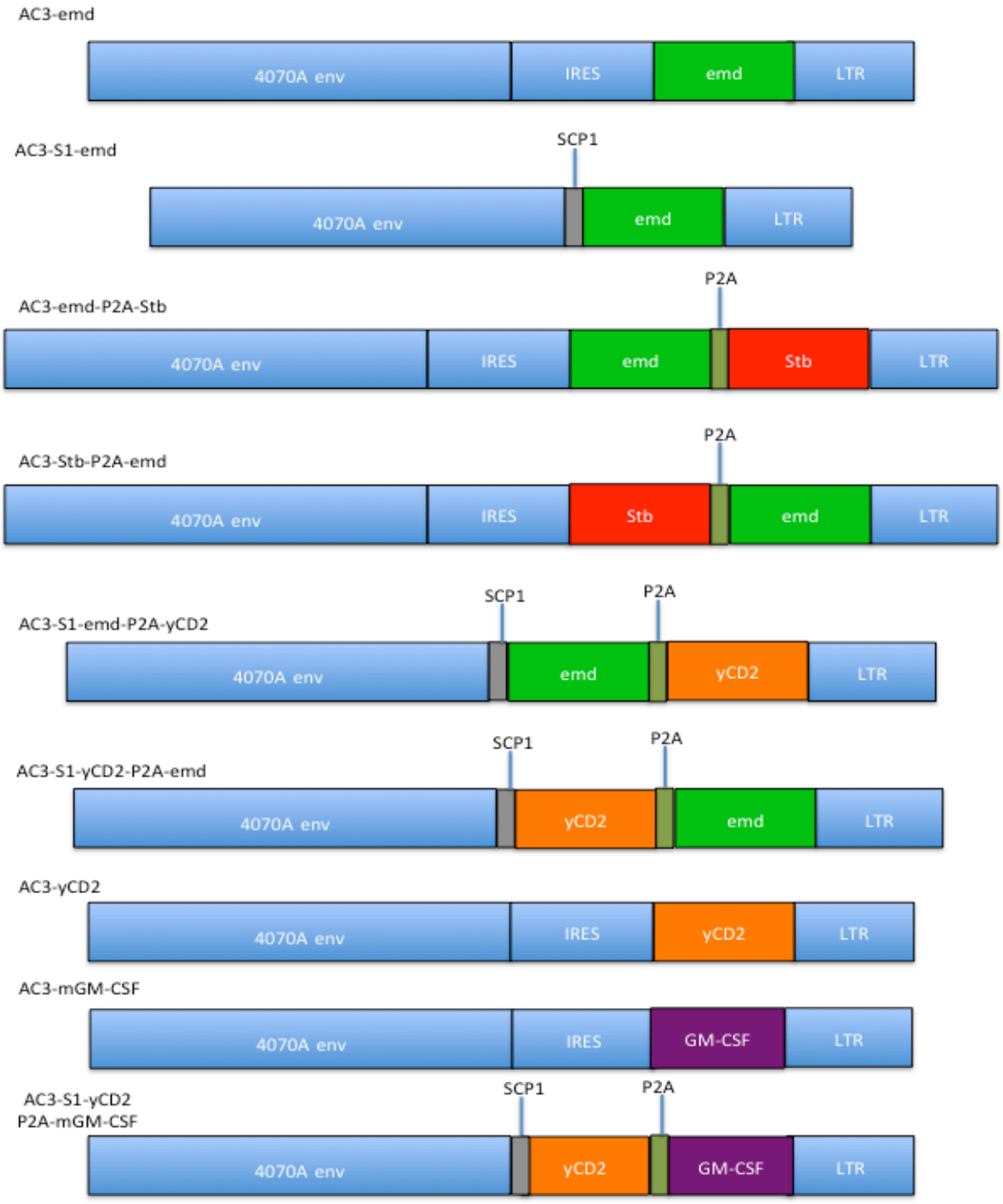

Figure 1-1
Vectors maps of different RRVs used in this experiment. The maps represent the envelope and transgene regions of RRV.

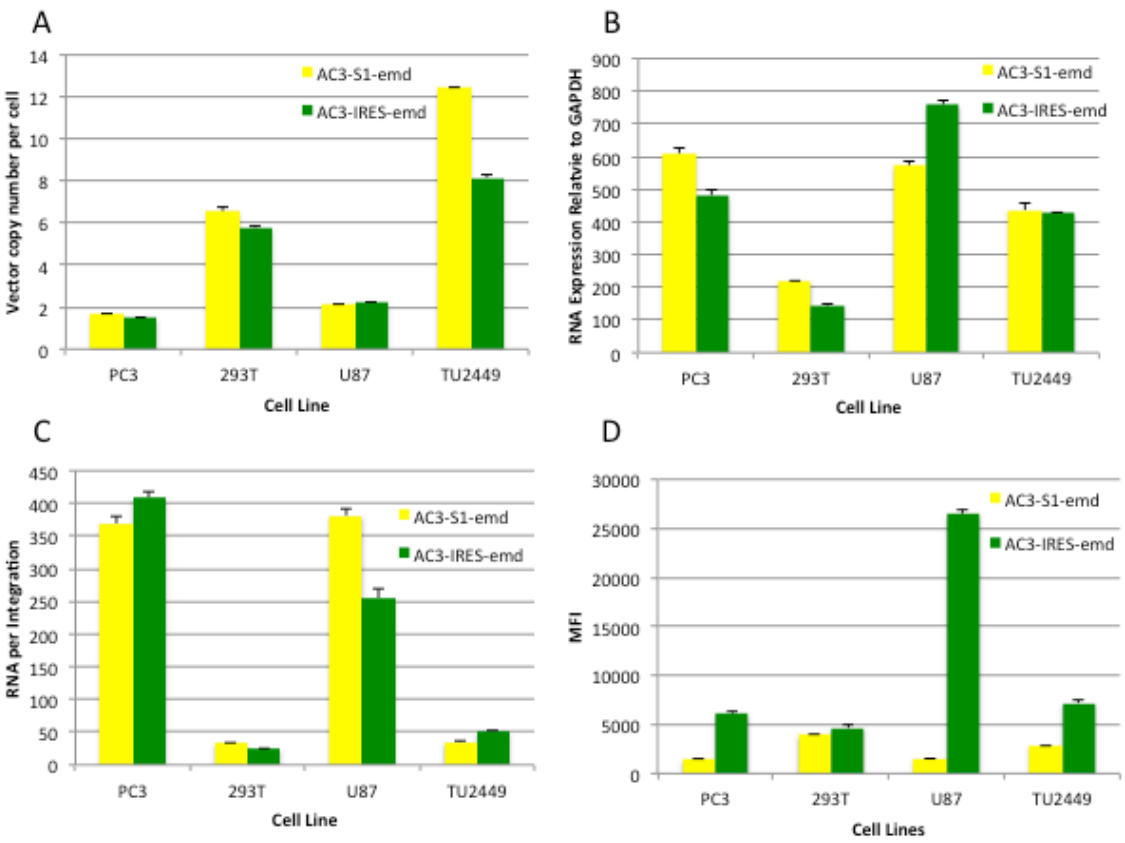

Figure 1-2
Vector copy number, RNA expression, and MFI were all taken more than 14 days after transduction with 0.05 MOI RRV. A) Vector copy number was measured by qPCR of the viral transgene emd and calculated by normalizing to GAPDH levels. B) RNA transgene expression of AC3-emd and AC3-S1-emd in different cells lines. RNA was reverse transcribed, analyzed by qPCR and compared relative to the amount of GAPDH RNA in each sample. C) Ratio of RNA expressed per viral copy. D) FACs analysis of the transgene expression by MFI.

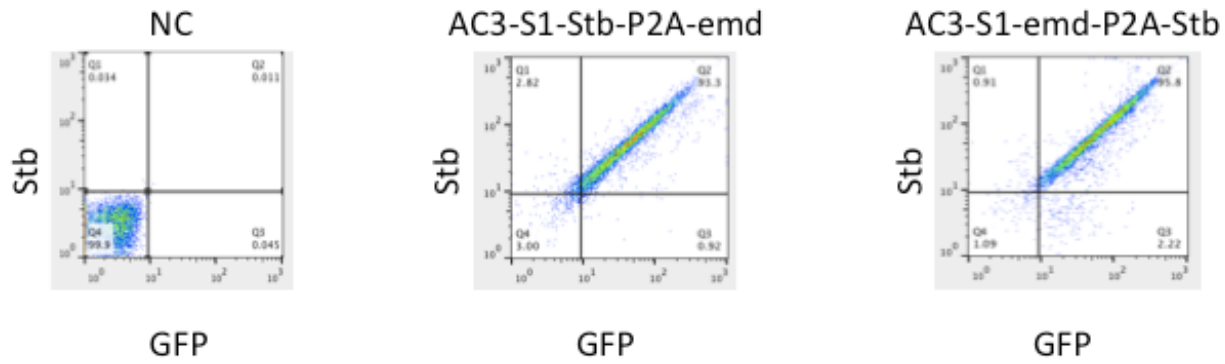

Figure 1-3
FACS analysis of SPC1-driven emd and Stb fluorescent proteins either oriented 5' or 3' of P2A to assess transgene expression and function in U87 cells 21 days post transduction.

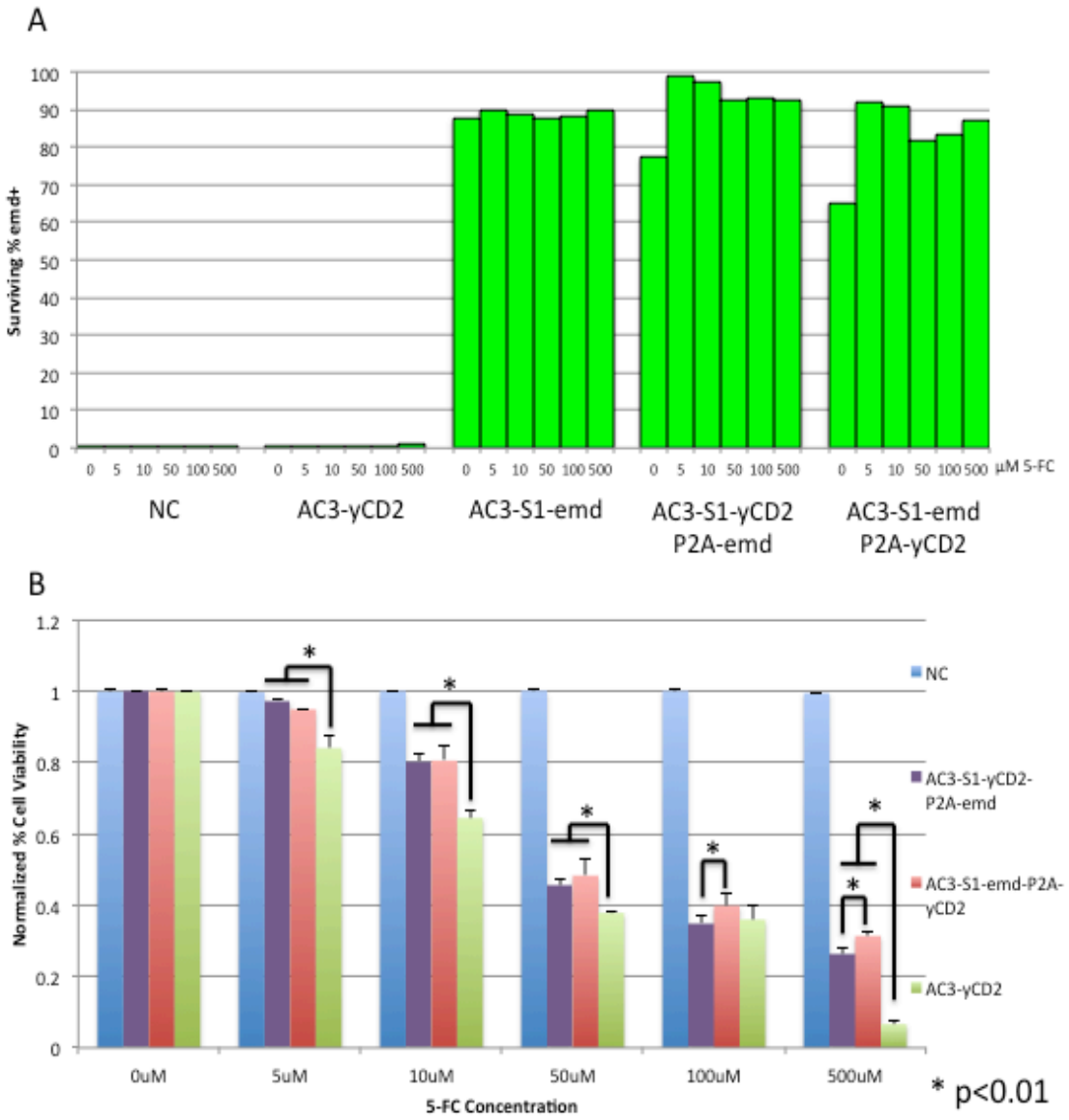

Figure 1-4
A) Percent population of surviving emd positive cells in U87 cells transduced with AC3-yCD2, AC3-S1-emd. AC3-S1-yCD2-P2A-emd, and AC3-S1-emd-P2A-yCD2 treated with 5-FC at varying concentrations. B) MTS cell viability assay of U87 cells transduced with AC3-yCD2, AC3-S1-yCD2-P2A-emd, and AC3-S1-emd-P2A-yCD2 9 days after treatment with varying concentrations of 5-FC.

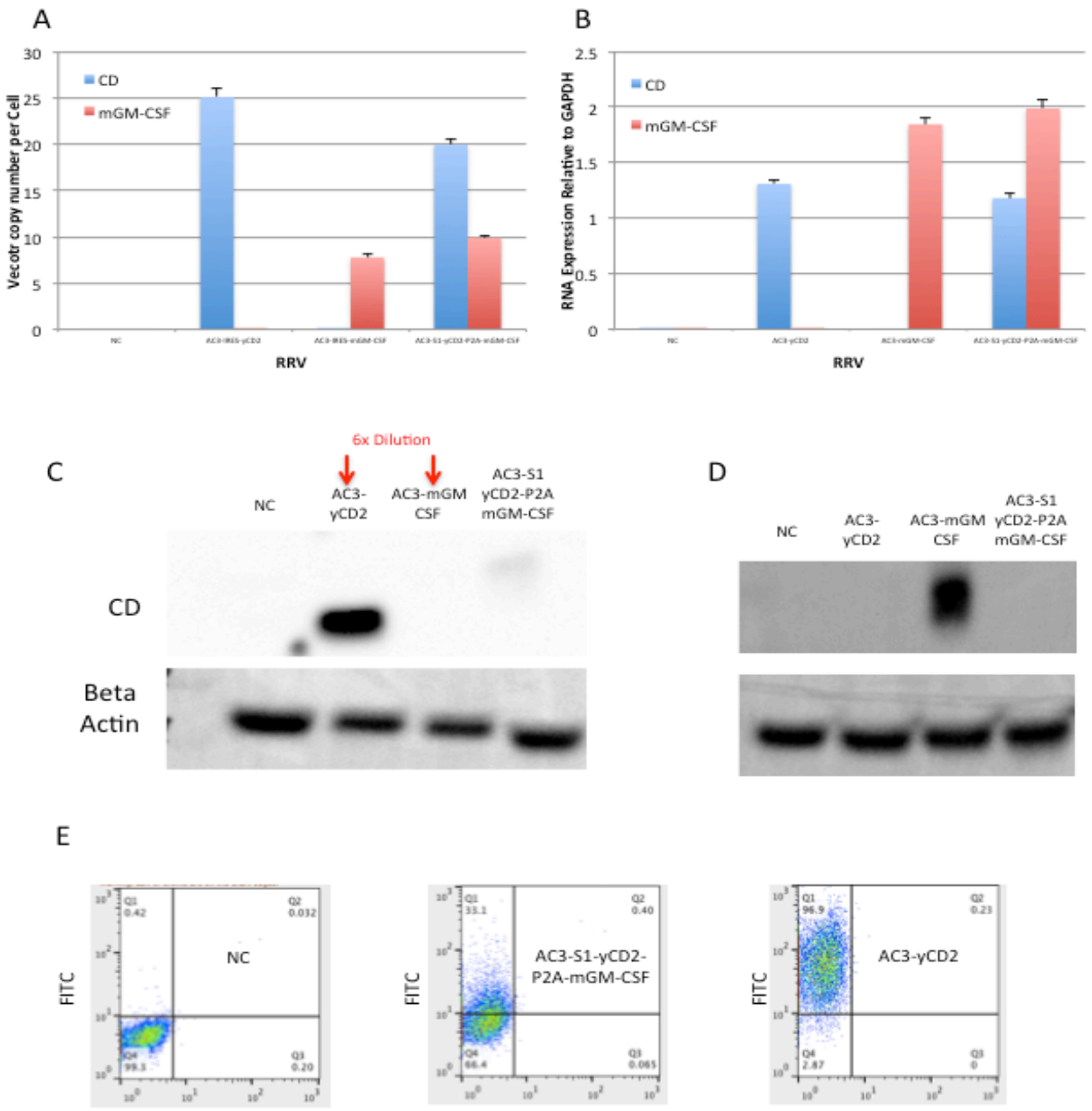

Figure 1-5
Proviral Vector copy number, RNA expression, and protein expression of AC3-yCD2, AC3-mGM-CSF, and AC3-S1-yCD2-P2A-mGM-CSF RRVs in TU2449 cells. A) Vector copy number was measured by qPCR of the viral transgenes yCD2 or mGM-CSF and calculated by normalizing to GAPDH levels. B) RNA transgene expression of different RRVs in TU2449 cell line. RNA was reverse transcribed, analyzed by qPCR and compared relative to the amount of GAPDH RNA in each sample. C) Western Blot for yCD in TU2449 cells transduced with the RRVs mentioned above. AC3-yCD2 and AC3-mGM-CSF were diluted 6x in these studies. D) Intracellular staining for yCD2 in AC3-yCD2 and AC3-S1-yCD2-P2A-mGM-CSF. Cell were fixed, permeabilized, and stained with primary and secondary antibodies, then analyzed through FACs.

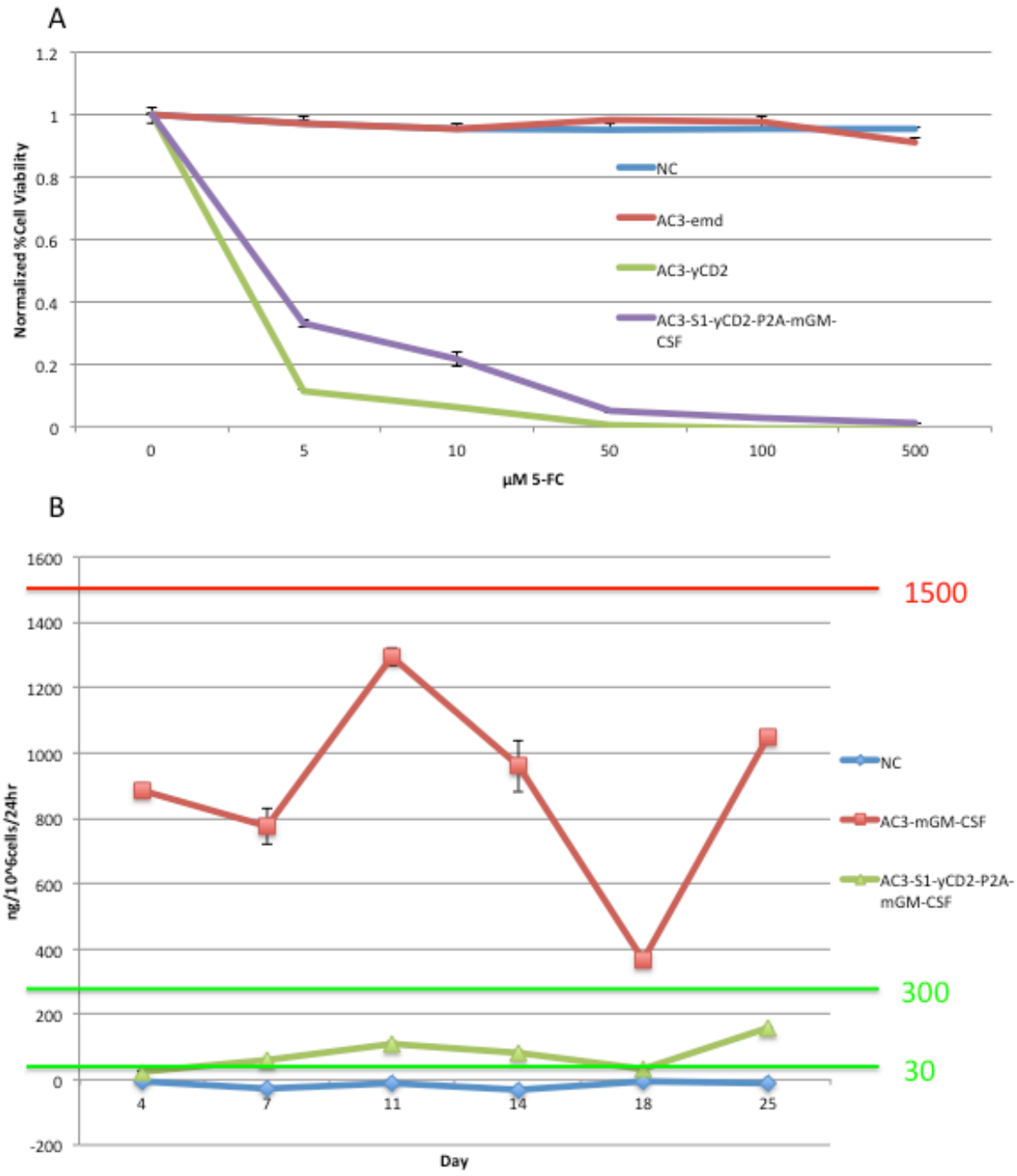

Figure 1-6
A) MTS cell viability assay of TU2449 cells transduced with AC3-yCD2 and AC3-S1-yCD2-P2A-mGM-CSF 8 days after treatment with varying concentrations of 5-FC. B) mGM-CSF concentrations in supernatant of TU2449 transduced by AC3-mGM-CSF and AC3-S1-yCD2-P2A-mGM-CSF. ELISA calculated levels were normalized to cell count and incubation time. Concentration 30, 300, and 1500 are marked to reference ideal therapeutic range of mGM-CSF.

Chapter 2: Delivery of Two Retroviral Replicating Vectors, Pseudotyped With Different Non-Interfering Envelopes, Increases Transgene Expression and Therapeutic Efficacy

Introduction

Retroviral Replicating Vectors (RRV) are capable of spreading throughout a tumor mass, as opposed to non-replicating vectors, which usually remain very close to the injection site and result in very low levels of tumor transduction[2]. One such virus, Toca 511, is currently under investigation in Phase I/II clinical trials for the treatment of advanced stage glioma (https://clinicaltrials.gov/; NCT01156584, NCT01470794, NCT01985256). Toca511 delivers the codon optimized yeast cytosine deaminase (yCD2) suicide gene, which acts by converting the non-toxic anti-fungal drug, 5-FC, into the chemotherapeutic agent, 5-FU. This conversion results in cell death via two main mechanisms: (1) inhibition of thymidylate synthase (TMS), which results in decreased intracellular pools of thymidine leading to DNA replication errors, and (2) at higher concentrations, integration into RNA and DNA. Most chemotherapeutic regimens involve the delivery of multiple drugs in order to combat the heterogeneous nature of most cancers. Although 5-FU is a potent anticancer agent, delivery of multiple therapeutic transgenes could increase the clinical efficacy of RRV-mediated cancer gene therapy. Delivery of multiple transgenes from a single RRV is complicated by “superinfection resistance,” a phenomenon common to many types of viruses. Cells already infected with RRV cannot be re-infected with an RRV expressing the same envelope protein. The current theory is that the viral envelope proteins on the surface of the virus, which bind specific membrane receptors on the cell surface, end up sequestering those viral receptor proteins once the cell has been infected, thereby inhibiting the entry of any new virus via the same viral receptor. This poses a problem to delivering two transgenes with the current RRV system, since RRVs bearing the same envelope protein but two different transgenes will not be able to infect the same cell, and thus each infected cell would still only receive one transgene.

Luckily, through genetic engineering, we can replace the envelope protein of the RRV with a different envelope protein that uses different viral receptors for cell entry. Toca511 expresses the MLV 4070A envelope of MLV, which binds the inorganic phosphate transporter, PiT2. By replacing this envelope protein, we can create RRVs that utilize different viral receptors and therefore are capable of cotransducing a single cell. This will bypass the problem of superinfection resistance, and allow for the delivery and expression of multiple transgenes to each cell in a tumor.

In this study, RRVs were pseudotyped RRV with four different envelope proteins: (1) 4070A, which binds PiT2, (2) Gibbon Ape Leukemia Virus (GALV) envelope, which enters through the inorganic phosphate transporter, PiT1, (3) 10A1 envelope, a variant of the MLV 4070A envelope, which can bind either Pit1 or Pit2, and (4) xenotropic murine leukemia virus-related virus (XMRV) envelope, which binds the XPR1 receptor. Pseudotyped RRVs expressing the emerald GFP (emd) and strawberry (Stb) fluorescent proteins were characterized for their ability to cotransduce different cell lines. Based on these results, we selected optimal candidates for cotransduction and further analyzed the vector copy numbers, RNA expression levels, transgene stability, and protein expression levels for these vectors. Finally, a functional analysis of two different RRVs with the optimal combination of envelope proteins containing two suicide transgenes was carried out to establish how well this combination therapy would work *in vitro*.

Materials and Methods

Cloning

GALV envelope was cloned into the RRV pAC3-emd to produce pGC3-emd as previously described[18]. This virus underwent selection and analysis to silently mutate out a splice sequence within GALV. 10A1 envelope was cloned into pAC3-emd by cutting 5' at the SalI site and 3' at the NgoMIV site of pTZ3-emd, cutting 5' at the NgoMIV site and 3' at the MluI site of a synthetic sequence provided by Operon to complete the 10A1 envelope sequence, and cutting

at 5' MluI and 3' SalI of the original pAC3-emd plasmid, and ligating all three together. XMRV envelope was provided by Dr. Sam Chow and ligated into pAC3-emd using 5' SphI and 3' BssHII sites from the envelope to produce XC3-emd. Fluorescent protein Strawberry (Stb) was swapped out for emd by PCR products that created an MluI site 5' of IRES and a NotI site 3' of Stb from a construct provided by UCLA Vector Core that already contained an IRES-Stb sequence. This was then ligated with all four different envelope plasmids cut with the respective enzymes. pAC3-S1-Tet-ON was cloned from the original pAC-S1-emd, where a Tet-ON PCR fragment containing a 5' HpaI site and a 3' NotI site replaced the emd transgene. pGC3-Tight-emd was cloned by Tight-GFP PCR containing 5' MluI and 3' NotI sites replacing SCP1-emd in pGC3-S1-emd.

Cell Culture

HeLa human adenocarcinoma cells (ATCC-CCL-2) and WiDr human adenocarcinoma cells (ATCC-CCL-218) were grown in MEM Corning (Cellgro Ref# 15-010-CV). U87 human glioblastoma(ATCC-HTB-14) were grown in DMEM (Corning Cellgro Ref# 10-0130-CV). PC3 human adenocarcinoma (ATCC-CRL-1435) were grown in RPMI (Corning Cellgro Ref# 10-040-CV). All media was supplemented with 10% FBS 10% FBS (Hyclone) and 1% Pen-Step.

Viral Production

Viruses were produced on 293T cells by calcium-phosphate mediated transfection, as previously described. Functional viral titers were calculated by transduction of U87s at various volumes, then treatment with AZT 24-hours later. Quantitation was done by either FACs in the case of either emd or Stb, or qPCR in the case of yCD2 or TKO.

Transduction

Cells were transduced in triplicate with an MOI of 0.05. 4 ug/mL polybrene was supplemented into the media to promote transduction. Sequential transductions were given 7-10 days to fully transduce the cell population and primary transductions were monitored by FACs to ensure

complete transduction. Simultaneous transductions were done within seconds of each other. Cells were split 10% into new wells every 3-4 days and remaining cells were analyzed by FACs.

FACs analysis

Cells were analyzed by a BD Biosciences FACs Canto II. Negative controls were run and gated for the live population of cells, 10,000 of these samples were then run for emd+ or Stb+ fluorescence. Untransduced negative control cells were gated in the lower quadrant of the emd-Stb axises. Transduced cells were then run and analyzed for percent population and MFI by FlowJo (www.flowjo.com).

Passaging

Cells were transduced in triplicate with an MOI of 0.05. 4 ug/mL polybrene was supplemented into the media to promote transduction. Each day before passaging, naïve U87 cells were split onto a new 6-well plate for the next passage and media was replaced and incubated for 24-hours on the previous passage. On the day of passage, 10% of supernatant was transferred to naïve cells supplemented with polybrene. Triplicates were combined for gDNA isolation.

Genomic DNA/RNA Extraction

Genomic DNA extraction kit was provided by Qiagen DNeasy Blood and Tissue Kit (Qiagen Cat# 69506. Cells were either processed directly or frozen at -80C before processing. RNA was isolated by Aurum total RNA minikit (BioRad Cat# 7326820) from 10cm plates directly with the lysis buffer. Both gDNA and RNA isolations were done according to the kit manufacture's protocol.

qPCR

10 ng-1 µg of RNA was reverse-transcribed to cDNA utilizing Transcriptor First Strand cDNA Synthesis Kit (Roche Applied Sciences, 04379012001) following the manufacturer instructions. Primers and probes were designed from Roche's Universal Probe Library. Primers for the genes were synthetized at Valuegene Inc. Quantitative PCR relative expression experiments were performed on a LightCycler 480 Real-Time PCR System (Roche), and data was further

analyzed with LightCycler 480 Software release 1.5.0. with 1-10 ng of sample in a total of 20 µL of reaction mix consisting of 10 µM UPL probe, 20 µM each of forward and reverse primers, and 20 µM 2X-LightCycler 480 Probes Master Mix. Triplicate experimental samples were paired using the all-to-mean pairing rule ΔCt value calculation with three housekeeping genes run in triplicate for advanced relative quantification.

Viability Assay

Viability assays were done with Promega CellTiter 96® AQ_{ueous} One Solution Cell Proliferation Assay (Cat#G3580). Cells were split into 2x10^3 cells per well on a 96-well plate and treated with prodrug one day after seeding. Media was removed from wells before addition of fresh media containing 20uL assay solution and 100uL media. Plates were then analyzed in a BioTek Synergy H1 Hybrid Reader at 490 nm. Plates were analyzed on days 3, 6, and 8 for TU2449 cells and days 3, 6, and 9 for U87 cells. Fro each day, time points were taken every half hour up to 4 hours.

Results

Sequential cotransduction in multiple cells lines using pseudotyped RRVs

In order to investigate the effect of envelope pseudotyping on cotransduction, multiple cell lines were sequentially transduced with each envelope pseudotyped RRV expressing either emd or Stb (Table 2-1). After initial full transduction was achieved, as monitored by FACS, cells were exposed to a second RRV, expressing the other fluorescent protein. For instance, cells were initially transduced with RRV expressing the 4070A envelope and emd transgene, and then, once the entire cell population was emd positive, were transduced with RRV expressing the GALV envelope and Stb transgene. Viral spread was monitored by FACS every 3-4 days. Different cell lines showed different patterns of cotransduction interference. HeLa cells were unable to be fully transduced by single RRV transduction, other than in the case of 10A1-pseudotyped RRV (TC3) (Table 2-2, Supplementary 2-1). Cotransduction with a second virus in

all cases resulted in either inhibition (no expression of second transgene) or incomplete cotransduction (less than 100% transduction with second transgene). In all cases where the second virus expressed the same envelope as the first, inhibition occurred. This was also the case when 4070A-RRV (AC3) challenged cells already transduced with TC3. All other combinations resulted in incomplete cotransduction. In WiDr cells pretreated with AC3, secondary transduction with GALV-RRV (GC3) or XMRV-RRV (XC3) resulted in incomplete cotransduction, while challenge with AC3 or TC3 resulted in complete inhibition. Conversely, when WiDr cells were pretreated with GC3, secondary transductions with all other pseudotyped RRVs, except GC3, resulted in full cotransduction. Pretreatment of WiDr cells with TC3 resulted in full cotransduction with XC3, although at a slower rate, incomplete cotransduction with GC3, and full inhibition against AC3 and TC3 challenges. Finally, XC3 pretreated WiDr cells showed complete cotransduction when challenged with AC3 and TC3, incomplete cotransduction when challenged with GC3, and inhibition against re-challenge with XC3. PC3 cells had different interference patterns from both the HeLa and WiDr cell lines. Pretransduction with AC3 lead to complete cotransduction by either GC3 or XC3, incomplete cotransduction with TC3, and inhibition against re-challenge with AC3. Pretreatment of PC3 cells with GC3 allowed for complete cotransduction by TC3 and XC3, but, interestingly, incomplete cotransduction by both AC3 and GC3. TC3 pretransduction led to complete cotransduction with XC3, slowed cotransduction with GC3, and complete inhibition of both AC3 and TC3. XC3 pretransduced cells showed slowed cotransduction with GC3, complete cotransduction with AC3 and TC3, and inhibition against rechallenge with XC3. U87s proved to be the most capable of achieving full cotransduction. In general, each pseudotyped-RRV was able to fully cotransduce cells that were pretransduced with RRV expressing a different pseudotype. However, cells pretransduced with AC3 slowed the spread of secondary transduction by TC3, and cells pretransduced TC3 inhibited secondary transduction by AC3. As anticipated, and consistent with results in other

cell lines, pretransduction by a certain pseudotyped-RRV inhibited cotransduction by RRVs expressing the same envelope.

Simultaneous cotransduction in multiple cell lines using pseudotyped RRVs

To further investigate how these envelope pseudotypes interact, cells were exposed to two RRVs simultaneously. In HeLa cells, all combinations of RRVs failed to achieve full cotransduction (Table 2-2, Supplementary 2-1). In WiDr cells transduced with two RRVs expressing the same envelope, incomplete cotransduction occurred in all cases. Additionally, cotransduction by AC3 and TC3 also yielded incomplete cotransduction. Exposure to TC3 and XC3 resulted in full cotransduction. With all other combinations, results were variable depending on the pairing of the envelopes with the fluorescent transgenes. In PC3 cells, complete cotransduction was achieved only by the simultaneous exposure to TC3 and XC3. Cotransduction with AC3 and XC3 or GC3 and XC3 gave variable results. All other combinations showed incomplete cotransduction. U87s, again, proved most susceptible to cotransduction. Treatment of U87s with XC3, TC3 or GC3 in combination with any other pseudotype resulted in full cotransduction, with the exception of AC3 and TC3, which showed an interference pattern. Although some interference is expected between AC3 and TC3, since they both enter through the PiT2 receptor, the effect was larger than expected given that TC3 can also utilize PiT1 for cellular entry. AC3 seemed to confer superinfection resistance, as around 10% of the population was transduced only with the fluorescence protein carried by AC3. AC3 and GC3 showed no interference between each other when simultaneously cotransduced. Finally, exposure to RRVs expressing the same envelope, which inhibited cotransduction when done sequentially, resulted in incomplete cotransduction when done simultaneously. A small population of the exposed cells was successfully cotransduced, while the remaining population expressed only a single transgene. The ratios varied depending on the envelope in question. Nearly 40%-50% of cells exposed to two AC3-RRVs were cotransduced, while 25%-40% of the cells were singly transduced. Transduction with two GC3-

RRVs resulted in a much higher percentage of the population being cotransduced, about 90%, while singly transduced cells accounted for only 10% of the population. For cells exposed to two TC3-RRVs, cotransduction efficiency ran between 50%-70%, while cells exposed to two XC3-RRVs were cotransduced 40%-50% of the time (Supplementary 2-1).

Transgene expression in single transduction by pseudotyped RRVs

In order to compare the transgene expression levels, cells were transduced with pseudotyped-RRVs expressing the emd transgene, and the mean fluorescence intensity (MFI) in U87 cells was compared as a measure of emd expression level. Compared to cells infected with AC3-emd, those infected with TC3-emd had the greatest increase in MFI; emd expression was roughly 3 times higher in these cells (Figure 2-1). Expression levels in cells transduced with GC3-emd were comparable to those in AC3-emd transduced cells, while cells infected with XC3-emd showed a 50% decrease compared to AC3-emd.

RRV-TC3 is cytotoxic in U87 cells.

An unexpected side effect of TC3 transduction was significantly slowed growth of U87 cells (Figure 2-2). An MTS assay following treatment of U87 cells with different MOIs of both AC3 and TC3 showed that cell viability decreased in a dose-dependent manner with increasing TC3 MOI, although no such decrease was observed in cells transduced with AC3 (Figure 2-2C). Transduction with TC3 had no effect on the viability of PC3 and WiDr cells (Supplementary 2-2). The cytotoxic effect in U87s was confirmed by propdium iodine (PI) staining and FACS analysis which showed increased uptake of PI in TC3 transduced cells at both MOIs compared to both untransduced cells and cells transduced with AC3 (Figure 2-2B).

Characterization of cells cotransduced with AC3-RRV and GC3-RRV

Since TC3 was cytotoxic in U87s and transgene expression in cells transduced with XC3 was reduced expression, further cotransduction experiments were focused on the use of AC3 and GC3. We measured the vector copy number per cell, using primer/probes specific to the transgene, as well as levels of transgene RNA and protein expression, by qPCR and FACS.

U87s singly transduced with AC3-emd, AC3-Stb, or GC3-Stb were compared to those cotransduced with AC3-emd and AC3-Stb or AC3-emd and GC3-Stb. As expected, cotransduction with two AC3-RRVs resulted in decreased vector copy number per cell, and well as reduced transgene RNA and protein expression (Figure 2-3A). Interestingly, cotransduction with AC3-emd and GC3-Stb significantly increased vector copy number for AC3-emd, while GC3-Stb remained equivalent. Expression of the transgene RNA also increased significantly for AC3-emd, while RNA expression levels of GC3-Stb decreased by about 10% as compared to single transductions (Figure 2-3B). MFI levels showed similar results, as levels decreased with same-envelope cotransduction, but increased for AC3-emd and decreased slightly for GC3-Stb, as compared to single transduction controls (Figure 2-3D).

Transgene stability of 4070A-GALV envelope pseudotype cotransductions

To measure the transgene stability of pseudotyped-RRVs during cotransduction, we infected U87 cells with either AC3-emd and GC3-Stb, or AC3-Stb and GC3-emd. Viral supernatants were serially passaged onto naïve cells every 3-4 days. FACS analysis of viral spread revealed that loss of transgene expression occurred more rapidly in cotransduced cells than in those infected with a single vector (Figure 2-4A). PCR analysis of integrated virus in genomic DNA confirmed that transgene drop out occurred in earlier passages in cotransduced cells (passage 9-11) compared to in cells infected with a single virus (passage 14-16) (Figure 2-4B).

Cotransduction of suicide genes yCD2 and TKO using vectors MLV and GALV

To examine the effect of cotransduction on the cytotoxic effect of RRVs carrying suicide genes, we utilized an AC3-RRV and GALV (GS4) virus expressing the suicide transgenes yCD2 and TKO. As TKO is a larger transgene (1.1 kb), it was driven by the SCP1 promoter as previously described. Cells were transduced with either single AC3-yCD2, AC3-S1-TKO, or GS4-S1-TKO or cotransduced with AC3-yCD2 and AC3-S1-TKO or AC3-yCD2 and GS4-S1-TKO. After treatment with 5-FC or ganciclovir (GCV) prodrugs, cell viability was measured by MTS at days 3, 6, and 9. Cell killing was slightly higher in cells cotransduced with two AC3-RRVs, compared

to those transduced with a single transgene. However, when cells were cotransduced with two viruses with non-competing envelopes, there was significantly more cell death compared to singly transduced cells at the same prodrug concentrations (Figure 2-5, Supplementary 2-3).

Discussion

In these experiments, we investigated the interactions of RRVs pseudotyped with four different envelope proteins. During sequential cotransduction, the interference patterns of the pseudotyped RRVs varied between cell lines. Additionally, we found that TC3 inhibited growth of U87 cells, although other cells lines were unaffected, and transgene protein expression from XC3-RRVs was decreased. Based on these results, and the non-interference between AC3 and GC3 RRVs, combination AC3-GC3 treatment is a prime candidate for dual transgene delivery. Cotransduction with these two RRVs actually increased transgene vector copy number, RNA expression, and protein expression for the transgene from the AC3 vector. Using these vectors to deliver two suicide genes, yCD2 and TKO, resulted in increased cell killing *in vitro*. Sequential cotransduction with two pseudotyped RRVs yielded differing levels of single and double positive populations, depending on the cell line used. Variations in viral receptor availability among different cell lines may explain the disparate results. However, incomplete cotransduction was occasionally observed in cells that were cotransduced with two RRVs with non-interfering envelopes. For instance, in WiDr cells, incomplete cotransduction occurred with GC3 and XC3 RRVs, suggesting that receptor sequestering may not be the reason for incomplete cotransduction, as GC3 uses the Pit1 receptor for entry and XC3 utilizes XPR1[19]. Antiviral immune factors or other host proteins may also play a role in susceptibility to cotransduction and may vary among cell lines.

In PC3, pretreatment with AC3 and challenge with GC3 or XC3 RRVs resulted in full cotransduction, but challenge with TC3 only achieved partial cotransduction. These results suggest that TC3 is unable to completely transduce PC3 cells by utilizing Pit1 receptors, as is

seen in U87 cells. Interestingly, pretreatment with GC3 allowed for partial cotransduction with the same envelope, suggesting there might be an overabundance of Pit1 receptors on PC3 cells. Pretreatment with GC3 and XC3 lead to slowed cotransduction rates of AC3 and GC3 challenge, respectively. This again suggests that other factors aside from receptor availability may be at work in superinfection resistance.

Results from simultaneous administration of two RRVs to WiDr and PC3 cell lines were inconsistent and varied depending on the combination of transgene and envelope. These experiments should be repeated in order to establish if the results are real and whether the transgene has an effect on cotransduction efficiencies. Despite the fact that envelopes of the same pseudotype inhibited each other when sequentially transduced, they were able to achieve varying percentages of cotransduction when applied simultaneously. GC3-GC3 cotransductions were around 90%, while AC3-AC3 was roughly 50%. According to BioGPS (http://biogps.org), U87 cells express significantly higher levels of PiT1 RNA than most cell lines, while expressing a median level of PiT2 RNA[14]. This may explain why GC3 had higher cotransduction efficiency than AC3 in U87 cells, as more Pit2 receptor is available for vector entry. Vector copy number analysis supports this theory, as copies of GC3-Stb were nearly 50% increased in U87 cells compared with AC3-Stb. As the variability of both sequential and simultaneous cotransduction between cell lines suggests, there are many factors, even outside of receptor expression levels, that can affect the ability of different pseudotypes to cotransduce. Even envelopes with no common target receptors can have an effect on each other in certain cell lines.

Studies of the transgene expression levels of the different pseudotypes in U87 cells also revealed differences in MFI values. XC3-emd expressed the lowest MFI intensity, possibly due to receptor levels of XPR1 or other intrinsic mechanisms mentioned above specific to the XMRV envelope. AC3 and GC3 had relatively equal MFIs, while 10A1 MFI was double that of both AC3 and GC3. This makes sense, as 10A1 is capable of entering the U87 cells through both PiT1 and PiT2 receptors, so there should be an increase in vector copy number, and therefore,

protein expression. However, TC3 proved to inhibit U87 cell growth. Although it was found that after initial transduction, U87 cells eventually regained their normal growth rates, it seems that transduction of TC3 can actually cause cell death, which is counterproductive to the suicide gene therapy, as the cells are required to stay alive to produce more RRV to transduce new dividing cells. The cause of this cytotoxicity may be due to the viral envelopes sequestering the PiT1 and PiT2 receptors to the point that the cell is starved of inorganic phosphate. Slight growth inhibition was noticed with AC3-GC3 cotransduction, but not to the extent of TC3. 10A1 also attaches to a different site on PiT1 as GALV, so it is possible that the binding site of 10A1 is more restrictive to the functioning of PiT1. Another theory is that the transgene load itself is cytotoxic to the cell. If the cell is too busy making the transgene, it may starve itself of essential nucleotides and proteins, causing apoptosis.

Despite the reduced transgene expression and increased cytotoxicity observed in U87 cells, 10A1 and XMRV may still be candidates for pseudotyping RRVs used to cotransduce other cell types. As was shown with the initial cotransduction experiments, interference patterns can vary greatly, depending on the cell line used. Cells with higher surface expression levels of XPR1 may be more amenable to transduction with XC3. Furthermore, TC3 was not cytotoxic to PC3 and WiDr cells. In this case, 10A1 could be an ideal candidate for use with XC3, as full cotransduction was observed among these two cell lines with this combination of RRVs in both sequential and simultaneous cotransductions.

When cells were cotransduced with AC3 and GC3 RRVs, vector copy number per cell, as well as transgene RNA and protein expression increased, at least for the transgene carried by the AC3 virus. Although these results were unexpected, they illustrate that, should the focus of a particular gene therapy be to maximize transgene expression, cotransduction with AC3 and GC3 can lead to increased transgene expression. The current theory is that when cells are cotransduced with both RRVs, these cells will produce both envelope proteins 4070A and GALV. This means that as the RRVs mature into the second generation of virus, this RRV will

have both 4070A and GALV envelope proteins expressed on the surface, meaning the new generation can enter cells via either the PiT1 or PiT2 receptors. Along with this chimeric envelope protein expression, RRVs carry two RNA templates within their capsid for reverse transcription during the next round of replication. This would mean that, if both AC3 and GC3 templates were transcribed and packaged equally, 25% of the population would contain homologous AC3-AC3 templates, 25% of the population would be homologous GC3-GC3, and 50% of the population would contain one AC3 and one GC3 template. In this population, AC3 templates, now armed with the ability to infiltrate the cells with the GALV envelope through the PiT1 receptor, would replicate to higher vector copy numbers per cell, thereby increasing RNA and protein expression. As mentioned earlier, PiT1 is more abundant in U87 cells than other cell lines. Different cell lines with different PiT1/PiT2 expression could result in different results. For example, a cell line with a higher level of PiT2 receptor could show an increase in transgene expression carried by GC3, as this template would now have more access to the cells after the first transduction cycle through the Pit2 receptor.

Despite the fact that cotransduction with AC3 and GC3 increases transgene expression in U87 cells, the combination of these two RRVs leads to a faster rate of transgene dropout in both constructs. This puts it at a disadvantage to single transductions, that can retain the transgene for more passages and therefore, transfer the transgene to a larger percentage of the tumor mass. The increase in transgene dropout could be linked to the idea of heterogeneous RRVs, with two different templates. Usually, when a retrovirus has two homologous templates, the reverse transcriptase (RT) produces DNA from both templates by switching back and forth between the two. When switching templates, RT usually finds a homologous region to bind to. However, in the case of two templates that don't have homology, the RT may skip further down the RNA strand. If this skipping takes place within a functional region of the virus, such as the heterogeneous regions in 4070A and GALV, the DNA integrated into the cell would produce non-functional RRV. On the other hand, if this kind of skipping took place in the transgene

region, functional genetic material would still produce RRV and continue to replicate. While this is worrisome, experiments have been done with other more heterogeneous transgenes (yCD2 and TKO) that cause the transgene region to actually become more stable over passages. Further passaging experiments should be carried out to determine if the genetic homogeneity of the transgene could have some effect on the stability.

Finally, experiments combining two suicide transgenes showed promising functional results. As should be expected, cotransduction with the same envelope results in incomplete cotransduction of each transgene. This is seen when U87 cells are treated with a combination of both prodrugs. The result is not additive, but median. Cells receiving only AC3-yCD2 RRV actually produced a more cytotoxic effect on the cells treated with prodrug combination than cells cotransduced with both, while cells receiving single transduction of GS4-S1-TKO showed less cytotoxicity. This makes sense, as a certain population of the cotransduced cells (around 25% according to fluorescence data) would only be expressing the TKO transgene, which was not as effective at killing cells at these levels of GCV. yCD2, on the other hand, resulted in higher levels cytotoxicity at these levels of 5-FC, but was unable to transduce the entire cell population, due to superinfection resistance from AC3-S1-TKO. Thanks to the data found earlier, we were able to apply TKO to GC3 to produce GC3-S1-TKO, a virus that would not interfere with AC3-yCD2 transduction in U87 cells and allow the entire cell population to express both transgenes. This was clearly illustrated, as the effect of both prodrugs was additive, rather than median.

This experiment opens up more options in the treatment of cancers with RRVs. As cancers are currently treated with a regimen of chemotherapeutics to combat tumor heterogeneity, the current RRV system relies on a single gene and a single prodrug. As this new biotechnology develops, options for more transgenes and more prodrugs must become available to combat this same heterogeneity in cancers. By using envelope pseudotypes and studying the

interactions of envelopes in different cell lines and different types of cancer, it will be possible to deliver more transgenes to the entire tumor mass and increase the therapeutic affect of RRVs.

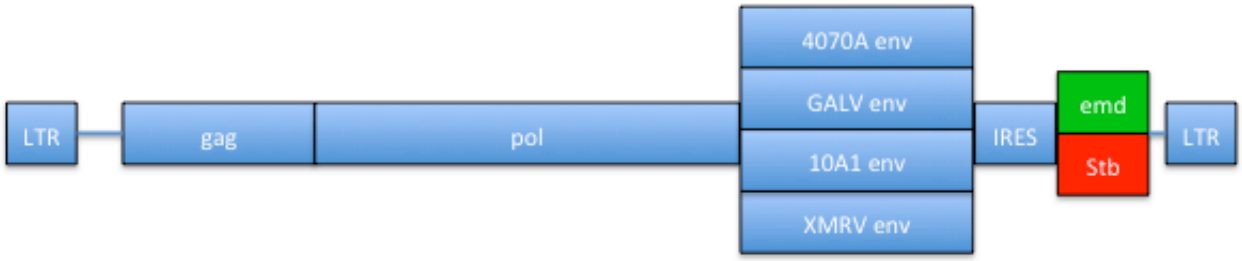

	4070A (MLV)	GALV	10A1 (MLV)	XMRV
Virus	Murine Leukemia Virus	Gibbon Ape Leukemia Virus	Murine Leukemia Virus	Xenotropic Murine Leukemia Virus
Species Tropism	Human+Mouse	Human	Human +Mouse	Human Mouse (?)
RRV	AC3	GC3	TC3	XC3
Receptor	Pit2	Pit1	Pit1+Pit2	XPR1
Receptor Function	Inorganic phosphate intake	Inorganic phosphate intake	Inorganic phosphate intake	Unknown
Base Pairs	1965	2037	1941	1938

Table 2-1
A) Vector map of different pseudotypes and fluorescent transgenes carried.
B) Details on different envelopes used for RRV envelope pseudotyping, including nomenclature, receptor binding targets, and tropism.

A

Pretrans	Challenge	PC3 emd-stb	PC3 stb-emd	U87 emd-stb	U87 stb-emd	HeLa emd-stb	HeLa stb-emd	WiDr emd-stb	WiDr stb-emd
AC3	AC3	I	I	I	I	I	I	I	I
	GC3	C	C	C	C	ICC	ICC	ICC	ICC
	TC3	ICC	ICC	SC	SC	ICC	ICC	I	I
	XC3	C	C	C	C	ICC	ICC	ICC	ICC
GC3	AC3	ICC	ICC	C	C	ICC	ICC	C	C
	GC3	ICC	ICC	I	I	I	I	I	I
	TC3	C	C	C	C	ICC	ICC	C	C
	XC3	C	C	C	C	ICC	ICC	SC	SC
TC3	AC3	I	I	I	I	I	I	I	I
	GC3	SC	SC	C	C	ICC	ICC	ICC	ICC
	TC3	I	I	I	I	I	I	I	I
	XC3	C	C	C	C	ICC	ICC	SC	SC
XC3	AC3	C	C	C	C	ICC	ICC	C	C
	GC3	SC	SC	C	C	ICC	ICC	ICC	ICC
	TC3	C	C	C	C	ICC	ICC	C	C
	XC3	I	I	I	I	I	I	I	I

B

	PC3 emd-stb	U87 emd-stb	HeLa emd-stb	WiDr emd-stb
AA	ICC	ICC	ICC	ICC
AG	ICC	C	ICC	ICC
AT	ICC	ICC	ICC	ICC
AX	ICC	C	ICC	ICC
GA	ICC	C	ICC	C
GG	ICC	ICC	ICC	ICC
GT	ICC	C	ICC	C
GX	C	C	ICC	C
TA	ICC	ICC	ICC	ICC
TG	ICC	C	ICC	ICC
TT	ICC	ICC	ICC	ICC
TX	C	C	ICC	C
XA	C	C	ICC	C
XG	ICC	C	ICC	ICC
XT	C	C	ICC	C
XX	ICC	ICC	ICC	ICC

C — Cotransduction
SC — Slowed Cotransduction
ICC — Incomplete Cotransduction
I — Inhibition

Table 2-2
Sequential and simultaneous cotransduction interference patterns of different RRV pseudotypes across multiple cell lines. For sequential transductions, the top row indicates cell line used and what order the fluorescent proteins were introduced, first FP being pretransduced, second being the challenge. The left column shows which RRVs were pretransduced and which RRVs challenged. Simultaneous cotransductions show the pairing of RRVs with their FPs in the left column and the cell lines in the top row.

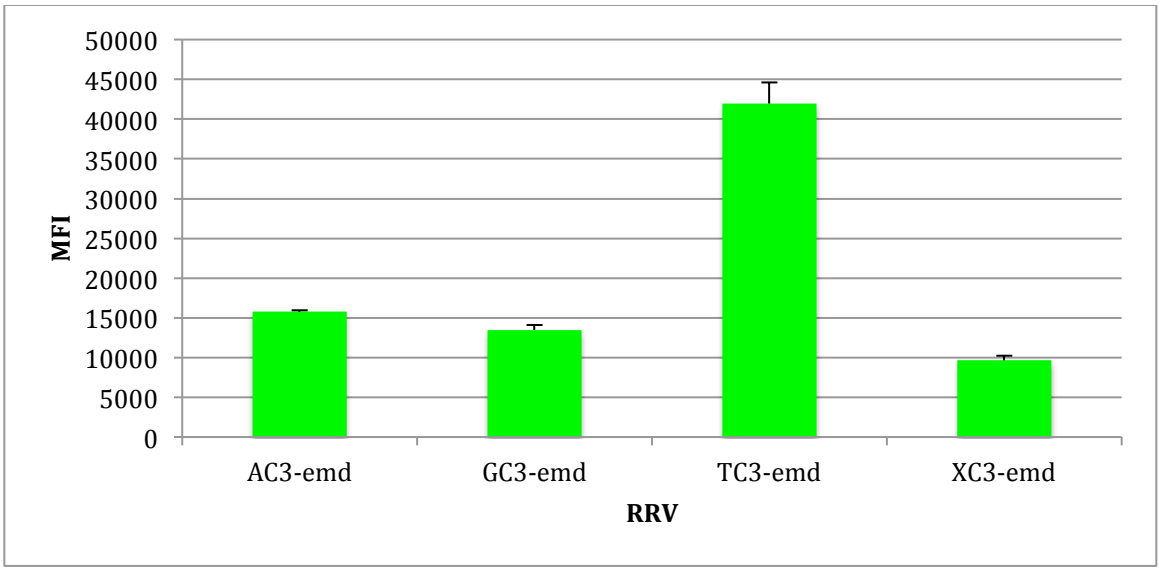

Figure 2-1
MFI FACs analysis of single transduction from four different RRV envelope pseudotypes in U87 cells.

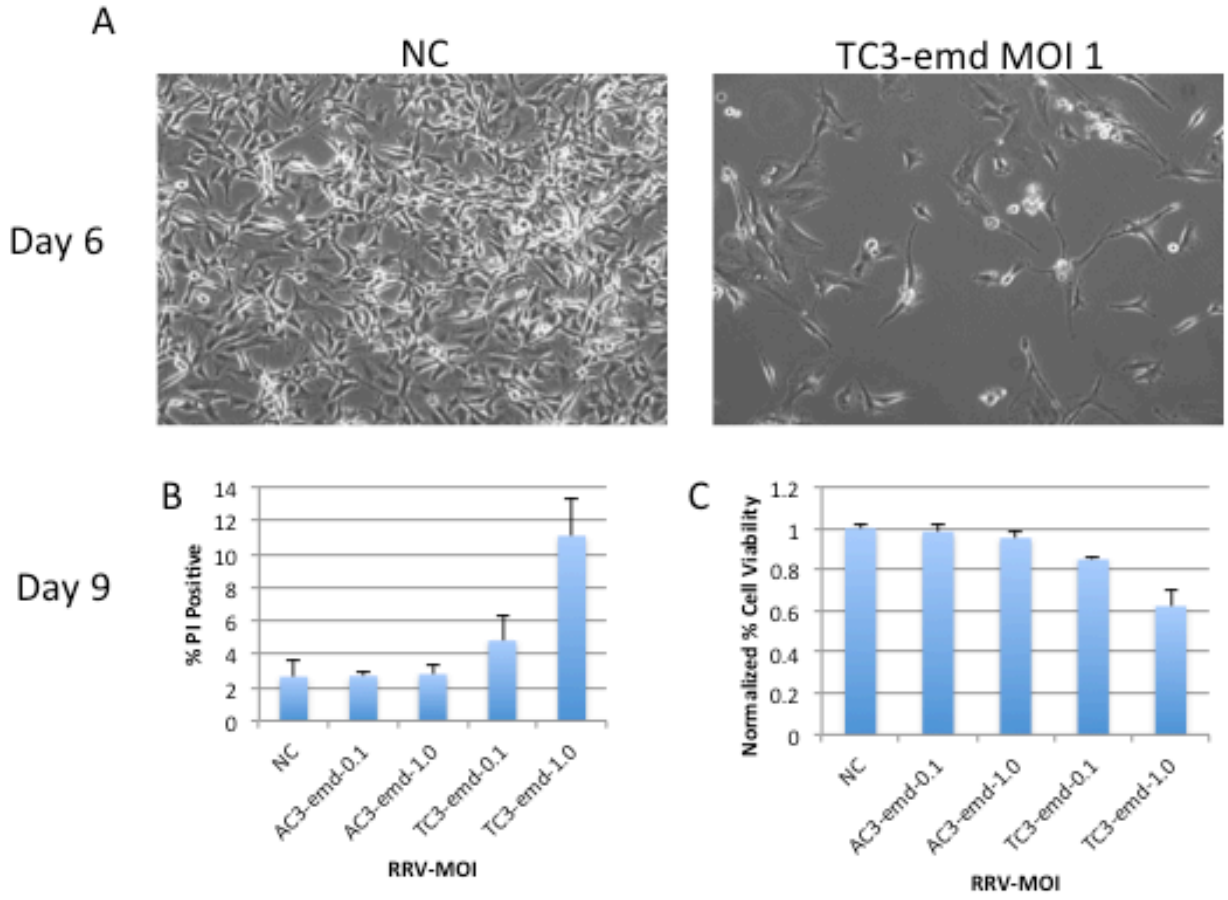

Figure 2-2
A) Inhibited growth of U87 cells transduced with TC3-emd. B) PI stain of U87 cells transduced at varying MOIs of AC3-emd and TC3-emd. C) MTS cell viability assay of U87 cells transduced at varying MOIs of AC3-emd and TC3-emd.

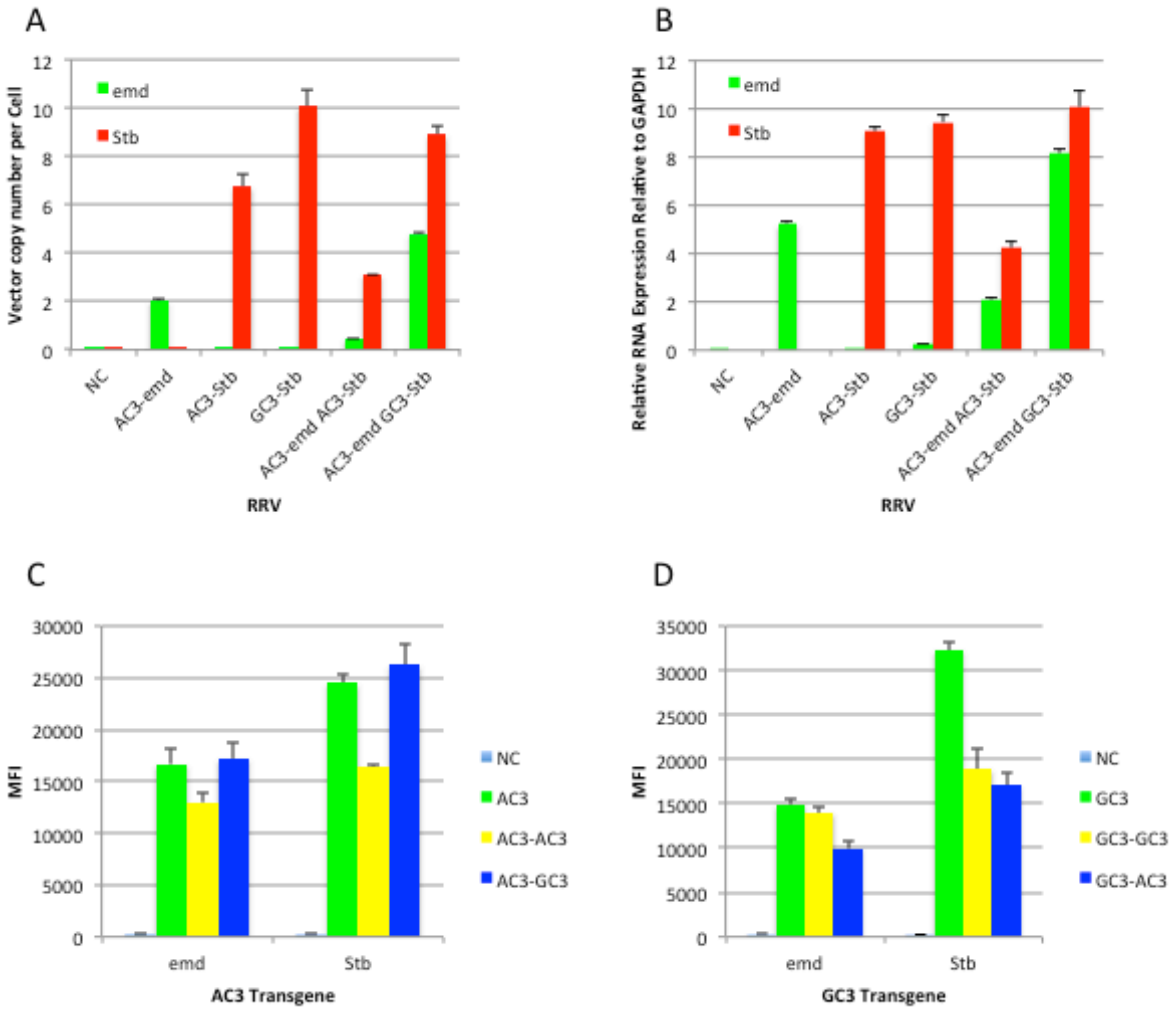

Figure 2-3
Vector copy number, RNA expression, and MFI were all taken more than 14 days after transduction with 0.05 MOI RRV. A) Vector copy number was measured by qPCR of the viral transgenes emd and Stb and calculated by normalizing to GAPDH levels. B) RNA transgene expression of AC3 and GC3 cotransduced U87 cells. RNA was reverse transcribed, analyzed by qPCR and compared relative to the amount of GAPDH RNA in each sample. C) Ratio of RNA expressed per viral copy. D) FACs analysis of the transgene expression by MFI in cotransduced U87s.

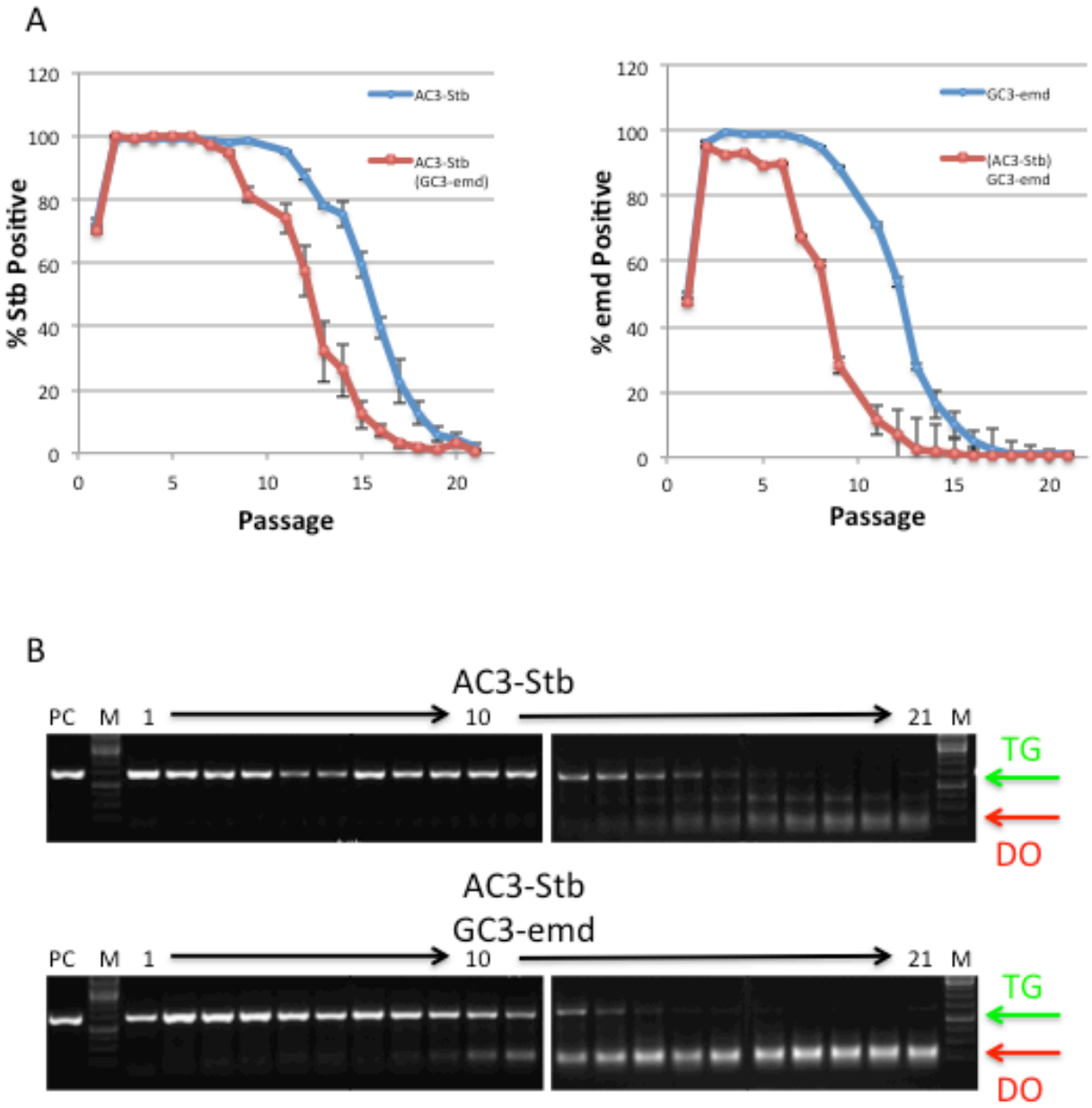

Figure 2-4
Passaging of cotransduced AC3 and GC3 RRVs expressing FPs. A) FACs analysis of the percent of the U87 population that still expressed the FP transgene over multiple RRV passages. B) PCR analysis of the transgene region of the provirus from genomic DNA. The longer product represents the full transgene (TG) while the shortened products represent dropout (DO).

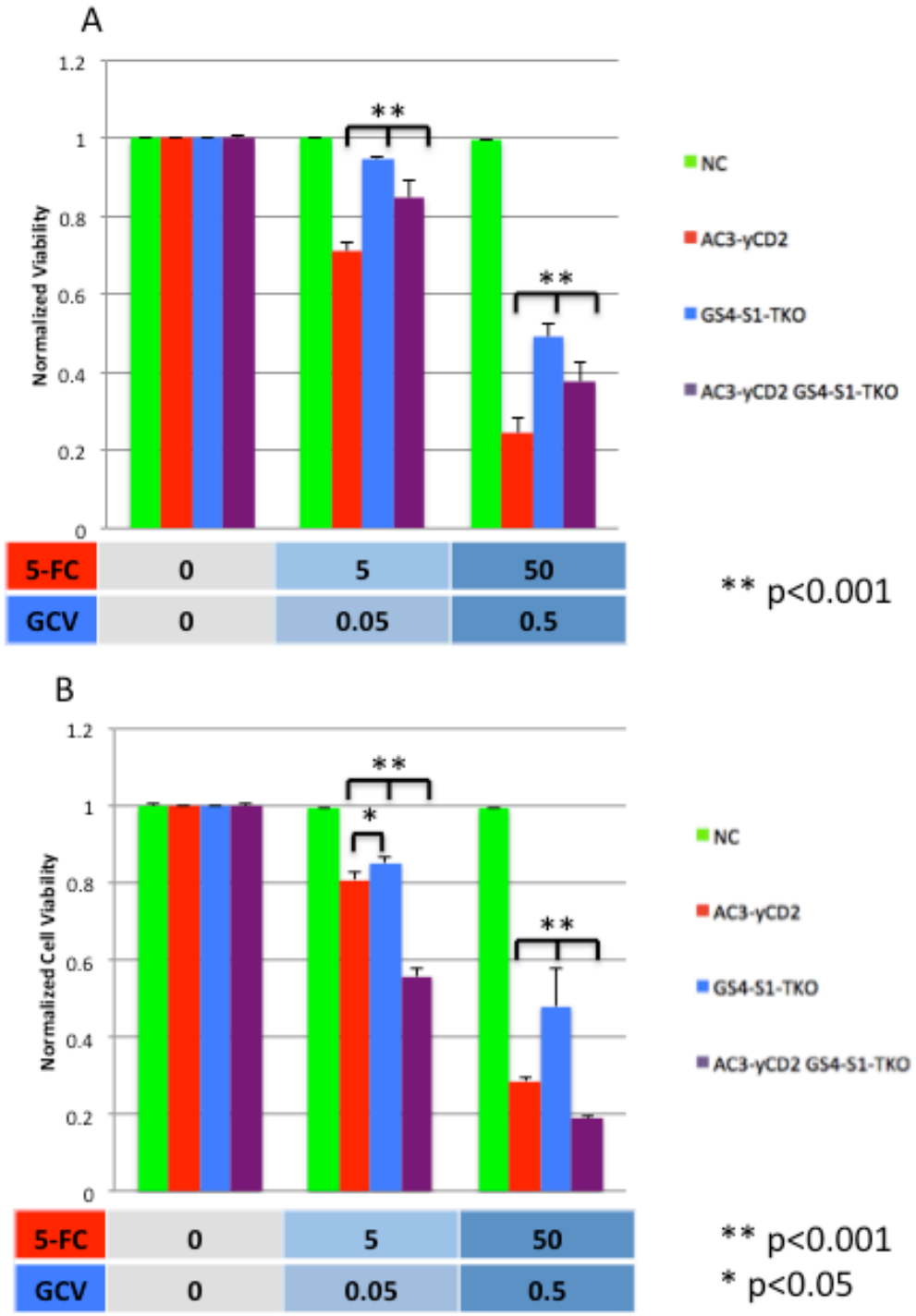

Figure 2-5
A) MTS cell viability assay of U87 cells transduced with AC3-yCD2, AC3-S1-TKO, or both, 9 days after treatment with varying concentrations of 5-FC and GCV. B) MTS cell viability assay of U87 cells transduced with AC3-yCD2, GS4-S1-TKO, or both, 9 days after treatment with varying concentrations of 5-FC and GCV.

Chapter 3 Envelope-Linked Oligonucleotide P2A Increases Transgene Expression From Retroviral Replicating Vectors

Introduction

Retroviral Replicating Vectors (RRV) are capable of spreading throughout a tumor mass, as opposed to non-replicating vectors, which usually remain very close to the injection site and result in very low levels of tumor transduction[2]. One such virus, Toca 511, is currently under investigation in Phase I/II clinical trials for the treatment of advanced stage glioma (https://clinicaltrials.gov/; NCT01156584, NCT01470794, NCT01985256). Toca511 delivers the codon optimized yeast cytosine deaminase (yCD2) suicide gene, which acts by converting the non-toxic anti-fungal drug, 5-FC, into the chemotherapeutic agent, 5-FU. This conversion results in cell death via two main mechanisms: (1) inhibition of thymidylate synthase (TMS), which results in decreased intracellular pools of thymidine leading to DNA replication errors, and (2) at higher concentrations, integration into RNA and DNA. Most chemotherapeutic regimens involve the delivery of multiple drugs in order to combat the heterogeneous nature of most cancers. Although 5-FU is a potent anticancer agent, delivery of multiple therapeutic transgenes could increase the clinical efficacy of RRV-mediated cancer gene therapy. We previously showed that delivery of both cytosine deaminase (yCD2) and thymidine kinase (TKO) from two different pseudotyped viruses results in increased cell killing. TKO is an enzyme that has a high specificity for the drug ganciclovir (GCV), to which it binds resulting in phosphorylation of GCV, which acts as a nucleotide analog. This analog works in a similar way to 5-FU at high concentrations, by integrating into replicating DNA and halting DNA synthesis. It has been suggested that, through the allosteric regulation of the nucleotide pool by ribonucleotide reductase (RNR), these two transgenes could have a synergistic affect when paired.

The TKO sequence, which is 1.1kb in length, is too large to package under the current RRV configuration. In order to properly accommodate a transgene this large, modifications to the RRV must be made to increase the space available for transgene sequences. We previously demonstrated that a synthetic promoter, SCP1, can be used to drive RRV transgene expression, and that the oligonucleotide P2A can be used to link two transgenes under the control of a single promoter. P2A is a short 66-bp amino acid sequence from picornavirus, which causes ribosomal skipping during translation. In this study, we utilized both SCP1 and P2A to coexpress TKO and yCD2 from a single RRV.

Materials and Methods

Cloning

pAC3-S1-emd was cloned by ligating the SCP1 sequence provided by BioBasic with 5' MluI and 3' HpaI sites, emd with 5' HpaI and 3' NotI sites, and backbone RRV with 5' NotI and 3 MluI sites. pAC3-S1-TKO was then cloned by removing emd with HpaI and NotI and replacing it with the TKO PCR product with matching restriction sites. SCP1-emd/TKO constructs were then cloned into the GC3 backbone by cutting and extracting at the 5' MluI and the 3' NotI sites. pAC3-P2A, pAC3-P2A-emd, pGC3-P2A, and pGC3-P2A-emd were cloned by PCR of the envelope region of both constructs with a 5' SphI site and a blunt site at the end of the envelope ORF without the stop-codon. This was blunt ligated to PCR product from either pAC3-S1-emd-P2A or pAC3-S1-yCD2-P2A-emd constructs with a 5' blunt end and 3' SacI site. Both inserts were ligated into corresponding pAC3-emd or pGC3-emd backbones cut with SphI and SacI. pAC3-P2A-TKO and pGC3-P2A-TKO were cloned by cutting both pAC3-P2A and pGC3-P2A with both SacI+SmaI (extracted at 0.6 kb) and SacI+NotI (extracted at 10.4 kb) and ligating both pieces with TKO PCR product with a 5' blunt end and a 3' NotI.

Cell Culture

U87 (ATCC-HTB-14) cells were grown in DMEM (Corning Cellgro Ref# 10-0130-CV). All media was supplemented with 10% FBS (Hyclone) and 1% Pen-Step.

Viral Production

Viruses were produced on 293T cells by calcium-phosphate mediated transfection, as previously described. Functional viral titers were calculated by transduction of U87s at various volumes (between 1-200μL per mL) , then treatment with 50 μM AZT 24-hours later. Quantitation was done by either FACs in the case of either emd, or qPCR in the case of yCD2 or TKO.

Transduction

Cells were transduced with an MOI of 0.05. 4 ug/mL polybrene was supplemented into the media to promote transduction. Cell cultures were grown out for 14 days before analysis to assure complete transduction.

FACs analysis

Cells were analyzed by a BD Biosciences FACs Canto II. Negative controls were run and gated for the live population of cells, 10,000 of these samples were then run for emd+ or Stb+ fluorescence. Untransduced negative control cells were gated in the lower quadrant of the emd-Stb axises. Transduced cells were then run and analyzed for percent population and MFI by FlowJo (www.flowjo.com).

Passaging

Cells were transduced in triplicate with an MOI of 0.05. 4 ug/mL polybrene was supplemented into the media to promote transduction. Each day before passaging, naïve U87 cells were split onto a new 6-well plate for the next passage and media was replaced and incubated for 24-hours on the previous passage. On the day of passage, 10% of supernatant was transferred to naïve cells supplemented with polybrene. Triplicates were combined for gDNA isolation.

Genomic DNA/RNA Extraction

Genomic DNA extraction kit was provided by Qiagen DNeasy Blood and Tissue Kit (Qiagen Cat# 69506. Cells were either processed directly or frozen at -80C before processing. RNA was isolated by Aurum total RNA minikit (BioRad Cat# 7326820) from 10cm plates directly with the lysis buffer. Both gDNA and RNA isolations were done according to the kit manufacture's protocol.

qPCR

10 ng-1 µg of RNA was reverse-transcribed to cDNA utilizing Transcriptor First Strand cDNA Synthesis Kit (Roche Applied Sciences, 04379012001) following the manufacturer instructions. Primers and probes were designed from Roche's Universal Probe Library. Primers for the genes were synthetized at Valuegene Inc. Quantitative PCR relative expression experiments were performed on a LightCycler 480 Real-Time PCR System (Roche), and data was further analyzed with LightCycler 480 Software release 1.5.0. with 1-10 ng of sample in a total of 20 µL of reaction mix consisting of 10 µM UPL probe, 20 µM each of forward and reverse primers, and 20 µM 2X-LightCycler 480 Probes Master Mix. Triplicate experimental samples were paired using the all-to-mean pairing rule ΔCt value calculation with three housekeeping genes run in triplicate for advanced relative quantification.

Viability Assay

Viability assays were done with Promega CellTiter 96® AQ_{ueous} One Solution Cell Proliferation Assay (Cat#G3580). Cells were split into 2x10^3 cells per well on a 96-well plate and treated with prodrug one day after seeding. Media was removed from wells before addition of fresh media containing 20uL assay solution and 100uL media. Plates were then analyzed in a BioTek Synergy H1 Hybrid Reader at 490 nm. Plates were analyzed on days 3, 6, and 8 for TU2449 cells and days 3, 6, and 9 for U87 cells. Fro each day, time points were taken every half hour up to 4 hours.

Western Blot

Western Blots were done using whole cell lysate from cultured cells 21 days post-transduction. Wells were loaded with between 15-90ug/well, depending on abundance of protein. Antibodies used were cytosine deaminase antibody from Thermo Scientific (Cat# PA1-85365) and thymindine kinase antibody from Santa Cruz (Cat# sc-28038). Beta-Actin controls were from Santa Cruz (Cat#sc-47778). Secondary antibodies used were Rabbit Anti-Goat IgG H&L (HRP) (Cat#ab6741) to conjugate TK and Rabbit anti-sheep IgG H&L (HRP) (Cat#ab97130) to conjugate CD, both from abcam. Primary antibody dilutions were done at 1:500 and secondary antibodies at 1:2000. Membranes were blocked with 5% milk in TBS. Primary antibodies were incubated overnight at 4C in TBS supplemented with 0.1% Tween and 5% milk. Secondaries were incubated at room temperature for 1 hour in 5% milk T-TBS. Beta-Actin antibody was only incubated at RT for 1 hour as the antibody itself is already conjugated to HRP.

Intracellular Staining

Intracellular staining for CD was done by fixation of TU2449s in 4% paraformaldehyde, then permeation of the cellular membrane by 0.1% Triton. Cells were then stained with anti-Toca CD provided by Tocagen. Secondary staining was done with goat anti-mouse IgG (H+L)-Alexa 488 from Thermo (Cat#A-11001). Cells were then analyzed by FACs as described above. Controls were run either without primary antibody or without both primary and secondary antibody as controls. Two washes with staining buffer from BD Pharmigen (Cat#554656) were carried out between each step.

Results

Characterization of transgene expression from IRES, SCP1, and P2A RRVs

To establish how well each RRV construct performed in multiple cell lines, single transductions were carried out with AC3-emd, AC3-S1-emd, and AC3-P2A-emd on U87, PC3, 293T, and TU2449 cell lines. After full transduction was established, cells were analyzed by qPCR for vector copy number and transgene RNA expression, and MFI was measured by FACS.

Transgene expression, as measured by MFI, was significantly higher in all cell lines transduced with AC3-emd (Figure 3-2D). The extent of this increase varied depending on the cell line. For cells transduced with AC3-P2A-emd, the MFI was increased compared to AC3-S1-emd in all cell lines other than 293T. Vector copy per cell remained constant for AC3-emd and AC3-S1-emd, other than in TU2449s, in which AC3-S1-emd was present at higher copies per cell (Figure 3-2A). Relative to the AC3-emd, AC3-P2A-emd had 15% to 50% less vector copies per cell depending on the cell line. Despite this decrease, transgene RNA expression in cells transduced with AC3-P2A-emd was equivalent to AC3-emd in U87 and TU2449 cell lines and increased 20% in PC3 and 293T cell lines (Figure 3-2B). Transgene RNA expression in cells transduced with AC3-S1-emd was comparable to AC3-emd in TU2449 cells, was increased 20% and 55% in PC3 and 293T cells, respectively, and was decreased 25% in U87 cells. Overall, these data show that cells transduced with AC3-P2A-emd have increased transgene RNA expression per vector copy when, compared to AC3-emd, in all cell lines other than PC3, in which it remains equal. In cells transduced with AC3-S1-emd, transgene RNA expression per vector copy decreased 10% and 35% in PC3 and TU2449 cells, respectively, and increased 35% and 50% in 293T and U87 cells, respectively, when compared to AC3-emd (Figure 3-2C). We next engineered GC3-RRVs fitted with IRES, SCP1, or P2A and expressing emd (Figure 3-1). These constructs were compared directly, by FACS, to the same constructs expressing the AC3 envelope. Interestingly, the MFI of emd-positive cells transduced with GC3-P2A-emd was nearly twice as high as that of AC3-P2A-emd. GC3-P2A-emd also only decreased MFI relative to GC3-emd roughly 40%, whereas AC3-P2A-emd MFI dropped 80% compared to AC3-emd (Figure 3-3A and B).

Vector copy number, protein expression, function, and stability of suicide transgene TKO in GALV RRVs with SCP1 and P2A

Further experiments with the TKO transgene focused on the SCP1 and P2A constructs, as the transgene region would quickly dropout a construct containing both IRES and TKO. Also, as

AC3-yCD2 is a well-established and studied RRV, combination with GALV envelope is optimal in U87s. Constructs GC3-S1-TKO and GC3-P2A-TKO were used to transduce U87 cells (Figure 3-1). Cells transduced with GC3-P2A-TKO had fewer vector copies per cell compared to GC3-S1-TKO, with GC3-S1-TKO achieving an average of 2.6 copies per cell and GC3-P2A-TKO achieving 1.4 (Figure 3-3C). However, when analyzed by Western blot, levels of TKO protein were significantly lower in U87 cells transduced with GC3-S1-TKO than GC3-P2A-TKO (Figure 3-3D). When incubated with varying concentrations of prodrug, GC3-P2A-TKO significantly decreased the cell viability compared to GC3-S1-TKO at all concentrations other than the highest, 10 μM GCV (Figure 3-3E). Despite this interesting increase in therapeutic effect, GC3-P2A-TKO lost the transgene region of the RRV at a faster rate than GC3-S1-TKO (Figure 3-4). Transgene dropout was seen around passage 6 in GC3-P2A-TKO, whereas any dropout in GC3-S1-TKO was not witnessed until passage 12. However, despite appearance of a dropout mutant earlier in passaging, GC3-P2A-TKO retained the full transgene over longer passages compared to GC3-S1-TKO. This could be due to random mutation only occurring in one of the triplicate samples, rather than all of them.

Vector copy number, RNA expression, protein expression, function and stability of cotransduced RRVs pseudotyped with non-interfering 4070A and GALV to deliver yCD2 and TKO

As the envelope-P2A construct proved to have a much higher level of both transgene protein expression and function, this construct was used in further experiments. U87 cells were singly transduced with AC3-yCD2, AC3-P2A-TKO, or GC3-P2A-TKO, or cotransduced with AC3-yCD2and AC3-P2A-TKO or AC3-yCD2and GC3-P2A-TKO. Compared to single transduction, cotransduction with AC3-yCD2 and AC3-P2A-TKO resulted in decreased vector copy number per cell and transgene RNA expression (Figure 3-5A). The decrease in AC3-P2A-TKO was much more pronounced, as vector copies were reduced almost 10-fold when cotransduced with AC3-yCD2. As seen with previous data involving cotransduction in U87 cells with AC3 and GC3 constructs, the number of AC3-yCD2 copies per cell increased when cotransduced with GC3-

P2A-TKO, while the number of GC3-P2A-TKO copies decreased slightly, compared to single transduction. Transgene RNA expression was similarly affected; AC3-yCD2 expression levels increased when cotransduced and GC3-P2A-TKO expression levels decreased slightly (Figure 3-5B). Western blot revealed lower levels of TKO protein in U87 cells cotransduced with AC3-yCD2 and AC3-P2A-TKO (Figure 3-5E). As expected, however, when non-interfering RRV pseudotypes were used, yCD2 and TKO levels were comparable levels to those of single transduction, with a slight increase in yCD2 and a slight decrease in TKO expression (Figure 3-5E). Intracellular staining for yCD2 showed that levels of the transgene remained constant between single transduction with AC3-yCD2 and cotransduction with AC3-yCD2 and AC3-P2A-TKO (Figure 3-5C). However, the MFI of yCD2 staining was increased in cells cotransduced with AC3-yCD2 and GC3-P2A-TKO (Figure 3-5D).

Transduced cells were next treated with different combinations of the prodrugs, 5-FC and GCV. In all prodrug combinations studied, cotransduction with AC3-yCD2 and GC3-P2A-TKO resulted in decreased cell viability, with the exception of the highest concentrations of GCV (Figure 3-6, Supplementary 3-1). Finally, AC3-yCD2 and GC3-P2A-TKO were transduced either separately or together and serially passaged on U87 cells. In contract to previous data with the same RRVs carrying fluorescent proteins, cotransduced AC3-yCD2 retained the transgene through an equal amount of passages as single transduction, while GC3-P2A-TKO actually retained the transgene for more passages (Figure 3-7).

Discussion

In these experiments, a new RRV set-up was designed to allow the vector to carry larger transgenes. The P2A oligonucleotide was attached to the end of the envelope gene, allowing the transgene to be expressed in the same transcript as the viral envelope. It was found that, despite a decrease in vector copy number per cell, P2A still expressed higher levels of protein in most cell lines compared to SCP1. This was later confirmed, as SCP1 produced very low levels

of the transgene TKO in U87 cells compared to envelope-P2A. However, the rate of transgene dropout was much higher in GC3-P2A-TKO than GC3-P2A-TKO. Cotransduction of GC3-P2A-TKO with AC3-yCD2 resulted in increased vector copy number and transgene RNA expression of AC3-yCD3, while slightly diminishing these factors for GC3-P2A-TKO. When incubated with prodrug, U87s cotransduced two RRVs with non-interfering envelopes exhibited decreased cell viability at most concentrations. Finally, when serially passaged with AC3-yCD2 the transgene stability of GC3-P2A-TKO was increased compared to transduction with a single RRV.

Across all cell lines, the vector copy number per cell decreased for AC3-P2A-emd when compared to AC3-emd and AC3-S1-emd. This suggests that P2A at the end of the envelope may have some effect on the efficiency of the virus. As mentioned before, P2A attaches 18 amino acids to the C-terminus of any protein it is linked with. Although both 4070A and GALV envelope proteins cleave the C-terminus of the protein post-translation, the reduction in vector copy number suggests that the P2A does have some effect on the RRV. It could be that the P2A sequence hinders cleavage, causing many of the RRVs produced to be unable to fuse to the next host while still sequestering the active site of the targeted cellular receptor. Despite decrease vector copies per cell, P2A produced levels of transgene RNA equal to or greater than that of AC3-emd in all cell lines. This level of RNA expression does not translate directly to protein expression. Although two different RNA transcripts are transcribed from the viral LTR, only one transcript is used for translation of the transgene. In the case of AC3-emd, both viral transcripts result in transgene translation, since IRES causes independent binding of the ribosomes independent of upstream stop codons. Theoretically, the RNA expression per vector copy should be the same between AC3-P2A-emd and AC3-emd, but this is only the case in PC3 cells. 293T, U87, and TU2449 cells all have a significant increase in transgene RNA expression per vector copy of AC3-P2A-emd compared to AC3-emd. This could be the result of inherent differences in RNA stability of the P2A and IRES transcripts.

Transgenes driven off of SCP1 should have three RNA transcripts, two from the LTR and one from the SCP1, but only one of these, the SCP1 transcript, should theoretically be translated. Interestingly, a drop in RNA expression per vector copy of SCP1-emd is seen in TU2449 cells when compared with AC3-emd. It is possible that the SCP1 transcripts also have differing levels of RNA stability. Transgene protein expression was highest in AC3-emd across all cell lines studied, while AC3-P2A-emd showed the second most expression in cell lines excluding 293T, in which AC3-S1-emd had more robust expression. This may be due to the fact that relative RNA levels actually increased significantly compared to AC3-emd and AC3-P2A-emd in 293Ts, suggesting that the SCP1 is more active in this particular cell line.

SCP1 and P2A were then compared head to head with a larger transgene, TKO, in a GALV-envelope pseudotyped RRV transduced in U87 cells. Again, the number of GC3-P2A-TKO vector copies per cell decreased roughly two-fold when compared to GC3-S1-TKO. However, Western blot revealed that the transgene protein expression by GC3-S1-TKO was nearly undetectable by Western, while GC3-P2A-TKO showed an abundance of protein. These two data are concurrent with the data seen in the previous experiment, where SCP1 promoter does not produce high levels of protein in U87 cells compared to P2A because of decreased promoter activity. This decrease in protein was apparent in functional assays, as treatment with prodrug GCV resulted in increased cell killing at lower concentrations of GCV with GC3-P2A-TKO than GC3-S1-TKO. When passage stability was assessed, GC3-P2A-TKO showed faster dropout than GC3-S1-TKO, although it retained a mixed population of full transgene and dropout for a longer period. Potentially, reverse transcriptase (RT) could have produced a more stable form of the transgene, rather than a dropout form. This more stable form could be sequenced to confirm this theory, as well as produce a new, more stable transgene sequence. However, this mutation could affect the functionality of TKO if it occurs within the ORF and is not a silent mutation.

As GC3-P2A-TKO showed increased therapeutic effects compared to AC3-S1-TKO, this RRV was chosen to cotransduce along with AC3-yCD2. As previously shown, 4070A and GALV pseudotyped RRVs can both achieve full transduction in U87 cells. In a similar fashion seen in fluorescent protein transduction, cotransduction with AC3-yCD2 and GC3-P2A-TKO resulted in an increase of AC3-yCD2 vector copies per cell, while there was a slight decrease in GC3-P2A-TKO vector copies when compared to single transductions. The same was seen in RNA expression. As previously theorized, this is likely due to the viral proteins both being expressed in the second generation of RRV, allowing AC3-yCD2 to transduce through the Pit1 receptor, which has higher expression in U87 cells. Cotransduction with the same envelope showed that AC3-P2A-TKO vector copy number and RNA expression was much lower than seen in cotransduction with two fluorescent proteins. This could be due to P2A effecting the fusion of RRV. The R-peptide, which is cleaved post-translationally from the c-terminus of the envelope protein of both 4070A and GALV is essential for viral fusion[20,21]. Modification of the R-peptide can hinder viral fusion while still occupying the binding site of the Pit2 receptor. This would give AC3-yCD2 an advantage in transduction, allowing it to transduce more cells before being inhibited by superinfection resistance. Western blot revealed patterns similar to vector copy number and RNA expression results, as yCD2 was increased in cotransduction with GC3-P2A-TKO, while TKO was slightly decreased. AC3-AC3 transductions showed little decrease in yCD2 expression, but a large decrease in TKO expression when compare to single transduction. Cell viability analysis showed decreased cell viability in AC3-yCD2 GC3-P2A-TKO cotransduced lines at all concentrations studied with the exception of the highest levels of GCV. In this case, single transductions with TKO, either AC3 or GC3, decreased cell viability more affectively. This could be due to the decrease in TKO expression seen in cotransduction with AC3. While cotransduction with GC3 gives AC3 an advantage in U87 cells, it hinders GC3 transgene expression slightly, as the Pit1 receptors are now being sequestered by envelope chimeric RRV carrying AC3. As AC3-yCD2 achieved better transduction than AC3-P2A-TKO,

little effect was seen between single transduction with AC3-yCD2 and AC3-yCD2 AC3-P2A-TKO when treated only with 5-FC. On the other hand, treatment with only GCV showed diminished cytotoxicity when compared to single transduction of AC3-P2A-TKO.

When passaged, AC3-yCD2 and GC3-P2A-TKO showed different results than observed with AC3-emd and GC3-Stb cotransductions. When using fluorescent proteins, transgene dropout occurred in earlier passages than single transduction. In this case, AC3-yCD2 retained its transgene the same number of passages as single transduction, while GC3-P2A-TKO actually retained the transgene longer than single transduction. This suggests that the pairing of the transgenes may have some affect on dropout in cotransduced RRVs. It is possible that the homology between the two RNA strands somehow effects the RT skipping, and that less homology, such as the yCD2 and P2A-TKO sequences, can lead to more stable transgene passaging.

As RRVs move through clinical trails, the issue of tumor heterogeneity may come to light, as our current therapy relies on a single transgene and a single prodrug. The ability to attack cancer from multiple pathways using an array of chemotherapeutics is currently the Gold Standard in clinic. For RRV therapy to develop, new methods of delivering multiple transgenes to the tumor mass must be explored. By using different envelopes, it is possible for RRVs to not only reach more of the cancer mass through different receptors, but also, to deliver both transgenes throughout the cancer mass, rather than just a percentage that would be blocked off from both by superinfection resistance. This new strategy hold great promise for the future of cancer gene therapy.

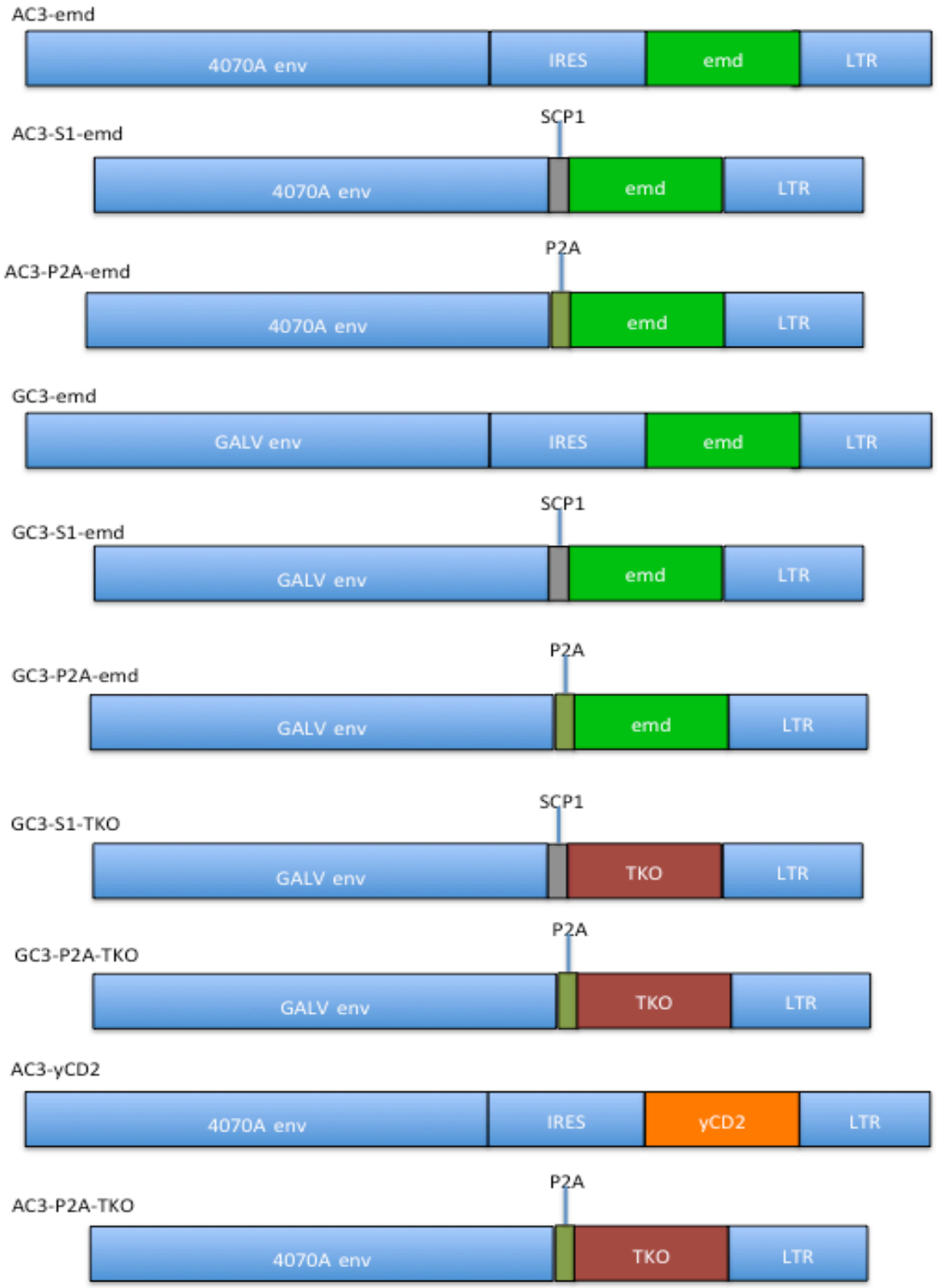

Figure 3-1
Vectors maps of different RRVs used in this experiment. The maps represent the envelope and transgene regions of RRV.

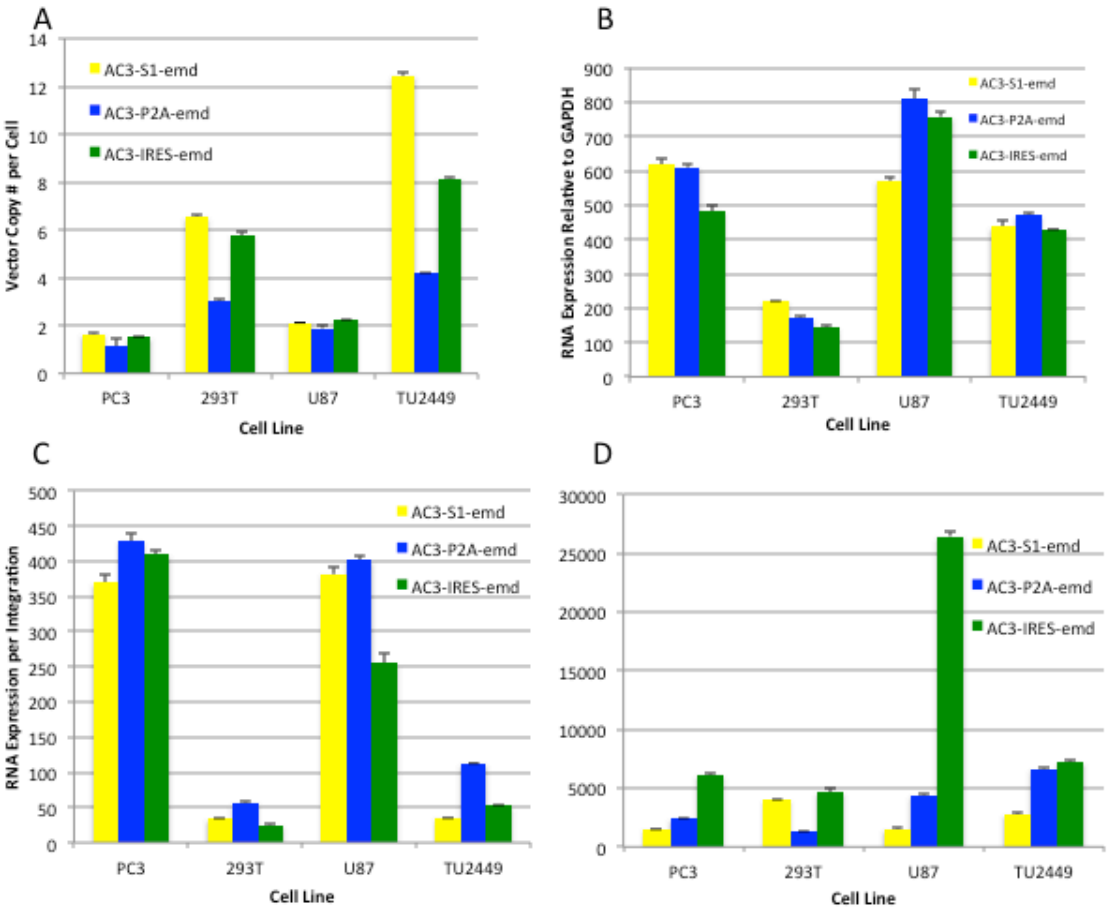

Figure 3-2
Vector copy number, RNA expression, and MFI were all taken more than 14 days after transduction with 0.05 MOI RRV. A) Vector copy number was measured by qPCR of the viral transgene emd and calculated by normalizing to GAPDH levels. B) RNA transgene expression of AC3-emd, AC3-P2A-emd, and AC3-S1-emd in different cells lines. RNA was reverse transcribed, analyzed by qPCR and compared relative to the amount of GAPDH RNA in each sample. C) Ratio of RNA expressed per viral copy. D) FACs analysis of the transgene expression by MFI.

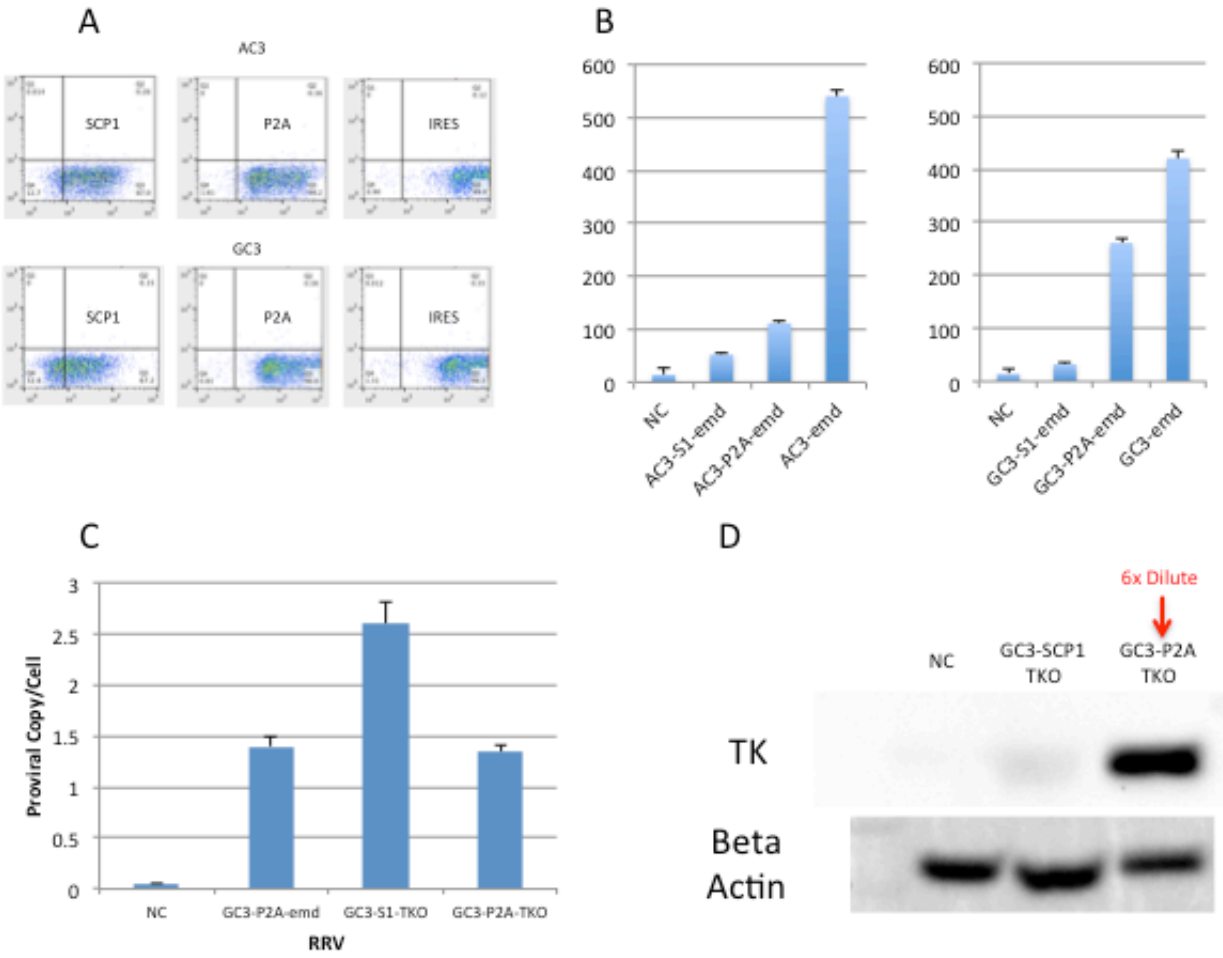
A
AC3
SCP1
P2A
IRES
GC3
SCP1
P2A
IRES
B
600
500
400
300
200
100
0
NC
AC3-S1-emd
AC3-P2A-emd
AC3-emd
600
500
400
300
200
100
0
NC
GC3-S1-emd
GC3-P2A-emd
GC3-emd
C
Proviral Copy/Cell
3
2.5
2
1.5
1
0.5
0
NC
GC3-P2A-emd
GC3-S1-TKO
GC3-P2A-TKO
RRV
D
6x Dilute
NC
GC3-SCP1 TKO
GC3-P2A TKO
TK
Beta Actin
E
Normalized % Cell Viability
1
0.8
0.6
0.4
0.2
0
0
0.1
0.5
1
5
10
μM GCV
**
**
**
**
NC
MLV-GALVenv-P2A-emd
MLV-GALVenv-S1-TKO
MLV-GALVenv-P2A-TKO
**
p<0.001

Figure 3-3
A) FACs plots of AC3 and GC3 RRVs equipped with IRES, SCP1, or P2A. B) MFI of emd positive U87 cells transduced with AC3-emd, AC3-S1-emd, AC3-P2A-emd, GC3-emd, GC3-S1-emd, GC3-P2A-emd. C) Vector copy number was measured by qPCR of the viral envelope GALV levels and calculated by normalizing to RNaseP levels. D) Western Blot for TK in U87 cells transduced with GC3-S1-TKO and GC3-P2A-TKO. GC3-P2A-TKO was diluted 6x in these studies. E) MTS cell viability assay of U87 cells transduced with GC3-S1-TKO and GC3-P2A-TKO 6 days after treatment with varying concentrations of GCV.

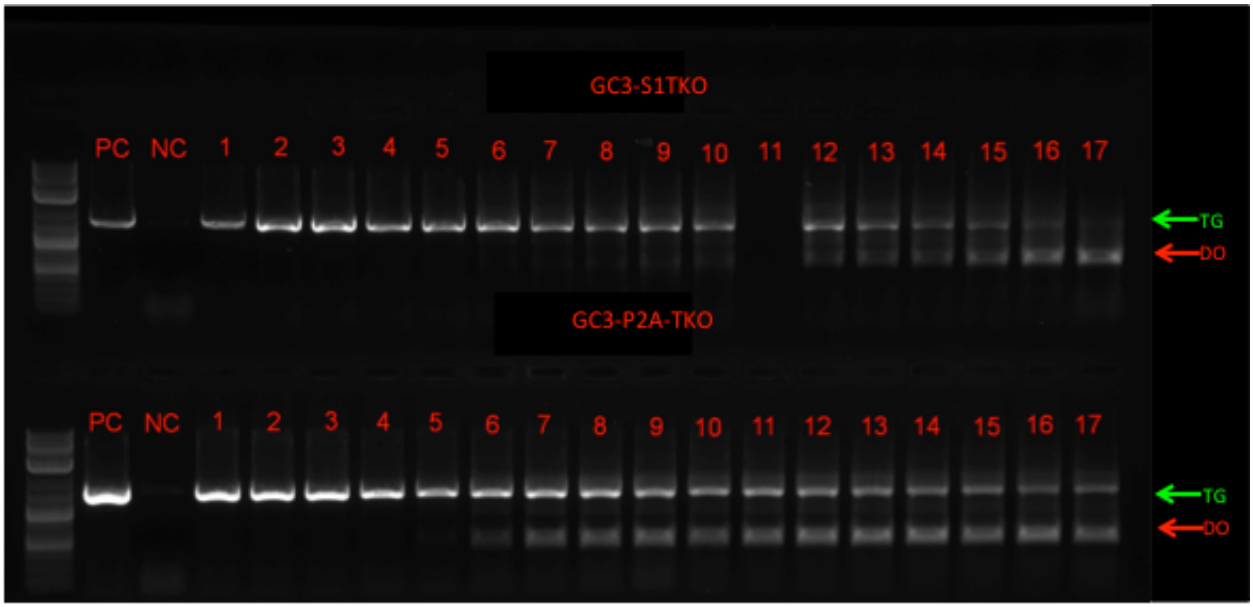

Figure 3-4
PCR analysis of the transgene region of the provirus from genomic DNA. The longer product represents the full transgene (TG) while the shortened products represent dropout (DO).

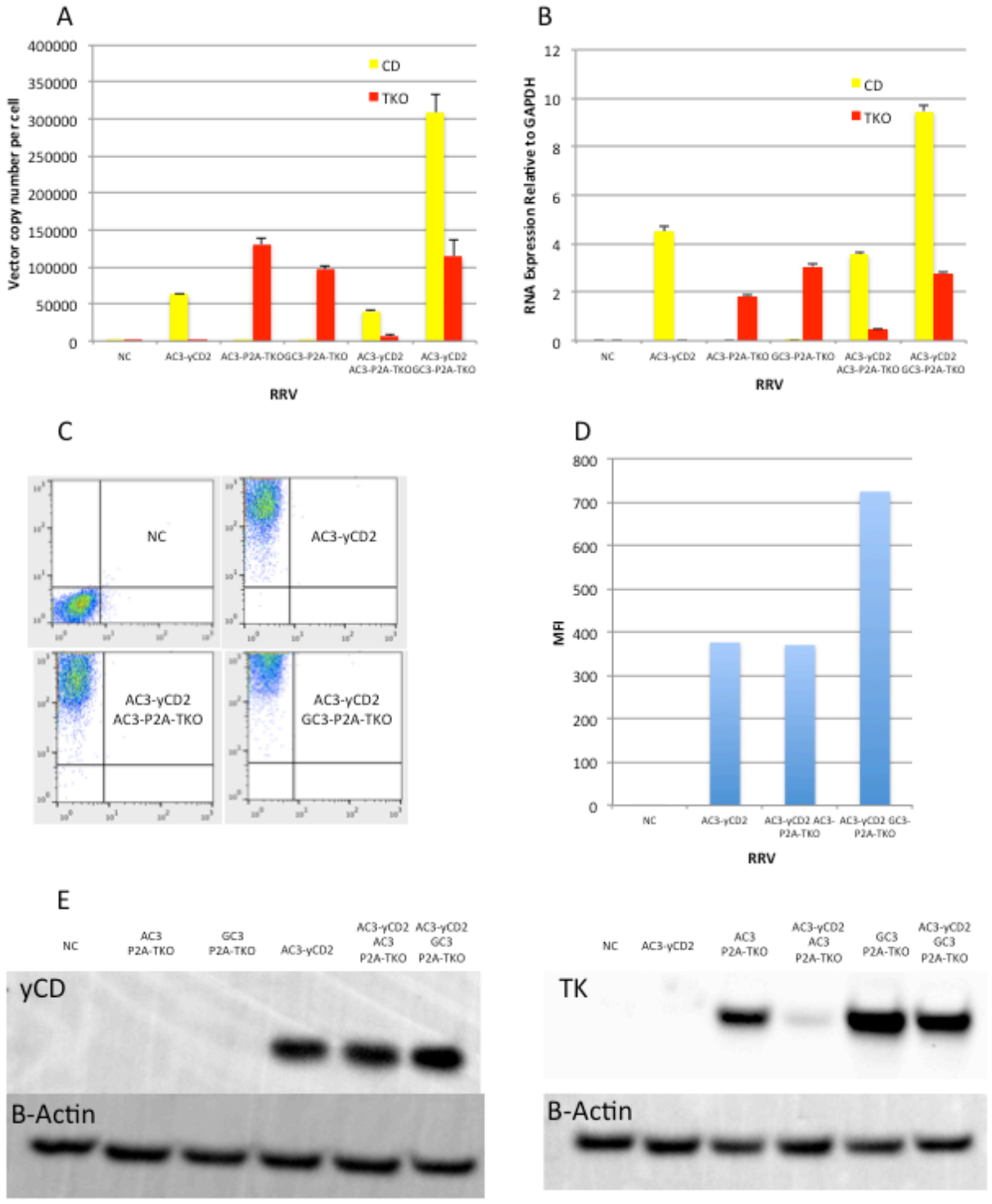

Figure 3-5
Vector copy number, RNA expression, and MFI were all taken more than 14 days after transduction with 0.05 MOI RRV. A) Vector copy number was measured by qPCR of the viral transgene yCD2 and TKO and calculated by normalizing to GAPDH levels. B) RNA transgene expression of AC3-yCD2, AC3-P2A-TKO, GC3-P2A-TKO, and cotransduction of these RRV in U87 cells. RNA was reverse transcribed, analyzed by qPCR and compared relative to the

amount of GAPDH RNA in each sample. C) Intracellular staining for yCD2 in AC3-yCD2 and AC3-yCD2 cotransduced with AC3-P2A-TKO or GC3-P2A-TKO. Cell were fixed, permeabilized, and stained with primary and secondary antibodies, then analyzed through FACs. D) MFI of intracellular staining results. E) Western Blot for CD and TK in U87 cells transduced with AC3-yCD2, AC3-P2A-TKO, GC3-P2A-TKO, and cotransduction of these RRV.

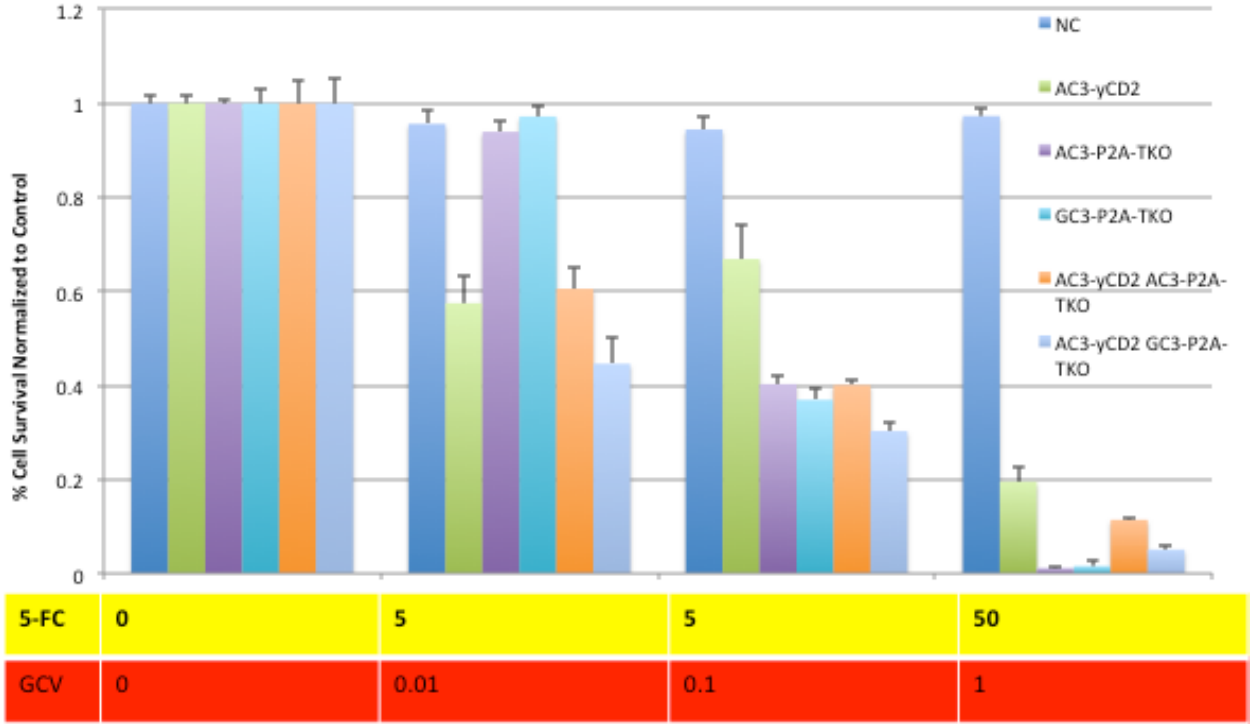

Figure 3-6
MTS cell viability assay of U87 cells transduced with AC3-yCD2, AC3-P2A-TKO, GC3-P2A-TKO, or combinations of the three, 9 days after treatment with varying concentrations of 5-FC and GCV.

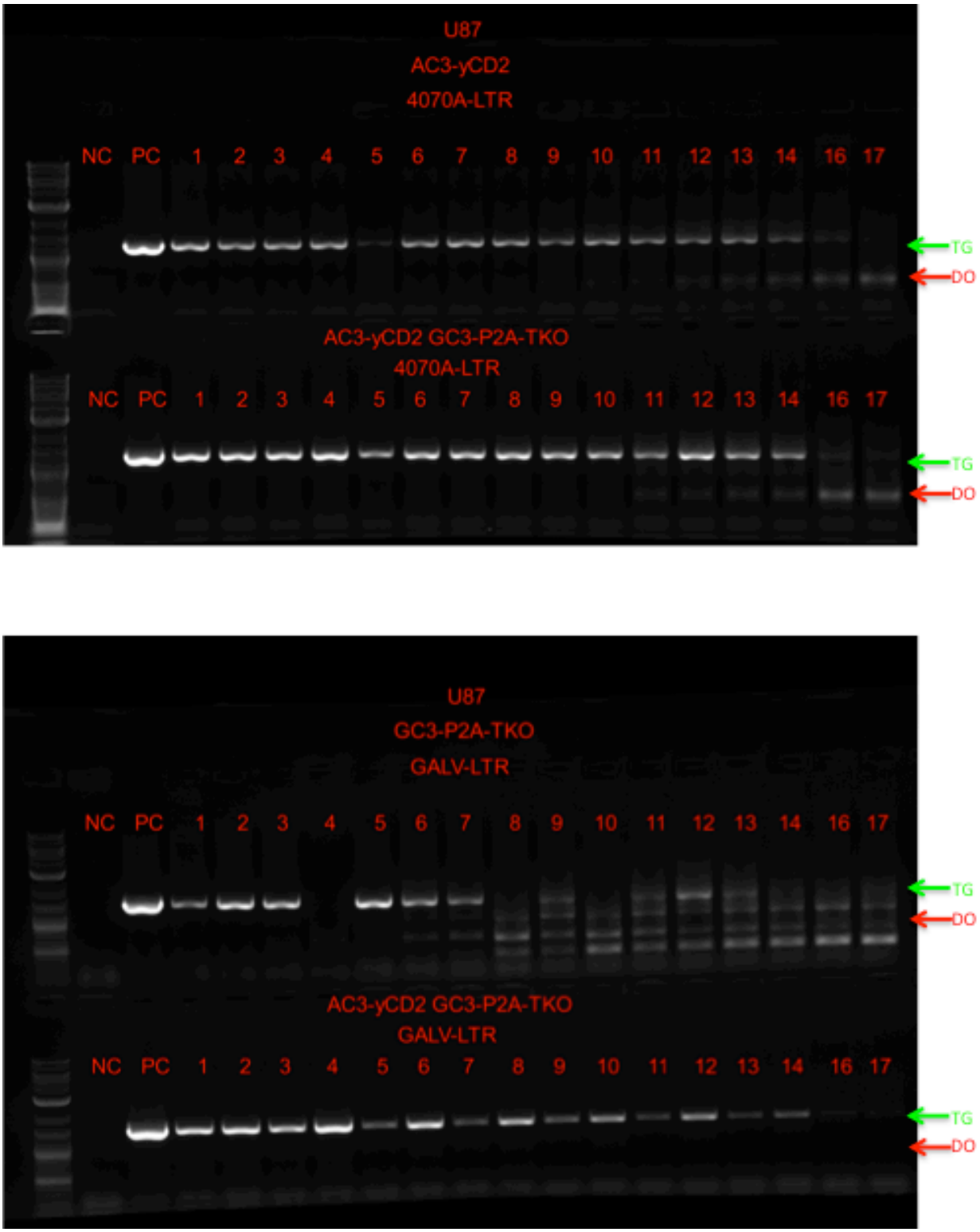

Figure 3-7
Passaging of cotransduced AC3 and GC3 RRVs expressing suicide genes. PCR analysis of the transgene region of the provirus from genomic DNA. The longer product represents the full transgene (TG) while the shortened products represent dropout (DO).

Conclusions and Future Directions

RRV-mediated gene therapy holds great promise in the cancer field. Although still in the early stages of developments, RRVs are capable of modifying the genetic makeup of tumors by delivery of specific transgenes. As it continues to develop, new avenues of treatment must be considered to add to and improve this field. The work presented here addressed two major constraints limiting the ability of RRVs to deliver multiple transgenes to a single cell: (1) the limited capacity RRVs are capable of retaining without transgene dropout and (2) superinfection resistance, which inhibits transduction of the same cell by two RRVs expressing the same envelope protein. Transgene capacity was increased by using promoters and linkers that occupied less of the limited transgene space, while superinfection resistance was overcome by pseudotyping the RRV with other viral envelopes.

Super Core Promoter And P2a Sequences Facilitate Combined Delivery Of A Suicide Gene And Cytokine By A Single Retroviral Replicating Vector

A synthetic promoter of minimal length, SCP1, was inserted into the transgene region of RRV to produce AC3-S1-emd. This promoter resulted in varying levels of transgene protein expression between cell lines when compared to AC3-emd. As vector copy number remained mostly equal between cell lines, it is likely that the difference in protein expression comes from the activity of the SCP1 promoter. The transcription factors that bind this synthetic promoter should be carefully studied to ascertain in which cell types this promoter would be most useful. In the studies shown here, maximal transgene expression was not our goal, as a therapeutic window exists for expression of GM-CSF.

The oligonucleotide P2A presented a means by which to save transgene space by expressing two proteins from the same promoter. When expressing two fluorescent transgenes, MFI levels correlated with each other, suggesting that equimolar amount of each transgene were being

produced, as previously described. However, a drawback to P2A is that it adds 18 amino acids to the C-terminus of the upstream gene, and a proline to the downstream gene. This can have an effect on protein function, as was evidenced by reduced activity of yCD2 when it was placed downstream of the P2A sequence. Further studies into the variations that an N-terminus proline would cause to yCD2 structure and active site could reveal the mechanism for this reduced activity.

Finally, in this study, yCD2 was paired with the cytokine mGM-CSF. After transduction of AC3-S1-yCD2-P2A-mGM-CSF, levels of this cytokine were concurrent with the optimal levels for *in vivo* stimulation. Future studies should concentrate on how this RRV works *in vivo*. Studies done with immune-competent mice would focus on quantitating the recruitment of APCs to the cancer mass, as well as testing the immune system against cancer, *in vitro,* by mixed lymphocyte tumor reaction (MLTR), and, *in vivo,* by re-challenging mice with a second tumor to assay immune memory and tumor recognition.

Delivery Of Two Retroviral Replicating Vectors Pseudotyped With Different Non-Interfering Envelopes Increases Transgene Expression And Therapeutic Efficacy

By pseudotyping RRVs with multiple different envelopes, different interference patterns were observed in different cell lines. Although the patterns of interference were not completely clear, there is potential that the access to membrane proteins may play some role in these patterns. Further analysis of Pit1, Pit2, and XPR1 receptor levels could yield insight into the interactions that are taking place between envelopes. For instance, overexpression or knockdown of a viral receptor, followed by cotransduction by various pseudotyped RRVs would further elucidate the effect of receptor availability on cotransduction efficiency. Intrinsic anti-viral restriction factors may have differential affects depending on the envelope pseudotype employed. For instance, RRV pseudotypes that undergo fusion in late stage endosomes may be more proximally localized to the nucleus and thus be less likely to encounter cytosolic antiviral immune factors.

Most importantly, all pseudotypes, except in one instance, were unable to cotransduce cells that had already achieved full transduction using an RRV with the same envelope. AC3 was also unable to cotransduce across all cell lines after TC3 transduction. In simultaneous cotransductions, however, cotransduction was achieved with the same envelopes, but at different degrees depending on the cell line in question. This would also benefit from further study into the expression levels of cellular receptors in each cell line.

The protein expression of each virus was then studied in U87s. Protein expression increased with TC3-emd transduction, but decreased with XC3-emd transduction in comparison to AC3-emd. Because of its low protein expression, XC3-emd was abandoned for further studies in U87 cells. It was also found that TC3-emd was cytotoxic to U87 cells, so this pseudotype was also abandoned in the U87 model. This left the AC3 and GC3 to be further explored in cotransduction experiments, but this does not mean that TC3 and XC3 should not be considered in other models. 10A1 did not inhibit growth or cause cytotoxicity in either WiDr or PC3 cells. XC3 could increase its transgene expression in a cell line with more XPR1 receptors, and is well suited for cotransduction as it showed the least amount of interference between envelopes across all cell lines.

Surprisingly, when AC3 and GC3 were cotransduced in U87 cells, a dramatic increase in AC3 vector copy number per cell and transgene RNA expression was observed, while GC3 vector copy number and transgene RNA expression were slightly decreased. This was an unexpected but welcomed result, as maximum transgene expression can increase therapeutic efficacy. The current theory is that, after a cell is cotransduced with both vectors, it will produce both forms of the envelope protein, which will then both be expressed on the surface of nascent budding RRVs. This will allow an originally AC3 RRV to display both 4070A and GALV envelope proteins and thus to enter subsequent cells through either the PiT1 or the PiT2 receptor. The mosaic virus can thus enter cells that were previously transduced by either parental virus,

resulting in increased vector copy number. Further studies should be carried out to test this RRV mosaic theory.

Chapter 3 Enveloped-Linked Oligonucleotide P2a Increases Transgene Expression From Retroviral Replicating Vectors

As mentioned above, P2A may alter protein function by addition of amino acids to both the upstream and downstream genes. In this study, we attached P2A to the end of the envelope protein of AC3 and GC3 RRVs. It was shown that this caused a decrease in vector copy number, which could be due to inefficient cleavage of the C-terminus of the envelope protein. This could result in production of non-fusogenic viruses capable of binding and occupying viral receptors, but incapable of infecting the next round of cells, thus leading to a decrease in vector copy number. Despite this decrease, P2A transgene expressed better in most cell lines than SCP1-driven transgenes. In attempting to combine suicide gene treatments with the larger TKO gene, P2A made for an ideal candidate. When cotransduced with AC3-yCD2, the number of AC3-P2A-TKO copies per cell fell drastically compared to single transductions. This can again be theorized to be the fault of inefficient cleavage of the envelope with P2A, as AC3-yCD2 would gain a kinetic advantage over this RRV over multiple infection cycles. GC3-P2A-TKO, on the other hand, does not compete directly with a fully functional form of GALV, so it would be able to cotransduce along with AC3-yCD2 with being hindered. Although this combination of RRVs has proven the most effective, the slight decrease that cotransduction has on GC3-P2A-TKO caused it to be less effective at decreasing cell viability at the highest concentrations of GCV than single transduction. Future studies can also look into TKO as a marker for viral spread, as TK can interact with the PET probe 9-4-[18F]fluoro-3-(hydroxymethyl)butyl]guanine ([18F]FHBG)[22]. This would allow for the tracking of viral spread *in vivo* to assess the amount of tumor transduced and monitor potential escape from the tumor mass.

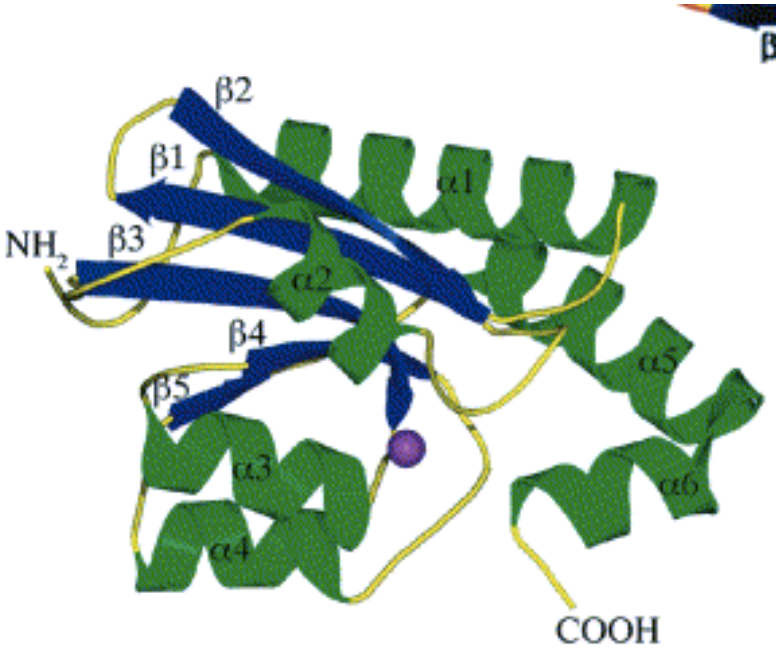

Supplementary Figure 1-1
Structure of yeast cytosine deaminase[15]

PC3 Simultaneous

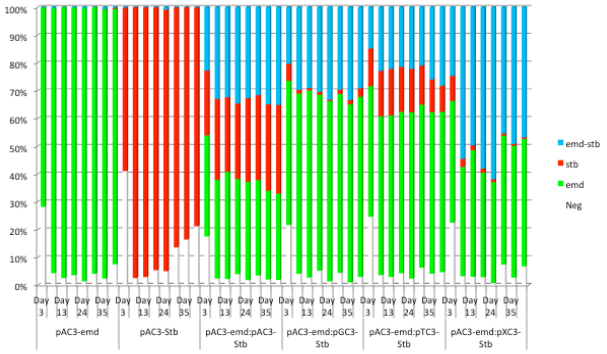

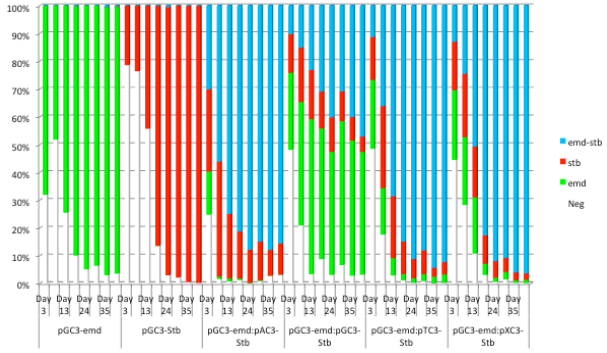

PC3 Simultaneous

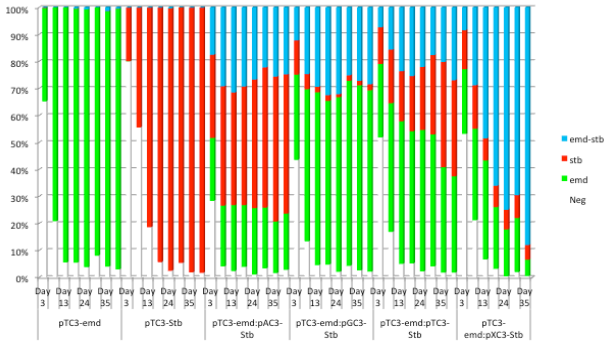

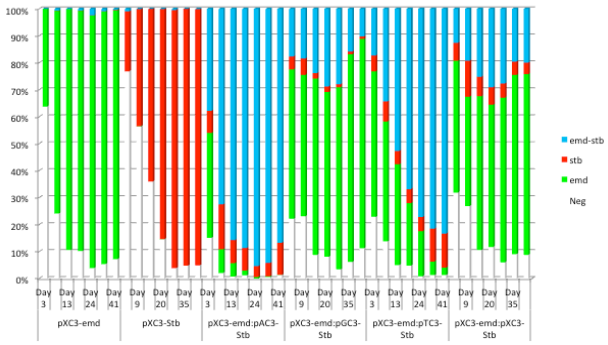

U87 Simultaneous

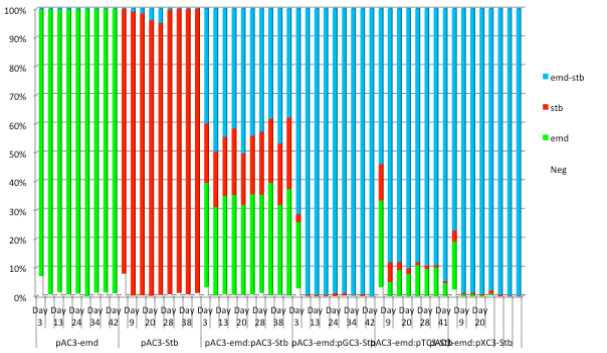

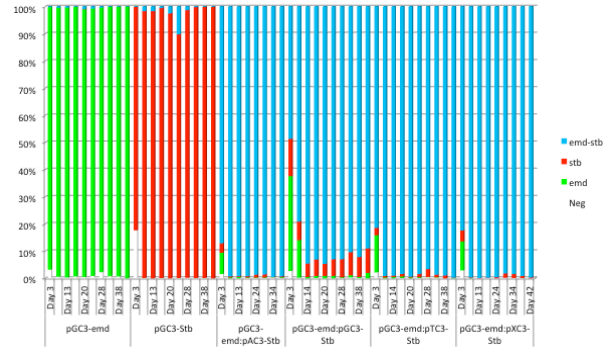

U87 Simultaneous

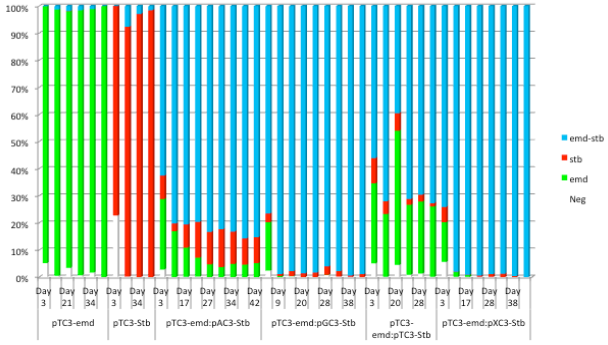

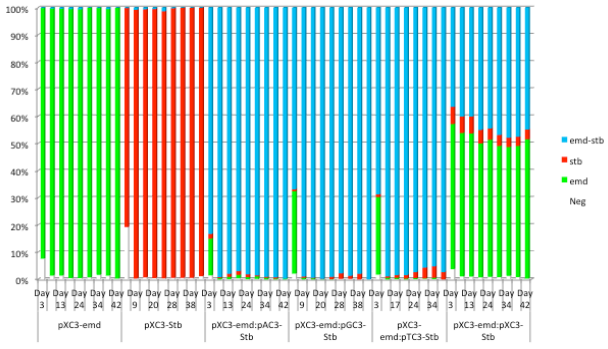

HeLa Simultaneous

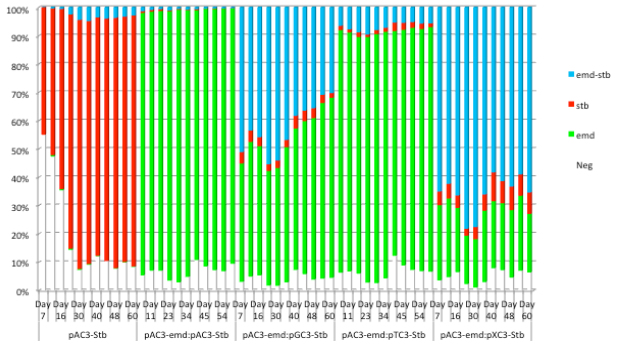

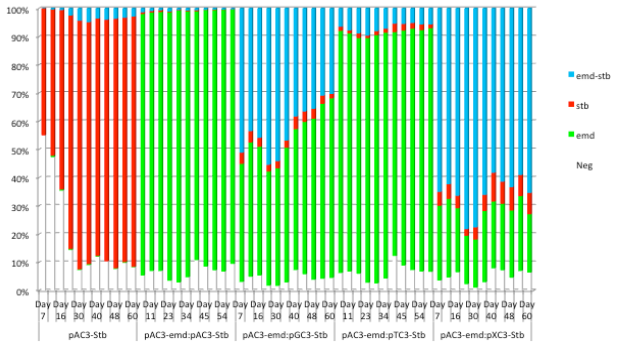

HeLa Simultaneous

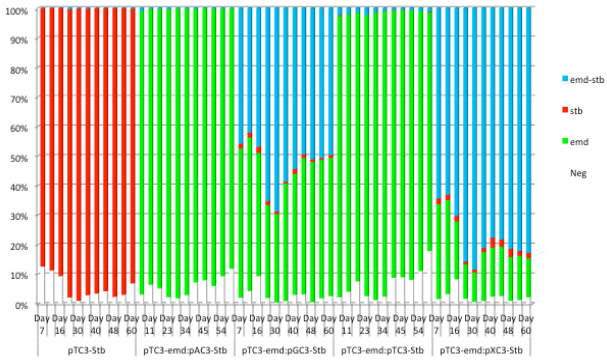

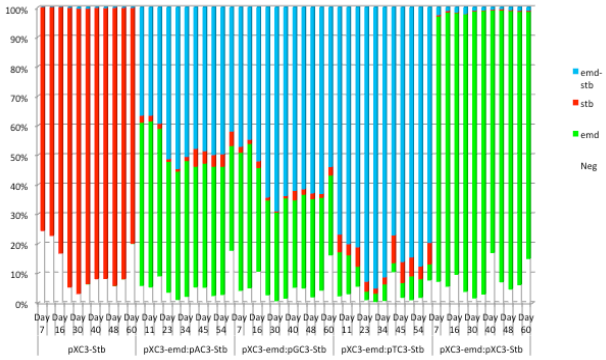

WiDr Simultaneous

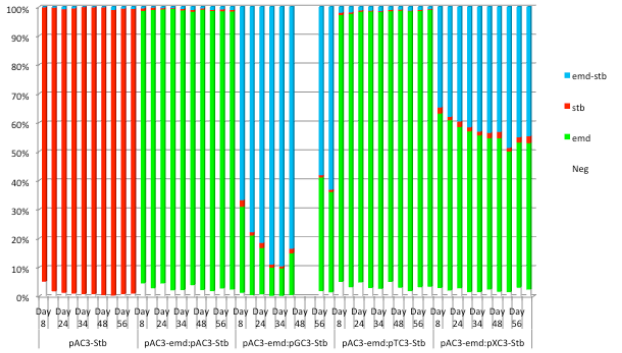

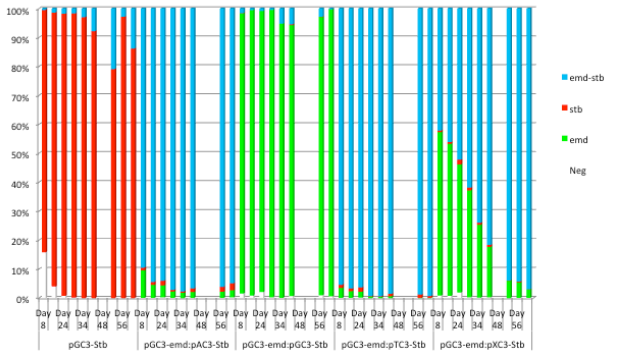

WiDr Simultaneous

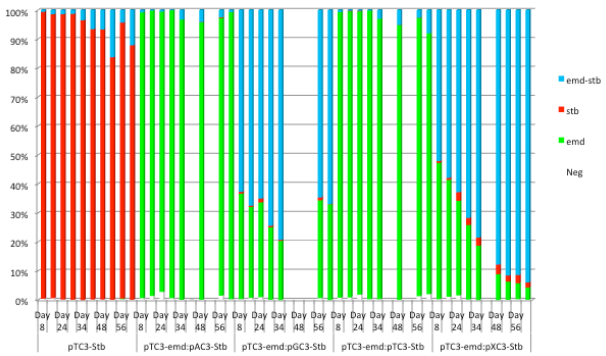

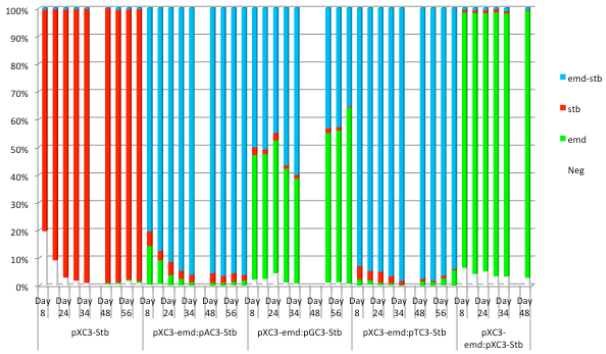

PC3 Sequential emd-Stb

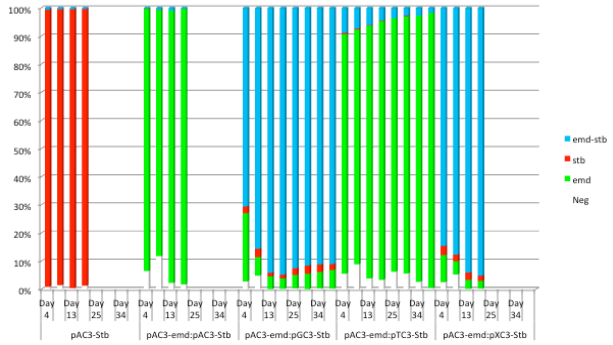

PC3 Sequential emd-Stb

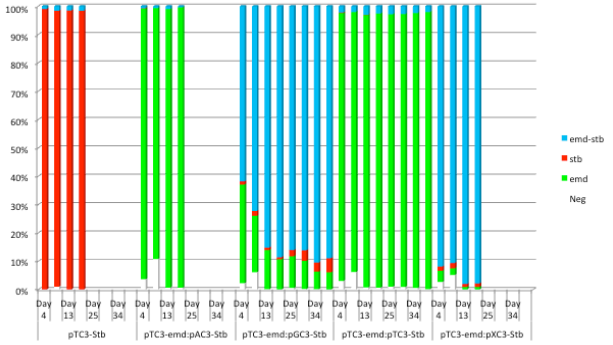

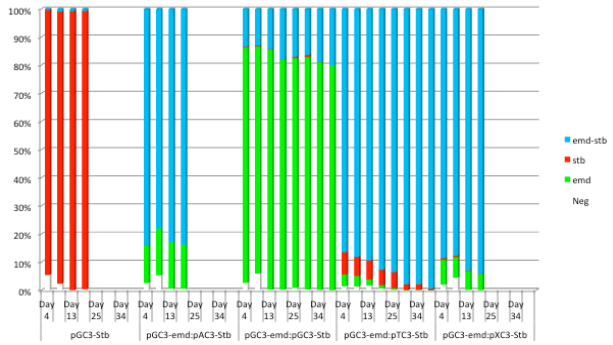

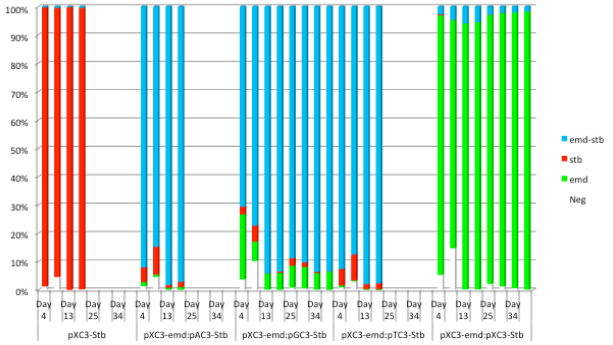

PC3 Sequential Stb-emd

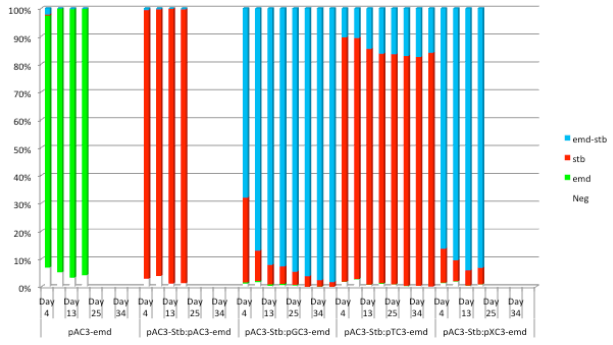

PC3 Sequential Stb-emd

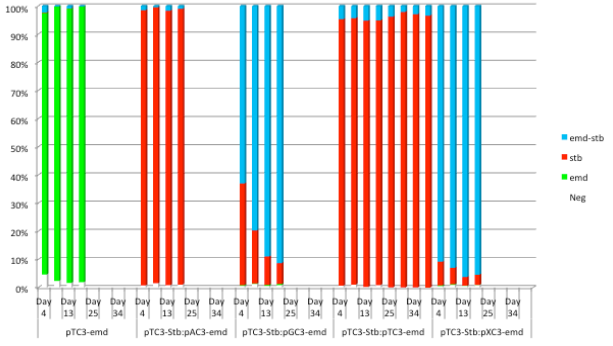

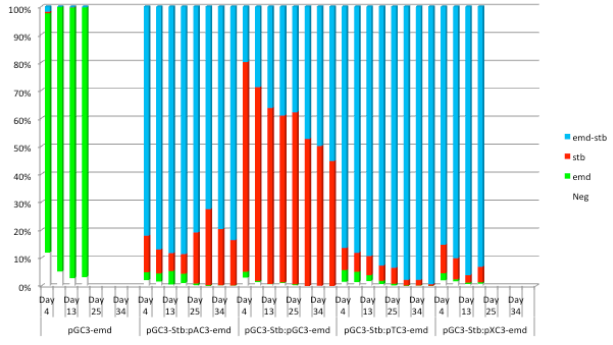

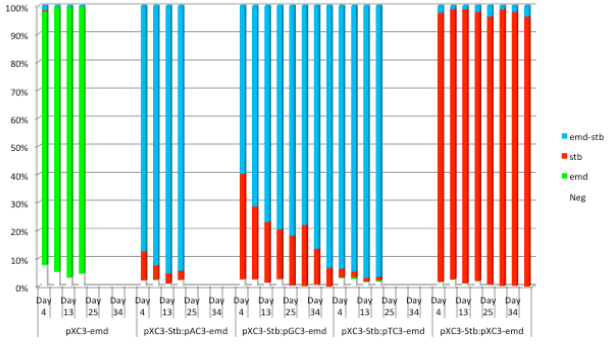

U87 Sequential emd-Stb

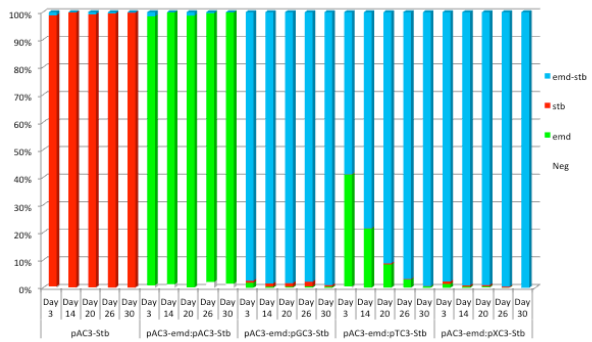

U87 Sequential emd-Stb

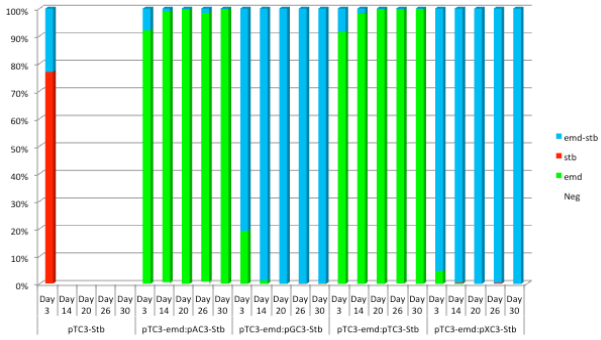

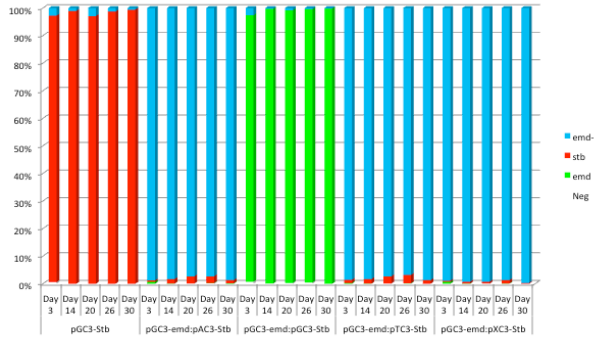

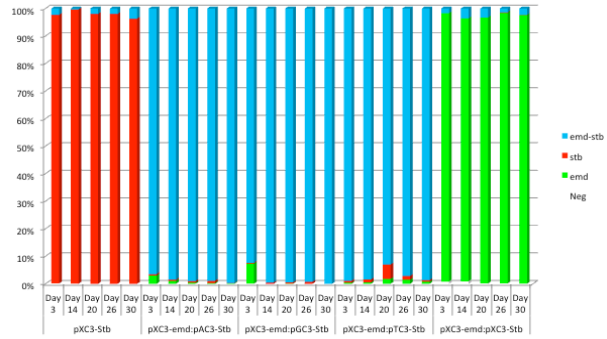

U87 Sequential Stb-emd

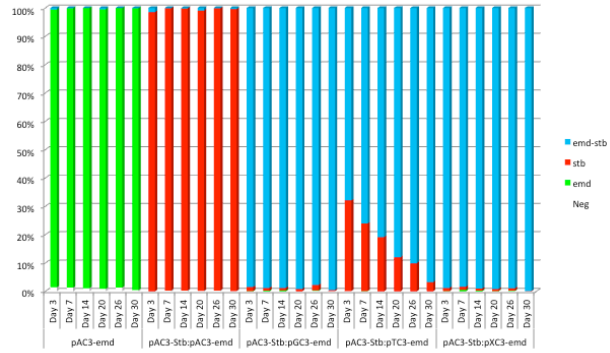

U87 Sequential Stb-emd

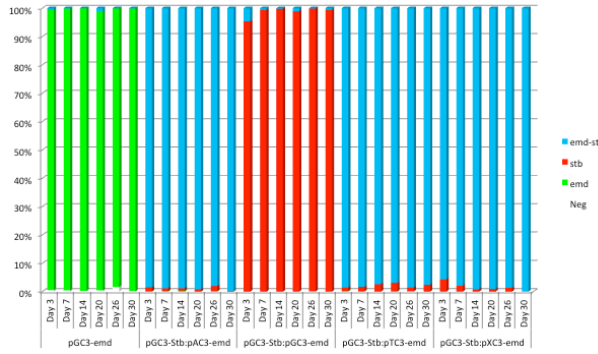

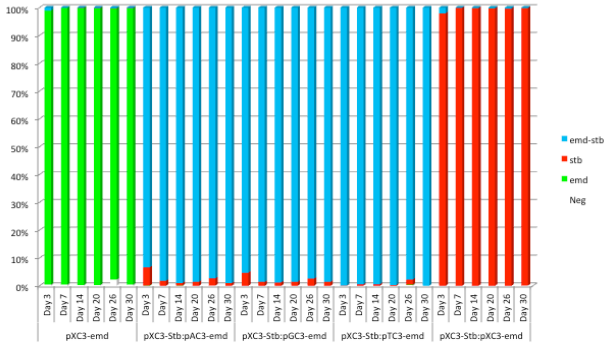

HeLa Sequential emd-Stb

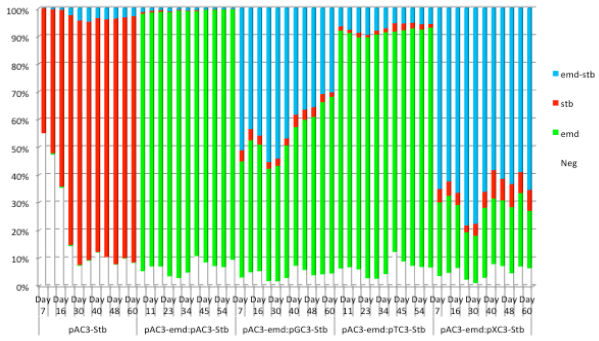

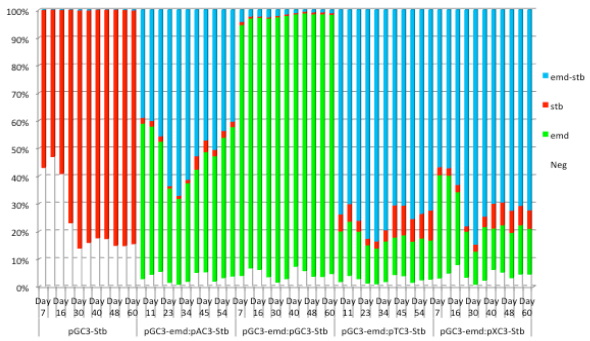

HeLa Sequential Stb-emd

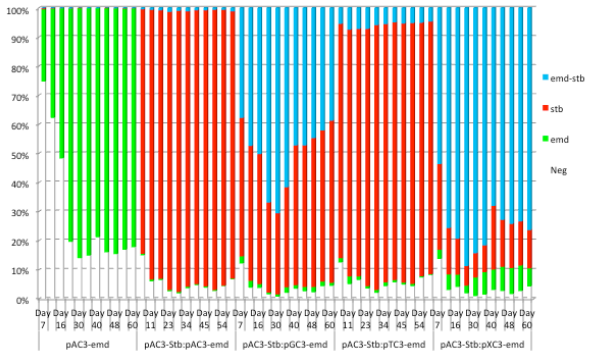

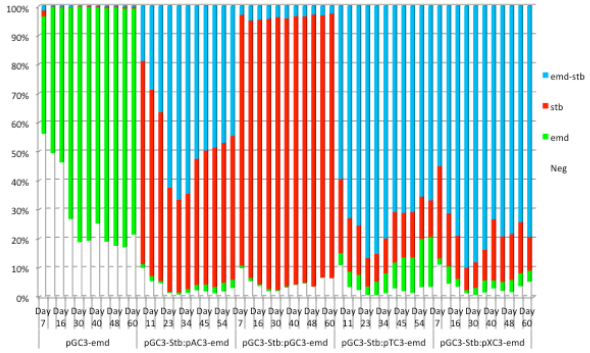

HeLa Sequential emd-Stb

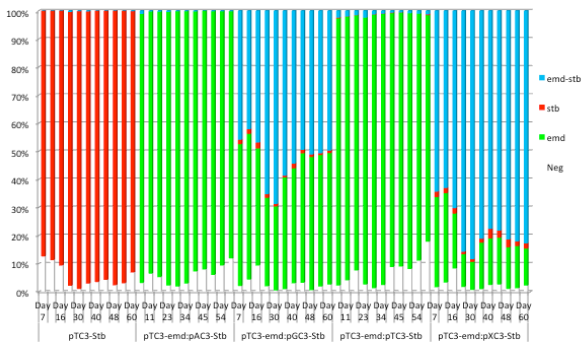

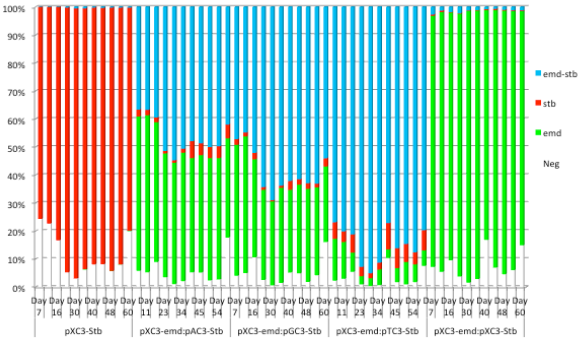

HeLa Sequential Stb-emd

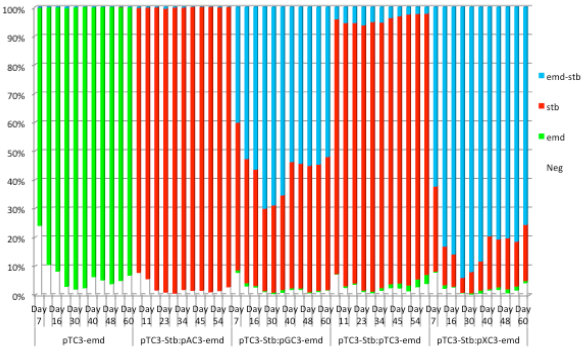

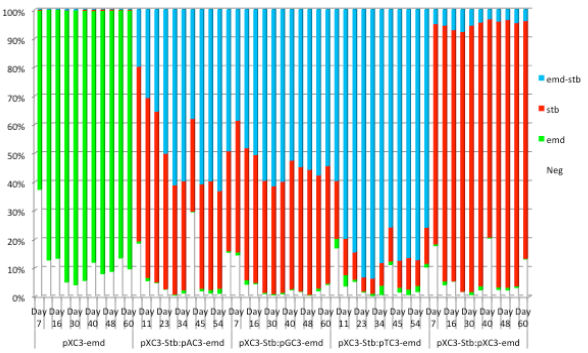

WiDr Sequential emd-Stb

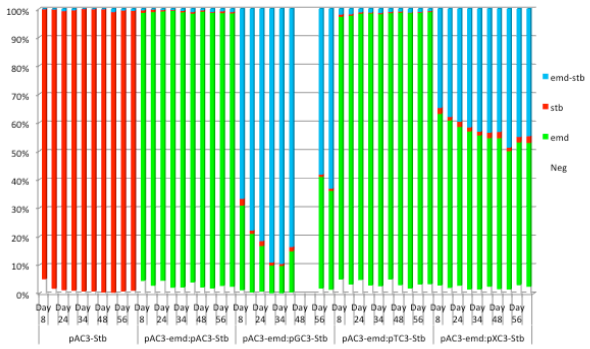

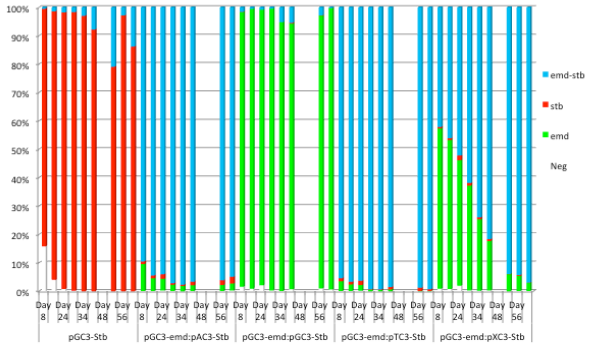

WiDr Sequential emd-Stb

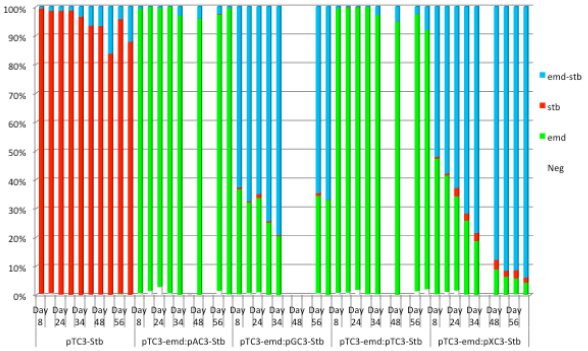

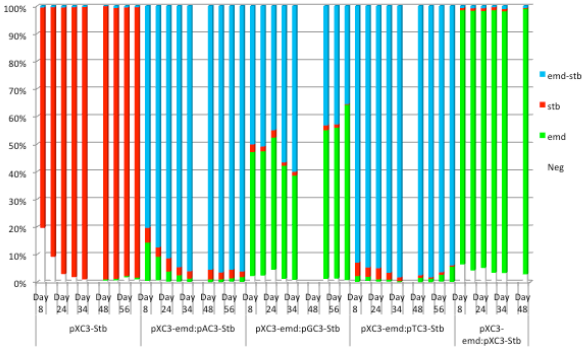

WiDr Sequential Stb-emd

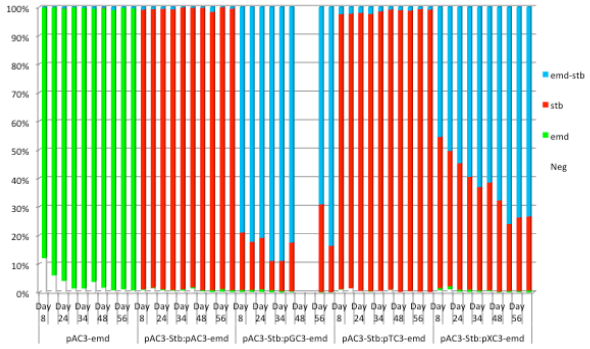

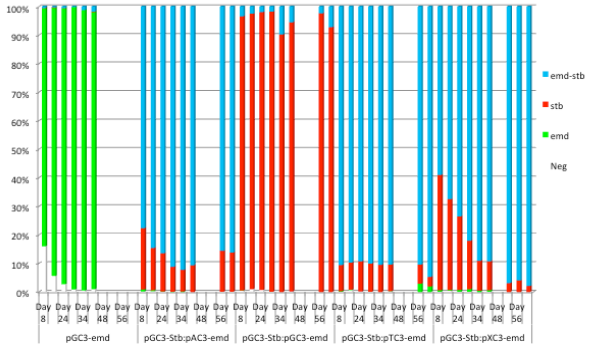

WiDr Sequential Stb-emd

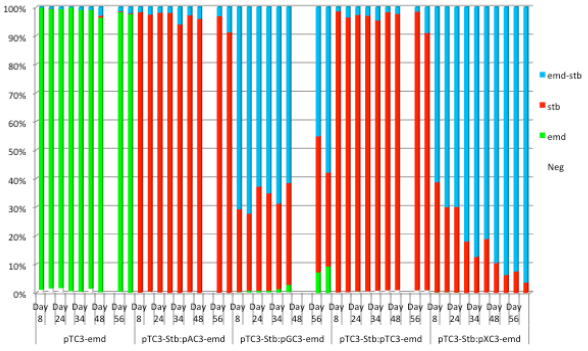

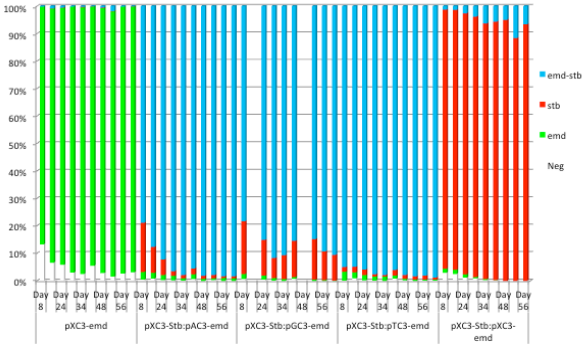

Supplementary Figure 2-1
Complete data on sequential and simultaneous cotransductions across cell lines. Graphs represent 100% of the population, as untransduced cells are represented by white, single transductions are represented by green or red, depending on the prevailing FP, and cotransduced cells are represented by blue.

PC3

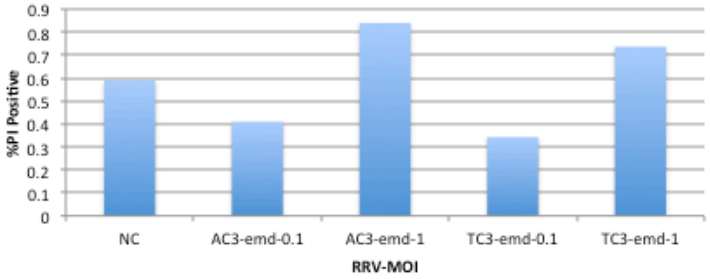

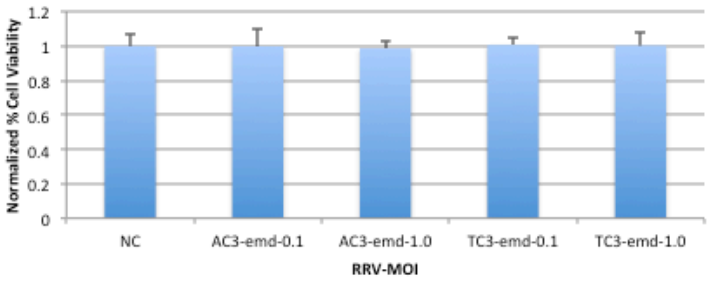

WiDr

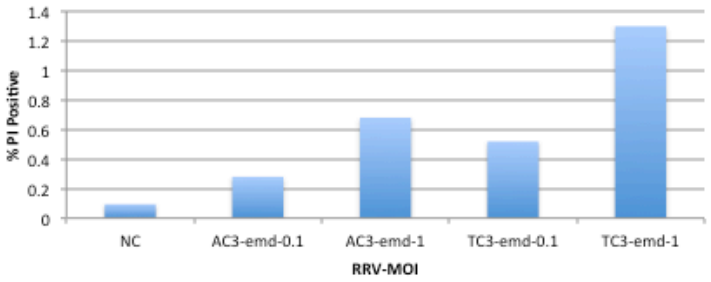

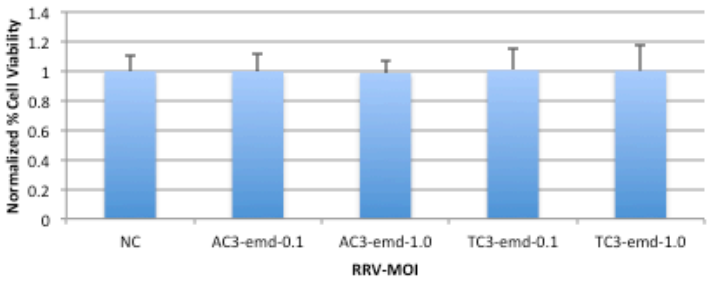

Supplementary Figure 2-2
Cell viability of PC3 and WiDr cell lines transduced with TC3-emd as measured by MTS and PI staining

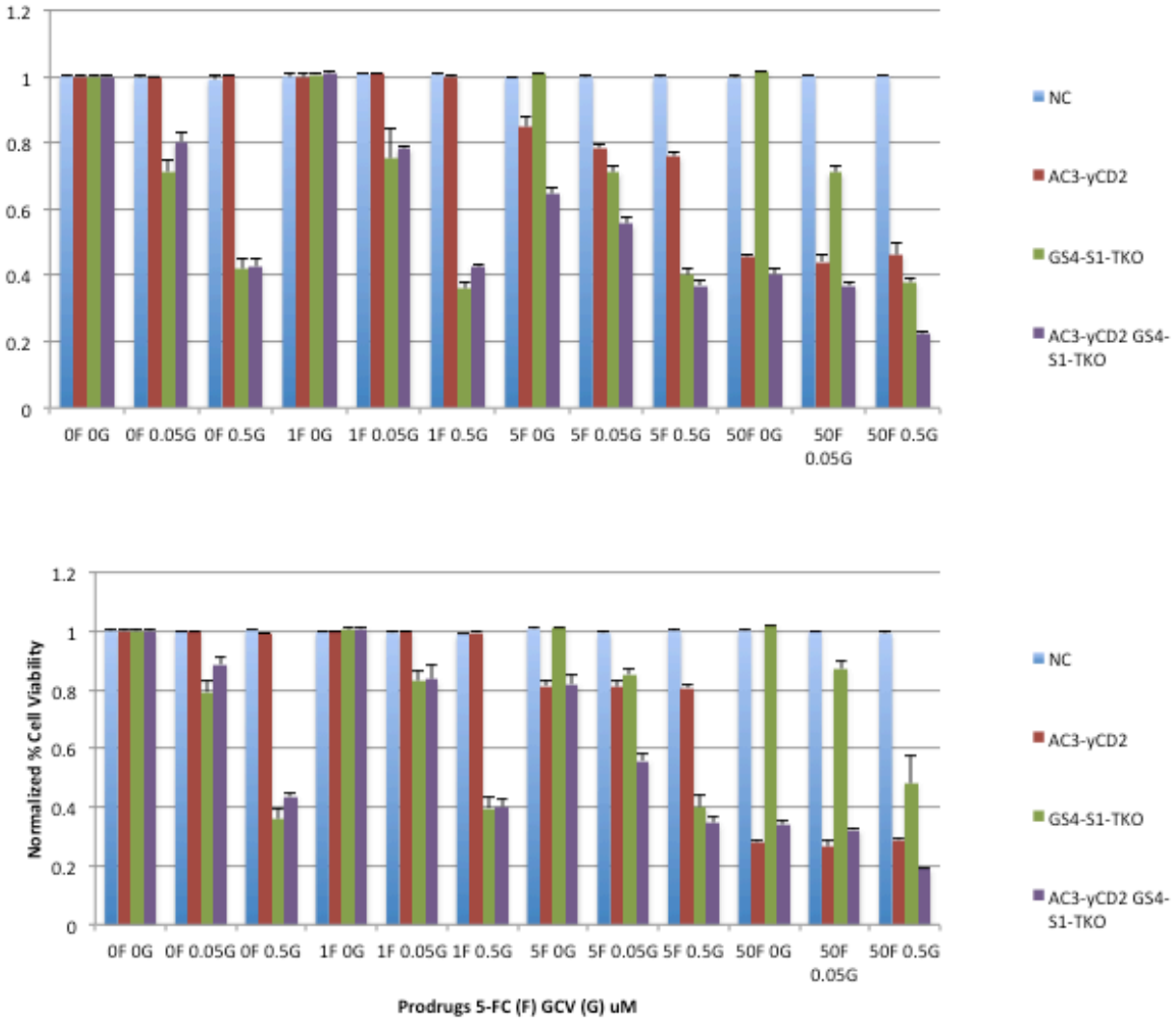

Supplementary Figure 2-3
MTS with full prodrug concentrations of AC3-yCD2 and GS4-S1-TKO cotransduced U87 cells.

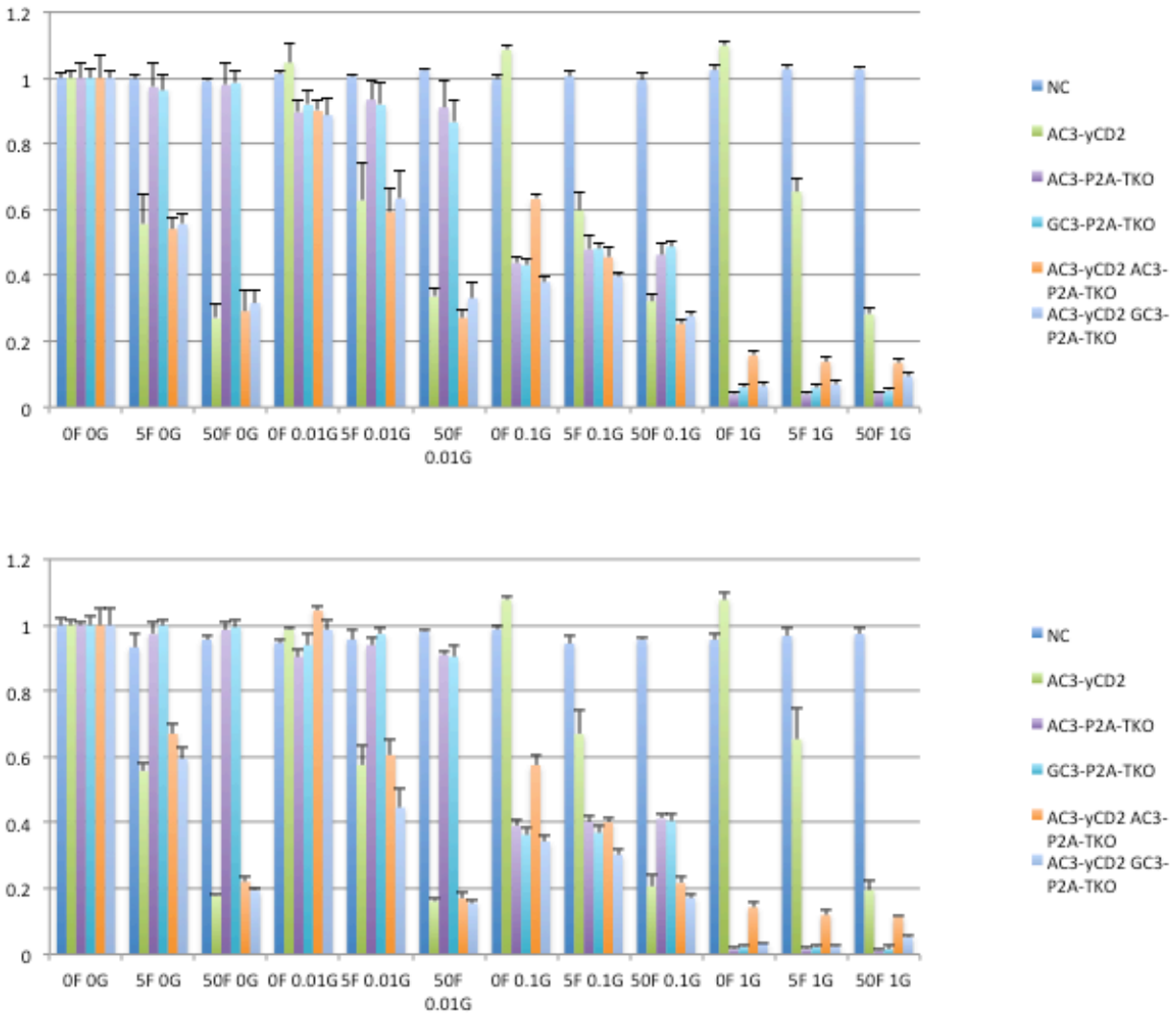

Supplementary Figure 3-1
MTS with full prodrug concentrations of AC3-yCD2 and GC3-P2A-TKO cotransduced U87 cells.

References1. Logg, C. R., Robbins, J. M., Jolly, D. J., Gruber, H. E. & Kasahara, N. *Retroviral replicating vectors in cancer. Methods in enzymology* **507,** (Elsevier Inc., 2012).

2. Derek Ostertag, Karin K. Amundson, Fernando Lopez Espinoza, B. M. *et al.* Brain tumor eradication and prolonged survival from intratumoral conversion of 5-fluorocytosine to 5-fluorouracil using a nonlytic retroviral replicating vector. *Neuro-Oncology* 14(2):145 – 159 (2012). at <http://neuro-oncology.oxfordjournals.org/content/14/2/145.full.pdf#page=1&zoom=auto,0,783>

3. Juven-Gershon, T., Cheng, S. & Kadonaga, J. T. Rational design of a super core promoter that enhances gene expression. *Nat. Methods* **3,** 917–922 (2006).

4. De Felipe, P. *et al.* E unum pluribus: multiple proteins from a self-processing polyprotein. *Trends Biotechnol.* **24,** 68–75 (2006).

5. Tang, W. *et al.* Faithful expression of multiple proteins via 2A-peptide self-processing: a versatile and reliable method for manipulating brain circuits. *J. Neurosci.* **29,** 8621–9 (2009).

6. Lang, F. *et al.* Phase I Trial of Adenovirus-Mediated p53 Gene Therapy for Recurrent Glioma: Biological and Clinical Results. *J. Clin. Oncol.* **21,** 2508–2518 (2003).

7. Logg, C. R., Tai, C. K., Logg, a, Anderson, W. F. & Kasahara, N. A uniquely stable replication-competent retrovirus vector achieves efficient gene delivery in vitro and in solid tumors. *Hum. Gene Ther.* **12,** 921–32 (2001).

8. Rainov, N. G. A phase III clinical evaluation of herpes simplex virus type 1 thymidine kinase and ganciclovir gene therapy as an adjuvant to surgical resection and radiation in adults with previously untreated glioblastoma multiforme. *Hum. Gene Ther.* **11,** 2389–2401 (2000).

9. Liu, B. L. *et al.* ICP34.5 deleted herpes simplex virus with enhanced oncolytic, immune stimulating, and anti-tumour properties. *Gene Ther.* **10,** 292–303 (2003).

10. Hu, J. C. C. *et al.* A phase I study of OncoVEXGM-CSF, a second-generation oncolytic herpes simplex virus expressing granulocyte macrophage colony-stimulating factor. *Clin. Cancer Res.* **12,** 6737–47 (2006).

11. Logg, C. R. *et al.* Genomic Stability of Murine Leukemia Viruses Containing Insertions at the Env-3 ′ Untranslated Region Boundary Genomic Stability of Murine Leukemia Viruses Containing Insertions at the Env-3 J Untranslated Region Boundary. (2001). doi:10.1128/JVI.75.15.6989

12. Hlavaty, J. *et al.* Comparative evaluation of preclinical in vivo models for the assessment of replicating retroviral vectors for the treatment of glioblastoma. *J. Neurooncol.* **102,** 59–69 (2011).

13. Serafini, P. *et al.* High-dose granulocyte-macrophage colony-stimulating factor-producing vaccines impair the immune response through the recruitment of myeloid suppressor cells. *Cancer Res.* **64,** 6337–6343 (2004).

14. Su, A. I. *et al.* A gene atlas of the mouse and human protein-encoding transcriptomes. *Proc. Natl. Acad. Sci. U. S. A.* **101,** 6062–6067 (2004).

15. Ireton, G. C., Black, M. E. & Stoddard, B. L. The 1.14 A crystal structure of yeast cytosine deaminase: Evolution of nucleotide salvage enzymes and implications for genetic chemotherapy. *Structure* **11,** 961–972 (2003).

16. Dranoff, G. GM-CSF-based cancer vaccines. *Immunol. Rev.* **188,** 147–54 (2002).

17. Jean, W. C. *et al.* Effects of combined granulocyte-macrophage colony-stimulating factor (GM-CSF), interleukin-2, and interleukin-12 based immunotherapy against intracranial glioma in the rat. *J. Neurooncol.* **66,** 39–49 (2004).

18. Logg, C. R., Baranick, B. T., Lemp, N. A. & Kasahara, N. Adaptive Evolution of a Tagged Chimeric Gammaretrovirus : Identification of Novel cis -Acting Elements that Modulate Splicing. 1214–1229 (2007). doi:10.1016/j.jmb.2007.04.026

19. Uckert, W., Willimsky, G., Pedersen, F. S., Blankenstein, T. & Pedersen, L. RNA levels of human retrovirus receptors Pit1 and Pit2 do not correlate with infectibility by three retroviral vector pseudotypes. *Hum. gene …* **2627,** 2619–2627 (1998).

20. Green, N. *et al.* Sequence-specific antibodies show that maturation of Moloney leukemia virus envelope polyprotein involves removal of a COOH-terminal peptide. *Proc. Natl. Acad. Sci. U. S. A.* **78,** 6023–6027 (1981).

21. Januszeski, M. M., Cannon, P. M., Chen, D., Rozenberg, Y. & Anderson, W. F. Functional analysis of the cytoplasmic tail of Moloney murine leukemia virus envelope protein. *J. Virol.* **71,** 3613–3619 (1997).

22. Yaghoubi, S. S. & Gambhir, S. S. PET imaging of herpes simplex virus type 1 thymidine kinase (HSV1-tk) or mutant HSV1-sr39tk reporter gene expression in mice and humans using [18F]FHBG. *Nat. Protoc.* **1,** 3069–3075 (2006).